Prediction of Sediment Delivery to Watercourses from Land Phase II

R & D Technical Report No P2-209

Marianne McHugh[1], Gavin Wood[2], Des Walling[3], Roy Morgan[2], Yusheng Zhang[3], Steven Anthony[4] and Mike Hutchins[4]

[1]National Soil Resources Institute, Cranfield University, North Wyke, Okehampton Devon EX20 2SB

[2]National Soil Resources Institute, Cranfield University, Silsoe Bedford MK45 4DT

[3]University of Exeter, Department of Geography, Amory Building, Rennes Drive, Exeter, Devon EX4 4RJ

[4]ADAS, Woodthorne, Wergs Road, Wolverhampton WV6 8TQ

Publishing Organisation
Environment Agency, Rio House, Waterside Drive, Aztec West, Almondsbury, Bristol, BS32 4UD.

Tel 01454 624400 Fax 01454 624409
Website www.environment-agency.gov.uk

© Environment Agency December 2002

ISBN 1-84432-078-2

All rights reserved. No part of this document may be reproduced, stored in a retrieval system, or transmitted, in any form or by any means, electronic, mechanical, photocopying, recording or otherwise without the prior permission of the Environment Agency.

The views expressed in this document are not necessarily those of the Environment Agency. Its officers, servants or agents accept no liability whatsoever for any loss or damage arising from the interpretation or use of the information, or reliance upon views contained herein.

Dissemination Status
Internal: No restrictions
External: No restrictions

Statement of Use
This research represents a collaboration between the National Soil Resources Institute (Cranfield University), the Geography Department (University of Exeter) and ADAS (Woodthorne).

Keywords
Arable, upland, grassland soil erosion vulnerability, sediment delivery to watercourses, connectivity

Research Contractor
This document was produced under R&D Project No P2-209 by:
Dr. Marianne McHugh, National Soil Resources Institute, Cranfield University, North Wyke, Okehampton Devon EX20 2SB
Tel: 01837 88198 fax: 01837 82139 www.silsoe.cranfield.ac.uk/nsri

Environment Agency's Project Manager
The Environment Agency's Project Manager for Project No P2-209 was:
Antony Williamson, Environmental Forecasting Advisor,
Environment Agency, Centre for Risk and Forecasting,
Kings Meadow House, Reading RG1 8DQ
Antony.williamson@environment-agency.gov.uk

Further copies of this report are available from:
Environment Agency R&D Dissemination Centre, c/o WRc, Frankland Road, Swindon, Wilts SN5 8YF

tel: 01793-865000 fax: 01793-514562 e-mail: publications@wrcplc.co.uk

EXECUTIVE SUMMARY

Phase I of this research was initiated to develop a clearer understanding of the processes involved in sediment delivery from arable land to surface waters. Its recommendations were that further work be undertaken to investigate the connectivity between land and watercourses using both field studies and modelling techniques to improve identification of areas at risk of erosion and of sediment movement to watercourses. It also highlighted that the approach could be usefully extended to other land uses, including grassland and upland, and that validation of the sediment delivery rates to watercourses using data collated from field studies was necessary.

The research conducted in Phase II sought to address some of these recommendations. Its main objectives were the identification of the risks of erosion from soils under arable, grassland and upland land uses and the combination of these with an index of the connectivity of eroding soils and watercourses. The final product comprises maps illustrating the risk of annual erosion vulnerability and sediment delivery to watercourses for different probabilities or return periods. Although time did not allow the detailed methodology or the maps to be validated, the results for the 1-in-10-year return period (p=0.999; Figure ES1) broadly confirm the findings of other researchers. The maps may therefore be used by EA personnel to identify potentially high risk areas of England and Wales.

It should be stressed that the map showing sediment delivery relates specifically to the movement of sediment from hillslopes into watercourses. It cannot be used to indicate sediment yield from specific catchments because issues such as the fate of sediment within the river channel and the supply of additional sediment to the watercourse from the channel bed and banks are not considered. These aspects were outside the scope of the project.

The greatest risk of erosion and diffuse pollution associated with sediment is shown to occur under arable agriculture in parts of Somerset, the Isle of Wight, Norfolk, the West Midlands and Nottinghamshire. The soils at risk are largely brown earths, brown sands and brown rendzinas with sandy loam, loamy sand and silty textures. Compared to previously published data, the erosion rates shown on the maps are rather low, reflecting the fact that individual events >10 m^3 ha^{-1} have higher return periods than 1-in-10 years and that such events usually relate to field sizes of 1-3 ha, whereas the data presented here represent averages over 1 km^2.

Phase II consisted of three stages:

1) Data from a series of objective and nationally-representative erosion monitoring studies on upland, lowland grassland and arable soils were used to calculate the probability of erosion of a given magnitude occurring for different soil-slope combinations. Such probability analysis allowed erosion rates for arable, upland and lowland grassland soils to be compared.
2) The efficiency of sediment delivery from land to watercourses, which in turn directly reflects the connectivity between the land surface and the river system, was characterised. Two measures of connectivity were developed: the connectivity index**,** which represents the relative efficiency of sediment transfer, and the connectivity ratio, which is based directly on the connectivity index and represents a scaling of that index to provide a quantitative measure of the efficiency of sediment transfer.
3) Using GIS, the probabilities of erosion for different soil-slope combinations were combined with the connectivity ratio to illustrate graphically the distribution of estimated annual sediment delivery to watercourses in England and Wales for different return periods.

The research output demonstrates the validity of the techniques used for the identification of areas at risk of erosion and sediment delivery to watercourses in England and Wales. Uncertainties remain, however. Although the dataset used is the most comprehensive available, it is not sufficient to quantify the risk of erosion from different soils at a more detailed level using, for example, soil series. Further calibration and validation of the connectivity ratio provided are needed: again, the collection of specific data is necessary for this to be possible. Finally, extrapolation of the erosion data across land use types nationally, using GIS, requires more accurate maps of vegetation cover and specific land uses than those currently available. The distinction between lowland grassland and grass leys in a rotational arable system particularly needs to be improved.

Although unvalidated, it would be possible to undertake a limited scoping validation exercise, which might inform how a more detailed validation survey could be carried out. This might involve examining the results of previously published erosion studies in more detail and comparing both erosion figures and the location of eroded fields with the outputs of this project. There is also some scope to consider using the current arable erosion data to produce maps showing erosion at different levels of probability for specific crop types such as winter cereals or sugar beet, i.e. the crops most frequently associated with serious erosion. There may also be possibility of using the upland data set to consider scenarios with different grazing intensities. There is little scope with the current data for further work on lowland grassland erosion.

The need for validation and improvement extends to the estimates of connectivity, where additional work is required to inform the calibration of the connectivity index used to produce estimates of the connectivity ratio and to validate the resulting values. In the longer-term, however, there is an important need to undertake further field-based and experimental investigations to improve existing understanding of sediment delivery and the factors controlling slope-channel connectivity. This improved understanding is likely to lead to the incorporation of further controlling factors into the procedure used to estimate the connectivity index, particularly factors related to adventitious effects on

slope-channel connectivity, such as field boundaries, the position of gateways and the role of tracks and roads in routing water and sediment.

Despite these reservations and the need for further work, the maps of vulnerability to erosion and sediment delivery to watercourses produced by the project can be used to identify broad regions at risk where more detailed local investigations can be targeted. The maps represent the first consolidated assessment at a national level, allowing comparisons of the situation across the range of slope, soil and land use combinations.

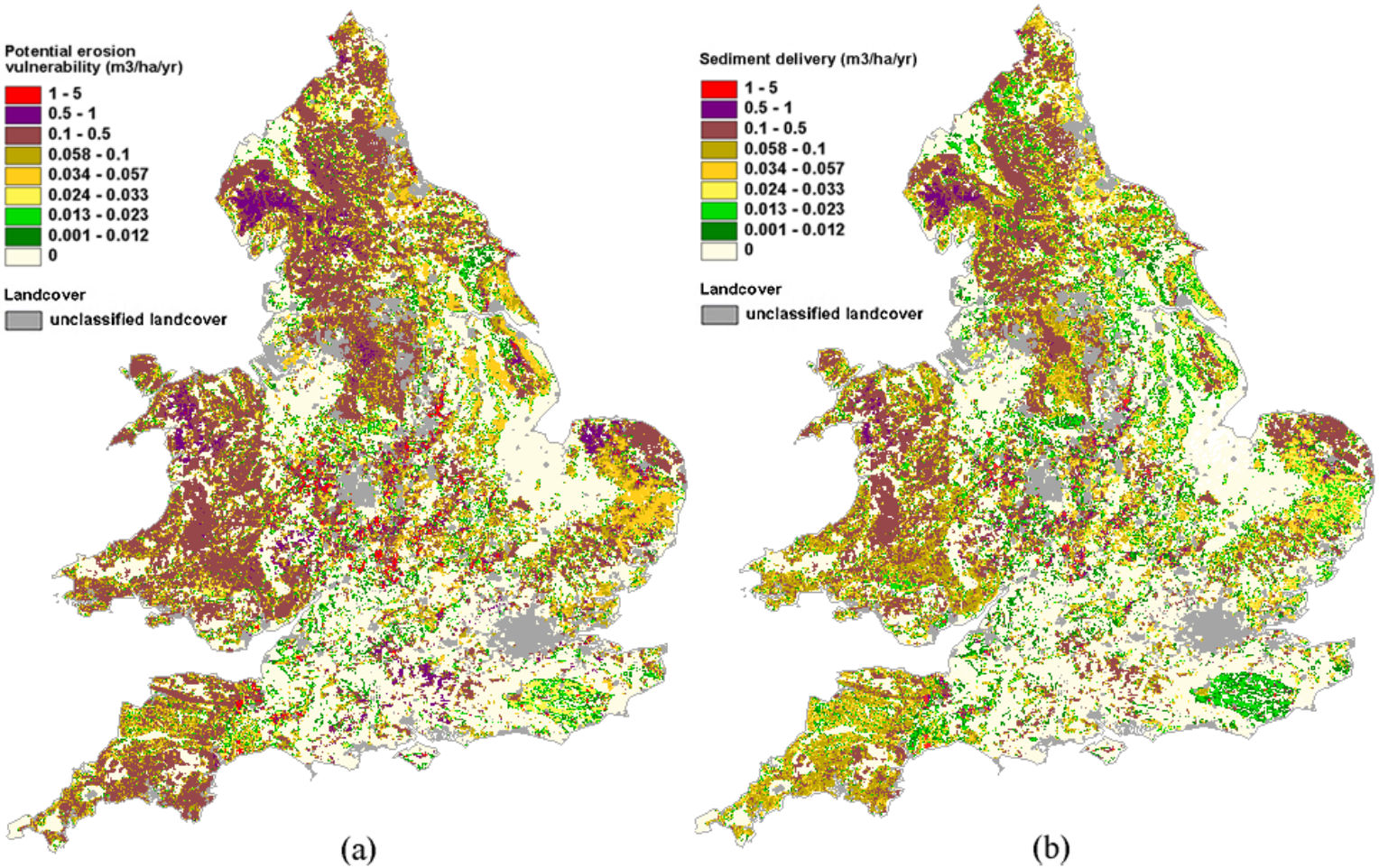

Figure ES1. The distribution of (a) of erosion vulnerability estimates and (b) estimated sediment delivery to watercourses expected to occur annually in England and Wales under 1-in-10 year events.

CONTENTS Page

EXECUTIVE SUMMARY iii

1. INTRODUCTION 1
1.1 Objectives and approach 1

2. EROSION VULNERABILITY AND RISK 3
2.1 Vulnerability classes 3
2.2 Erosion probability 6
2.3 General comments 12

3. ASSESSMENT AND CHARACTERISATION OF SLOPE-CHANNEL CONNECTIVITY 15
3.1 Introduction, aims and objectives 15
3.2. Identification of factors that control the efficiency of sediment delivery from hillslopes to watercourses 16
3.3 Parameterisation of the controlling factors 17
3.4 Derivation of the connectivity index 21
3.5 Derivation of the connectivity ratio 25
3.6 The final products: their use and limitations 25

4 SPATIAL DATA PROCESSING AND MAPPING 31
4.1 Introduction 31
4.2 Characterisation of slope gradient distribution 31
4.3 Soil distribution 35
4.4 Landcover mapping 37
4.5 Erosion modelling 41
4.6 Erosion vulnerability mapped output 44

5 FINAL OUTPUT: SEDIMENT DELIVERY TO WATERCOURSES 54

6 DISCUSSION 58
6.1 Sediment generation 58
6.2 Sediment connectivity 61
6.3 Sediment delivery 61

7 CONCLUSIONS AND RECOMMENDATIONS 64

8 REFERENCES 66
9 LIST OF FIGURES 71
10 LIST OF TABLES 74

APPENDIX 1 Data for classification of erosion vulnerability on arable, grassland and upland soils 76
APPENDIX 2 Data associated with slope-channel coupling 81
APPENDIX 3 Data relating to spatial data processing, analysis and mapping 96

1. INTRODUCTION

The accelerated erosion of land in England and Wales has been an issue of some concern to researchers and policy makers alike for several years (Morgan, 1995; Evans and Skinner, 1987; Robinson and Blackman, 1990). The implications of accelerated soil loss include the loss of agricultural land (Evans, 1996), the economic costs of sediment on roads (Evans, 1996) and in reservoirs and rivers (Butcher *et al.,* 1992), and the ecological impacts on fish stocks (Theurer *et al.,* 1998) and water quality. All highlight the importance of mitigating accelerated soil loss to watercourses.

Although information about the source and delivery of eroded sediment from a catchment area to water has implications for management strategies (Higgitt and Lu, 2001), frequently the management of sediment-related environmental problems is compromised by a lack of information on sediment mobilisation and delivery (Walling *et al.,* 2001). This research has been initiated by the Environment Agency to identify the risk to watercourses in England and Wales from erosion of soil by water, by investigating the connectivity between erosion and watercourses. Identification of watercourses at risk will allow resources to be focused on key areas of the country to reduce the overall scale and impacts of erosion and sediment generation.

Before resources can be effectively and appropriately focussed, it is necessary to identify key target areas for resource investment. Previously, remediation and mitigation have been on an *ad hoc* basis, with problems of soil erosion and sedimentation being dealt with locally. This research aims to provide information on erosion and sediment delivery at a national level, using nationally-representative data on erosion from arable, lowland grassland and upland ecosystems, by deriving an index of sediment connectivity using nationally-explicit data and by using GIS to combine these factors in national coverages.

1.1 Objectives and approach

Specifically, the project's objectives are to:

1) Construct algorithms to link soil physical and chemical properties with slope, land use and other relevant data to derive a soil erosion vulnerability score;
2) Propose coefficients to estimate amounts of sediment generated from different combinations of data such as soil, land use and slope;
3) Calculate sets of coefficients to represent the connectivity of the soil systems with watercourses with respect to sediment delivery;
4) Construct algorithms linking items (2) and (3) above to represent the risk of sediment delivery to watercourses;
5) Use existing data from river monitoring, erosion event reports and other field data to validate and revise the algorithms and coefficients produced in (1-4);
6) Produce ArcView GIS layers in grid format of the datasets derived from the base data using algorithms from items (1), (2), (3) and (4).

The research has been carried out by the National Soil Resources Institute of Cranfield University and by the Geography Department at the University of Exeter. In addition, peer-review and advice have been available to the research team throughout the project from the Environment Modelling and GIS Group at ADAS Woodthorne.

The work builds upon a pilot study for quantifying sediment export from arable land to water using a systematic, national-scale approach (Phase I; Fraser *et al.,* 2000). That study identified areas of arable land in England and Wales at increased risk of erosion and provided initial estimations of rates of sediment transfer and delivery to watercourses from arable land. The recommendations of Phase I have provided the basis for the development of this second phase of research.

The approach to the assessment used here broadly follows and builds upon that used in Phase I. The classification of erosion vulnerability and risk of arable soils developed in Phase I has been refined to provide assessments of the probability of erosion from arable, grassland and upland soils. The efficiency of sediment delivery from land to watercourses has been defined by identifying and applying data on the parameters that control sediment delivery efficiency. Probability of erosion and the sediment connectivity ratio were then combined using GIS to illustrate the estimated rates of sediment delivery to watercourses from lowland arable, lowland grassland and upland soils of England and Wales.

The algorithms developed to classify erosion vulnerability and risk on arable, lowland grassland and upland soils are based on three independent MAFF- (now DEFRA) funded research projects. Between 1996 and 1998, research was carried out to establish national budgets of phosphorus loss by assessing soil erosion on lowland arable and lowland grassland National Soil Inventory (NSI) field sites (Harrod, 1998). Between 1997 and 2000, a second MAFF-funded research project investigated soil erosion within the uplands of England and Wales, again using a database of NSI field sites (Harrod *et al.,* 2000). This upland study was partially repeated in 2001/2 (McHugh, 2002). All three studies objectively recorded details of erosion form and extent and these data were used in this study to quantitatively express the risk of erosion from soils in England and Wales.

2. EROSION VULNERABILITY AND RISK

The work described here addresses the first two objectives listed in Section 1.1, namely a classification of erosion vulnerability (Objective 1) and erosion risk (Objective 2). Research undertaken in Phase I of the project aimed to link soil and environmental data to derive a soil erosion vulnerability score and then determine the amount of sediment generated, using different combinations of soil, land use and slope data.

2.1 Vulnerability classes

A classification was developed for erosion vulnerability on lowland arable soils (Fraser *et al.,* 2000) based on five classes of topsoil texture and five slope gradient groups. Published research (Morgan, 1985; Evans, 1990a) shows that topsoil textures dominated by sand and silt are more vulnerable to soil erosion than those with a high clay content, and that erosion vulnerability increases with slope gradient (Fraser *et al.,* 2000). Phase II of the work was intended to improve on the classification for lowland arable soils, by using topsoil texture data at the soil series level instead of soil subgroups, and to develop similar classification systems for upland soils and soils under lowland grass. The database for the classification systems comprises sub-sets of the National Soil Inventory (NSI) used in extensive erosion monitoring projects for lowland arable soils (Harrod, 1998), upland soils (DEFRA Project SP0402; Harrod *et al.,* 2000; McHugh, 2002) and lowland grassland soils (Harrod *et al.,* 2000). The NSI database contains comprehensive data on soils for over 6000 field sites located at 5 km intervals across England and Wales.

For the lowland arable soils, erosion data were available for 270 field sites over three years, therefore allowing the calculation of annual rates of soil loss (Appendix 1, Table 1.1). In the original survey erosion was assessed by measuring the length, width and average depth of rills and gullies on each site visit, thus enabling the volume of soil lost per hectare of field to be established. The rates recorded underestimate the true value because the methodology is not able to account for erosion by raindrop impact and shallow unchannelled overland flow. However, these types of erosion will deliver very small amounts of sediment to watercourses. The data are therefore a good indicator of erosion vulnerability.

Using the NSI database, each site was assigned to a soil series and thereby to a topsoil texture class (Table 2.1). Topsoil texture was determined for each soil series in the national soil survey completed in the early 1980s (McGrath and Loveland, 1992) based on the proportions of sand, silt and clay in the uppermost soil horizon. The relationship between topsoil texture class and vulnerability to soil erosion was based on Evans (1990a). Fine sandy soils are more vulnerable to erosion than loamy or clay soils. Lowland peaty and humose soils are least vulnerable because of their high organic content which improves structure and cohesion, precluding the formation of a surface cap or seal and thus reducing runoff and erosion (Harrod, personal communication). Those soil series falling within a calcareous soil subgroup were advanced to the next vulnerability class because of the greater aggregate stability conferred on topsoils by the presence of $CaCO_3$ (Harrod, 1998). Soil series information was not available for 37 of the 270 field sites where their location differed from the original NSI grid points because of obstruction or difficult access.

Each of the remaining 233 sites was assigned to a slope class (Table 2.2) derived from the Ordnance Survey 50 m Panorama elevation data. Mean annual erosion rates were calculated for each combination of topsoil texture and slope gradient (Table 2.3).

The results do not support the expected patterns. The mean annual erosion rate does not increase consistently with either increase in topsoil texture class or increase in gradient. Previous studies (Evans, 1998) have indicated that simple relationships between erosion and factors such as soil type and slope are frequently masked by the interaction with land cover. Whether or not erosion occurs will often depend on which crop is grown, the extent of the crop cover when the erosion event occurs and the direction and method of tillage. The patterns shown in Table 2.3 reflect, therefore, the association of certain soil-slope combinations with certain crop types. As such, the data provide useful indicators of erosion vulnerability and the risk of sediment delivery to water bodies.

Table 2.1 Vulnerability of lowland arable soils to soil erosion based on texture and calcareous nature of the topsoil (after Evans, 1990; Harrod, 1998)

Texture group	Top soil texture	Vulnerability
A	Fine sand	Very high
	Fine loamy sand	
	Fine sandy loam	
	Fine sandy silt loam	
	Silty loam	
B	Medium and coarse sandy loam	High
	Medium and coarse sandy silt loam	
	Medium and coarse loamy sand	
	Medium and coarse sand	
	Silty clay loam	
	Textures as in A but calcareous	
C	Clay loam	Moderate
	Sandy clay loam	
	Silty clay	
	Sandy clay	
	Clay	
	Textures as in B but calcareous	
D	Textures as in C but calcareous	Slight
E	Peaty and humose soils	Negligible

Table 2.2 Slope gradients proposed for assessment of vulnerability of lowland arable soils to soil erosion

Slope group	Slope range	
	original	modified
I	>11°	7 - 12°
II	7 - 11°	
III	3 - 6.99°	3 - 6°
IV	1 - 2.99°	<3°
V	<1°	

Table 2.3 Mean annual soil erosion (m^3 ha^{-1}) for lowland arable soils according to topsoil texture classes (A-E) and slope classes (I-V) (Harrod, 1998). Blanks represent classes for which no data exist.

	A	B	C	D	E
I	0.000	0.024	0.002	0.000	
II	0.000	0.043	0.081	0.002	0.000
III	0.038	0.376	0.062	0.036	0.000
IV	0.000	0.284	0.010	0.034	0.054
V	0.000	0.000		0.123	

A similar approach was used with data for upland soils. Topsoil texture was not suitable for classifying the vulnerability of upland soils because many upland soils, such as deep blanket peats, have no discernible topsoil horizon. Since previous work (McHugh, 2000) has shown that vulnerability to erosion is greater on wetter upland soils, the inherent hydrological status of the soil was used as an alternative to topsoil texture (Appendix 1, Table 1.2). The soils were assigned, therefore, to one of four classes based on the HOST classification (Boorman *et al.,* 1995; Table 2.4). Data on upland erosion were obtained from a DEFRA-funded project on the assessment of upland erosion (Project SP0402) in which observations were made at 426 field sites in 1999 (Appendix 1, Table 1.3). Mean erosion rates were determined for each combination of HOST class and slope gradient (Table 2.5).

Table 2.4 Classification of upland soils into HOST classes (Boorman *et al.*, 1995)

HOST group	HOST class	Description
A: permeable with high water storage capacity	3	Free draining permeable soils on soft sandstone substrates with relatively high permeability and high storage capacity
	4	Free draining permeable soils on hard but fissured rocks with high permeability but low to moderate storage capacity
	6	Free draining permeable soils in unconsolidated loams or clays with low permeability and storage capacity
B: low storage capacity, occasionally waterlogged	17	Relatively free draining soils with a large storage capacity over hard impermeable rocks with no storage capacity
	18	Slowly permeable soils with slight seasonal waterlogging and moderate storage capacity over slowly permeable substrates with negligible storage
	19	Relatively free draining soils with moderate storage capacity over hard impermeable rocks with no storage capacity
	21	Slowly permeable soils with slight seasonal waterlogging and low storage capacity over slowly permeable substrates with negligible storage capacity
	22	Relatively free draining soils with low storage capacity over hard impermeable rocks with no storage capacity
C: seasonally waterlogged by groundwater	10	Soils seasonally waterlogged by fluctuating groundwater and with relatively rapid lateral saturated conductivity
	24	Slowly permeable, seasonally waterlogged soils over slowly permeable substrates with negligible storage capacity
D: perennially waterlogged	12	Undrained lowland peaty soils waterlogged by groundwater
	15	Permanently wet, peaty topped upland soils over relatively free draining permeable rocks
	26	Permanently wet, peaty topped upland soils over slowly permeable substrates with negligible storage capacity
	27	Permanently wet, peaty topped upland soils over hard impermeable rocks with no storage capacity
	29	Permanently wet upland blanket peat

Table 2.5 Amounts of soil loss (m^3 ha^{-1}) for upland soils (Harrod *et al.*, 2000). Values relate to variable and unspecified time periods.

Slope	HOST group			
	A	B	C	D
0-3°	87.75	0.49	0.00	238.00
4-6°	0.00	0.00	193.00	402.00
7-12°	69.67	5.08	1.43	242.00
>12°	4.82	14.40	2.37	356.00

Unfortunately, the results indicate no obvious pattern in erosion vulnerability with either HOST class or increasing slope steepness. Since the HOST class is indicative of the level of runoff generation at a small catchment scale, it may not be an appropriate indicator of runoff and associated erosion potential on hillslopes. Further, since the assessments of erosion were carried out in only one year, it is not possible to determine over what period the erosion has occurred. Some of the very high values may relate to erosion over several hundreds, if not thousands, of years whereas other values may reflect recent erosion along footpaths or in response to grazing pressure. Consequently, the upland data are not comparable with those for lowland arable sites. Any assessments of erosion vulnerability in the uplands would therefore have to be treated separately from those of the lowlands and it would not be possible to produce a single consistent output of erosion risk for England and Wales.

An attempt was made to assess the data for erosion of soils under lowland grass based on the hydrological properties of the soils and the risk of poaching, as represented by HOST (Table 2.6). Observations were made on 135 field sites but instances and volumes of erosion were limited (Harrod, 1998; Appendix 1, Table 1.4). The results indicate that the relationship with HOST class is poor, reflecting the fact that whilst some erosion was attributed to restricted infiltration or soil saturation, livestock damage and land management practices were often more important factors (Harrod, 1998). Further, the data are also limited by being based on single site visits made in 1997.

Table 2.6 Vulnerability of lowland grassland soils to erosion based on HOST poach classes.

HOSTpoach class	HOST classes	Vulnerability
1	1 - 5	Slight
2	6 - 8, 11, 16 - 20, 22	Moderate
3	10, 14, 21, 23	High
4	9, 13, 24, 25	Very high
5	12, 15, 26 - 29	Extreme

It was therefore clear that the approach developed in Phase I for the lowland arable sites could not be extended to upland and lowland grassland soils. An alternative approach was therefore investigated.

2.2 Erosion probability

One reason for the failure to obtain the expected relationships between erosion and either soil type or slope steepness is that such relationships are usually obtained from experimental studies in which other influencing factors, such as climate, are in some way controlled. For example, field studies often relate to different crop types or slopes

at a given location so that, although climatic events may vary over time, all treatments receive the same sequence of events. The erosion data used here for the lowland arable sites relate to individual events in different parts of England and Wales in different years and at different times in each year. They are therefore best considered as a database of random events in which the probability of erosion occurring depends on the severity of the climatic event, the extent and type of crop cover and the resistance of the soil at that time. Such data are amenable to an analysis to determine the probability of an erosion event of a given magnitude occurring.

The erosion data were therefore re-analysed to determine the probability of erosion of a given magnitude occurring for given soil-slope combinations. In order to ensure a uniform approach across lowland arable, upland and lowland grassland soils, topsoil texture and HOST class were replaced as soil descriptors by soil type. It was hoped, initially, to use soil series but, despite the database being the most comprehensive available on soil erosion in England and Wales and far more comprehensive than that which exists for many other countries, the number of observations occurring on most soil series was too small for analysis. The same was true for the soil association level. Data were therefore analysed at the subgroup level (Avery, 1980). In some cases it was necessary to combine subgroups and analyse data at the soil group level.

Each site was assigned to one of the following slope classes, defined to the nearest degree: 0-2°, 3-6°, 7-12°, 13-18° and >18°. The boundary at 3° was chosen because it represents the critical angle at which, for many soils in northern Europe, rill erosion begins (De Ploey, 1984). The boundary at 7° represents the upper limit of land considered suitable for arable farming in many land capability classifications (Hudson, 1981) and is the upper limit of land in the highest capability class in the UK (Bibby and Mackney, 1969). The 12° boundary was selected as that in the uplands at which erosion was found to decrease significantly compared with that on lower slopes (McHugh, 2000). It is also the upper limit at which ploughing can be carried out safely using standard equipment. The 18° boundary is the angle at which land is generally classed as steep (Young, 1972). For some soil subgroups it was necessary to group slope classes together either because the number of observations in a given slope class was very small or because there was no difference in the frequency of erosion between slope classes.

For each combination of soil subgroup and slope class, frequency histograms were produced showing the number of instances of erosion of different magnitudes. Figure 2.1 shows two examples from the lowland arable data set. As expected (Boardman, 1990; Evans, 1998), these show that the volumes of soil eroded are strongly negatively skewed. Such a skewed dataset in which the possibilities in one direction are limited by zero values and in the other direction by magnitude approximates a Poisson distribution which, in such cases, provides a better basis than the normal distribution for estimating the probability of rare events with a low probability of occurrence. The Poisson distribution is associated with events which occur singly and at random in a given interval of time or space and where the mean number of occurrences (λ) in a given interval is known and finite, so that:

$$P(X = x) = e^{-\lambda} \frac{\lambda^x}{x!} \text{ for } x = 0,1,2,3, \ldots \text{.to infinity} \qquad (2.1)$$

where X is the number of occurrences in the given interval. Table 2.7 gives the cumulative probability values of erosion for each magnitude class for the two data sets illustrated in Figure 2.1. From these, it is possible to estimate the magnitude of erosion that will occur for given levels of probability. Table 2.8 shows the values for p = 0.99, p = 0.995 and p = 0.999. By adopting the ergodic principle of statistical mechanics, spatial probabilities can be used to approximate temporal probabilities (Scheidegger and Langbein, 1966). This approach is based on the assumption that "in a steady state, the ensemble of all possible configurations of the system at a given time is identical to the ensemble obtained by watching the system evolve through all times $t_1, t_2 \ldots t_i$" (Scheidegger, 1970) and that, in geographical and geomorphological situations, 'ensembles' can be "replaced by sets of spatial points or areas" (Paine, 1985). In which case, these probabilities obtained from spatial data sets can be used as surrogates for the probability of events occurring over time. Events with annual probabilities of 0.99, 0.998 and 0.999 correspond to events with respective recurrence intervals of once in 1, 5 and 10 years.

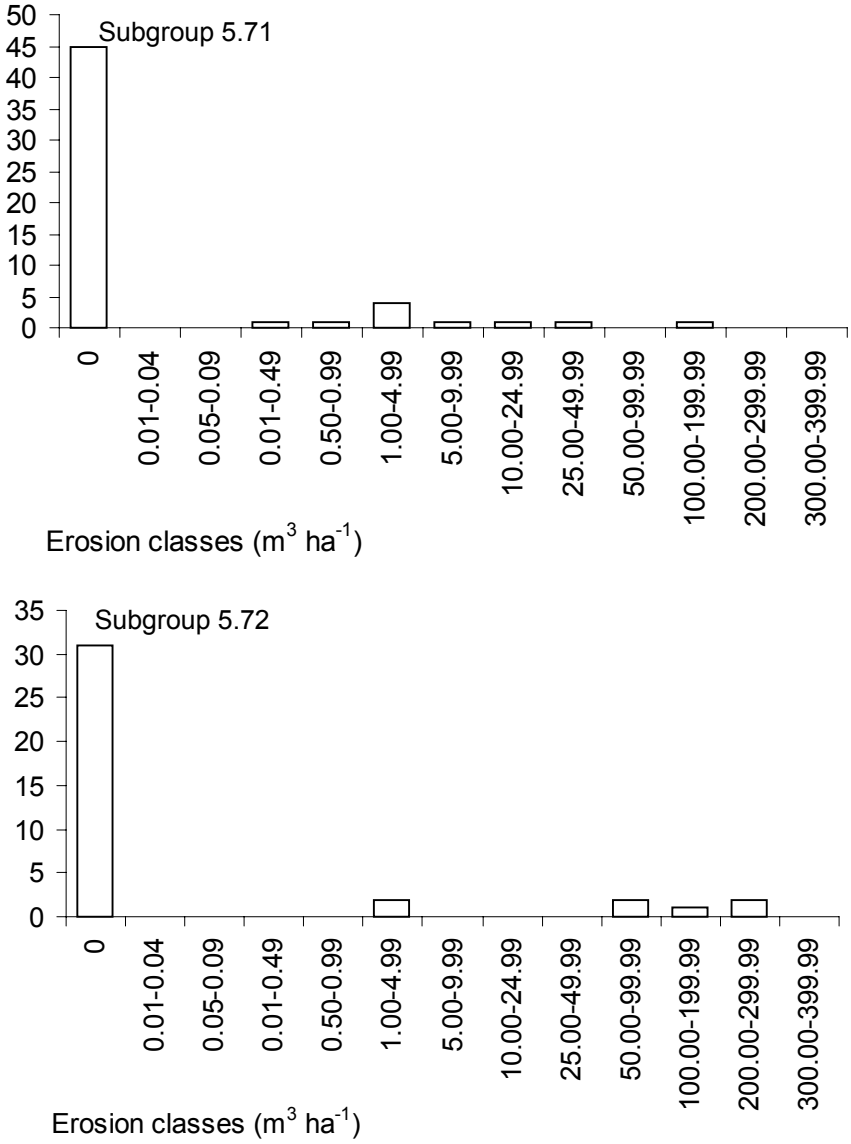

Figure 2.1 Frequency of erosion classes for soil subgroups 5.71 and 5.72 under lowland arable on slopes ≥ 3°.

Table 2.7 Cumulative probability distributions based on Poisson distribution for selected soil subgroups under lowland arable.

(a) Subgroup 5.71 - slopes ≥3° (λ = 1.0546)

Erosion class	Cumulative probability
0	0.348351
0.01-0.05	0.715702
0.05-0.09	0.909397
0.10-0.49	0.977483
0.50-0.99	0.995434
1.00-4.99	0.999219
5.00-9.99	0.999885
10.00-24.99	0.999985
25.00-49.99	0.999998

(b) Subgroup 5.72 - slopes ≥3° (λ = 1.57895)

Erosion Class	Cumulative probability
0	0.206192
0.01-0.05	0.531758
0.05-0.09	0.788784
0.10-0.49	0.924061
0.50-0.99	0.977460
1.00-4.99	0.994323
5.00-9.99	0.998760
10.00-24.99	0.999761
25.00-49.99	0.999959
50.00-99.99	0.999994
100.00-100.99	0.999999

2.2.1 Erosion risk on lowland arable soils

The annual erosion expected with given probabilities or return periods was determined for lowland arable soils from the same dataset used to produce Table 2.3, namely observations made at 270 NSI field sites visited over a period of three years (Harrod, 1998). The data indicate that 16 soil subgroups experienced soil erosion in the period 1997-1999. Table 2.8 gives the probabilities of erosion.

Overall, the brown earths are the major soil group with the highest vulnerability, which is in line with previous studies. The Soil Survey of England and Wales (1983) recognised soils in subgroups 5.41 (typical brown earths), 5.51 (typical brown sands), 5.54 (argillic brown sands) and 5.71 (typical argillic brown earths) as having a risk of water erosion. It is not surprising that these subgroups figure strongly in the dataset with 140 observations for 5.41, 46 for 5.51, 5.52 and 5.54 combined, and 87 observations for 5.71. In the 1997-1999 survey, there were 68 observations on subgroup 5.72 (stagnogleyic argillic brown earths) with two occurrences >100 m^3 ha^{-1}. The probabilities of erosion may be overestimated for typical paleo-argillic brown earths (5.81), colluvial brown earths (5.47) and stagnogleyic brown calcareous earths (5.13) where, in each case, two instances were recorded in data sets of ≤15 observations.

Table 2.8 Estimated annual soil erosion (m^3 ha^{-1}) for lowland arable soils with given return periods.

(a) 1-in-1 year

Soil Group	Slope		
	0-2°	3-6°	≥7°
3.43	0.00	0.00	0.00
4.11	0.00	0.07	0.07
5.11	0.00	0.02	0.02
5.13	0.06	0.06	0.06
5.41+5.47	0.04	0.09	0.07
5.51, 5.52, 5.54	0.00	0.19	0.19
5.71	0.04	0.38	0.38
5.72	0.05	0.87	0.87
5.81	0.18	0.18	0.18
7.11, 7.12, 7.13	0.02	0.07	0.07
8.31	0.05	0.05	0.05

(b) 1 in 5 years

Soil Group	Slope		
	0-2°	3-6°	≥7°
3.43	0.00	0.00	0.03
4.11	0.00	0.10	0.10
5.11	0.00	0.05	0.05
5.13	0.10	0.10	0.10
5.41+5.47	0.30	0.42	0.10
5.51, 5.52, 5.54	0.00	0.53	0.53
5.71	0.06	0.84	0.84
5.72	0.09	4.29	4.29
5.81	0.50	0.50	0.50
7.11, 7.12, 7.13	0.05	0.10	0.10
8.31	0.10	0.10	0.10

(c) 1-in-10 years

Soil Group	Slope		
	0-2°	3-6°	≥7°
3.43	0.00	0.00	0.05
4.11	0.00	0.50	0.50
5.11	0.00	0.05	0.05
5.13	0.50	0.50	0.50
5.41+5.47	0.42	0.49	0.50
5.47	0.00	4.00	4.00
5.51, 5.52, 5.54	0.00	0.81	0.81
5.71	0.08	0.97	0.97
5.72	0.10	6.00	6.00
5.81	0.79	0.79	0.79
7.11, 7.12, 7.13	0.05	0.32	0.32
8.31	0.14	0.14	0.14

2.2.2 Erosion risk on upland soils

As a supplement to the dataset on upland soils used to produce Table 2.5, some 206 eroded upland field sites were revisited in 2001 and further measurements of erosion made. These enabled the amount of upland soil erosion between 1999 and 2001 (actually 2.5 years) to be determined (McHugh, 2002). The two datasets were

combined to calculate the probabilities of erosion. The original dataset was used to determine the number of sites in each soil subgroup without erosion. The second dataset gave information on the eroded sites. In order to estimate annual erosion, the measured volumes of soil loss were divided by 2.5.

Table 2.9 gives the calculated probabilities of erosion on the upland soils. As expected (Bower, 1962; Evans, 1990b; Phillips *et al.,*1981; Tallis, 1987), peat soils (subgroups 10.11 - raw oligo-fibrous peat soils; 10.13 - raw oligo-amorphous peat soils) are the most at risk. The most vulnerable mineral soils are the podzolics (Major Group 6), particularly the wetter stagnopodzols (group 6.5).

Table 2.9 Estimated annual soil erosion (m^3 ha^{-1}) for upland soils with given return periods.

(a) 1-in-1 year

Soil Group	Slope	
	≤12°	>12°
3.11	0.02	0.02
5.41	0.03	0.03
6.11, 6.12, 6.21, 6.22, 6.31, 6.32, 6.42, 6.43, 6.51, 6.52, 6.54	0.04	0.06
7.21	0.01	0.01
10.11, 10.13	0.07	0.09

(b) 1 in 5 years

Soil Group	Slope	
	≤12°	>12°
3.11	0·04	0·04
5.41	0.04	0.04
6.11, 6.12, 6.21, 6.22, 6.31, 6.32, 6.42, 6.43, 6.51, 6.52, 6.54	0.16	0.20
7.21	0.02	0.02
10.11, 10.13	0.36	0.39

(c) 1-in-10 years

Soil Group	Slope	
	≤12°	>12°
3.11	0.09	0.09
5.41	0.12	0.12
6.11, 6.12, 6.21, 6.22, 6.31, 6.32, 6.42, 6.43, 6.51, 6.52, 6.54	0.19	0.31
7.21	0.03	0.03
10.11, 10.13	0.40	1.20

2.2.3 Erosion risk on lowland grassland soils

The dataset used to produce Table 2.6 was the only one available for assessment of erosion on lowland grassland soils, which is most commonly associated with either heavily-grazed permanent pasture or short-term rotational grass or leys (Heathwaite *et al.,* 1990a; 1990b). Ley grass is commonly resown every 7 to 10 years and any erosion usually occurs in the time between when the land is prepared for resowing and when grass cover has become established. For both heavily-grazed land and rotational grass, it is reasonable to assume that any erosion observed in the field has occurred

some time within the previous 1 to 4 years. In order to provide a temporal resolution to the data, the measured values of soil loss are divided by 3. Table 2.10 gives the erosion probabilities for soils under lowland grassland.

Table 2.10 Estimated annual soil erosion (m^3 ha^{-1}) for lowland grassland soils with given return periods.

(a) 1-in-1 year

Soil Group	Slope		
	0-2°	3-6°	≥7°
5.41	0.00	0.03	0.03
5.72	0.01	0.01	0.01
7.13	0.08	0.08	0.08

(b) 1 in 5 years

Soil Group	Slope		
	0-2°	3-6°	≥7°
5.41	0.00	0.17	0.17
5.72	0.03	0.03	0.03
7.13	0.20	0.20	0.20

(c) 1-in-10 years

Soil Group	Slope		
	0-2°	3-6°	≥7°
5.41	0.00	0.19	0.19
5.72	0.03	0.03	0.03
7.13	0.28	0.28	0.28

2.3 General comments

The following general points should be made about the data in Tables 2.8, 2.9 and 2.10, which provide the data for estimating annual hillslope erosion.

1) The dataset from which the erosion rates are derived is the most comprehensive available for England and Wales and is larger than that available for most other countries.
2) Probability analysis enables comparable data to be obtained on erosion rates for lowland arable, upland and lowland grassland soils. It is thus an improvement on the original methodology which was based on calculations of erosion rates for variable time periods.
3) The analysis is based on the assumption that spatial probabilities can be used to approximate temporal probabilities.
4) The risk of erosion changes with land use in the order of lowland arable > lowland grass > upland. With regard to the delivery of sediment to watercourses, the lower rates of erosion on upland soils may be offset by the steeper slopes, which will increase the proportion of eroded sediment discharging into rivers and reservoirs.
5) The probability of erosion may be overestimated for soil subgroups 5.13, 5.47 and 5.81.
6) Erosion rates are likely to be underestimates because the methodology used to measure soil loss did not account for erosion rainsplash and shallow unchannelled flow.

7) The probabilities of erosion reflect instances of erosion under the combinations of soil, slope and land cover at the time of survey. Thus vulnerability of the upland soils relates to vegetation covers of bracken, moorland grasses, heathland or bog. The data cannot therefore be used to estimate the erosion that would occur if the area under arable cultivation or rotational grass was extended onto upland soils. Tables 2.11a and 2.11b show the vulnerability to erosion of all the soil subgroups for which data were available for this study.

Table 2.11a Vulnerability of soil subgroups (3.11 to 5.83) to erosion under different land uses. Shading denotes vulnerable soils; n/a = conditions do not exist in surveyed data.

Soil subgroup		Lowland arable	Lowland grassland	Uplands
3.11	Humic rankers	n/a	n/a	
3.13	Brown rankers		n/a	
3.41	Humic rendzinas		n/a	n/a
3.42	Grey rendzinas			n/a
3.43	Brown rendzinas			n/a
4.11	Typical calcareous pelosols			n/a
4.31	Typical argillic pelosols	n/a		n/a
5.11	Typical brown calcareous earths			n/a
5.12	Gleyic brown calcareous earths		n/a	n/a
5.13	Stagnogleyic brown calcareous earths		n/a	n/a
5.14	Colluvial brown calcareous earths		n/a	n/a
5.21	Typical brown calcareous sands		n/a	n/a
5.32	Gleyic brown calcareous alluvial soils		n/a	n/a
5.41	Typical brown earths			
5.42	Stagnogleyic brown earths			
5.43	Gleyic brown earths		n/a	n/a
5.44	Ferritic brown earths		n/a	n/a
5.45	Stagnogleyic ferritic brown earths		n/a	n/a
5.47	Colluvial brown soils		n/a	
5.51	Typical brown sands			n/a
5.52	Gleyic brown sands		n/a	n/a
5.54	Argillic brown sands		n/a	n/a
5.61	Typical brown alluvial soils		n/a	n/a
5.71	Typical argillic brown earths			n/a
5.72	Stagnogleyic argillic brown earths			n/a
5.73	Gleyic argillic brown earths		n/a	n/a
5.81	Typical paleo-argillic brown earths			n/a
5.82	Stagnogleyic paleo-argillic brown earths		n/a	n/a
5.83	Gleyic paleo-argillic brown earths		n/a	n/a

Table 2.21b Vulnerability of soil subgroups (6.11 to 10.13) to erosion under different land uses. Shading denotes vulnerable soils; n/a = conditions do not exist in surveyed data.

Soil subgroup		Lowland arable	Lowland grassland	Uplands
6.11	Typical brown podzolic soils			
6.12	Humic brown podzolic soils	n/a	n/a	
6.21	Typical humic cryptopodzols	n/a	n/a	
6.22	Ferri-humic cryptopodzols	n/a	n/a	
6.31	Humo-ferric podzols		n/a	
6.32	Humus podzols	n/a	n/a	
6.42	Humo-ferric gley-podzols		n/a	
6.43	Stagnogley podzols	n/a	n/a	
6.51	Ironpan stagnopodzols	n/a	n/a	
6.52	Humus-ironpan stagnopodzols	n/a	n/a	
6.54	Ferric stagnopodzols	n/a	n/a	
7.11	Typical stagnogley soils			n/a
7.12	Pelo-stagnogley soils			n/a
7.13	Cambic stagnogley soils			
7.15	Sandy stagnogley soils		n/a	
7.21	Cambic stagnohumic gley soils	n/a	n/a	
8.11	Typical alluvial gley soils			n/a
8.12	Calcareous alluvial gley soils			n/a
8.13	Pelo-alluvial gley soils			n/a
8.14	Pelo-calcareous alluvial gley soils	n/a		n/a
8.21	Typical sandy gley soils			n/a
8.31	Typical cambic gley soils			n/a
8.41	Typical argillic gley soils		n/a	n/a
8.51	Typical humic-alluvial gley soils	n/a		n/a
8.52	Calcareous humic-alluvial gley soils		n/a	n/a
8.71	Typical humic gley soils	n/a	n/a	
10.11	Raw oligo-fibrous peat soils	n/a	n/a	
10.13	Raw oligo-amorphous peat soils	n/a	n/a	

3. ASSESSMENT AND CHARACTERISATION OF SLOPE-CHANNEL CONNECTIVITY

3.1 Introduction, aims and objectives

Working as part of the collaborative research team assembled for the project, the work of the group based at the Department of Geography of the University of Exeter focused on characterising the efficiency of sediment delivery or transfer from the land surface to watercourses. The efficiency of sediment delivery directly reflects the connectivity between the land surface and the river system and two measures of this connectivity have been developed. The first, which has been termed the ***connectivity index,*** is essentially *qualitative* and represents the *relative* efficiency of sediment transfer. Values for the index range between 0 and 1, with a value close to 1 indicating very high connectivity and a value close to 0 very low connectivity. The second measure is based directly on the connectivity index and represents a simple scaling of that index to provide a more specific *quantitative* measure of the efficiency of sediment transfer, namely the *fraction* of the sediment eroded or mobilised from the land surface that reaches the stream network (i.e. >0 - <1). This derivative of the connectivity index has been termed the ***connectivity ratio***. It is analogous to the sediment delivery ratio, that is widely used in studies of sediment yield from catchments and which represents the proportion of the gross erosion within the catchment that reaches the catchment outlet as the sediment yield. The two are, nevertheless, different in that the connectivity ratio expresses the proportion of the gross or on-site erosion from the slopes of a catchment that reaches the stream network, whereas the sediment delivery ratio expresses the proportion of the gross erosion within the catchment that reaches the catchment outlet. The sediment delivery ratio must therefore, also take account of deposition of sediment as it passes through the channel and floodplain system. For a given catchment the value for the connectivity ratio, will be greater than that for the sediment delivery ratio, since the latter will involve further conveyance losses within the channel and floodplain system. In addition, the connectivity ratio can be applied to a small area of the catchment surface (e.g. a grid cell), whereas the sediment delivery ratio is applicable only to a complete catchment. If estimates of the gross or on-site erosion rate (t ha^{-1} $year^{-1}$) associated with the surface or slopes of a catchment are available, these estimates can be multiplied by the connectivity ratio to provide a quantitative estimate of the sediment input to the stream network from the land surface (t ha^{-1} $year^{-1}$).

In undertaking the task of developing these measures of slope-channel connectivity, the following objectives were identified and addressed:

1) To review existing understanding of the controls on sediment delivery efficiency, with particular reference to arable land, in order to establish the key variables and parameters to be used in deriving the connectivity index.
2) To formulate a connectivity index which provides a measure of the relative efficiency of sediment transfer from the land surface to watercourses.
3) To provide relevant algorithms and tools for estimating the connectivity index from existing datasets.
4) To produce a dataset providing national scale coverage of values of the connectivity index.
5) To develop a procedure for calibrating the connectivity index to provide values of the connectivity ratio.

6) To produce a dataset providing national scale coverage of values of the connectivity ratio.

A number of basic requirements for the connectivity index and connectivity ratio were also established. These were as follows:

1) They should have a raster-based spatial data structure to be compatible with existing data sets. A national coverage at a spatial resolution of a 1 km x 1 km grid was required.
2) They should represent the delivery of sediment from the land surface or slopes to well defined drainage channels by surface runoff. Transfer of sediment by drain flow, additional inputs of sediment to the stream network from bank erosion, in-stream sediment storage, and deposition of sediment in ponds and reservoirs are not considered.
3) No attempt should be made to represent the temporal variability of slope-channel connectivity according to event magnitude or season. The values obtained for the index should represent lumped mean annual values.
4) The connectivity index should reflect the transfer of sediment from the land surface within a cell to watercourses in the cell or adjacent to the cell. It should provide a measure of the relative efficiency of sediment transfer and be expressed as a ratio value between 0 and 1.
5) It should be possible to scale the values of the connectivity index to produce a value for the connectivity ratio, which represents the fraction of the sediment eroded or mobilised from the land surface within the 1 km grid cell that reaches the watercourses in the cell or adjacent to the cell. The product of the connectivity ratio and an estimate of the gross or on-site soil loss within the grid cell should provide an estimate of the sediment contribution from the land surface within the grid cell to the stream network.
6) The resulting connectivity index and connectivity ratio datasets are intended to be used primarily as tools to inform national and regional scale sediment-related risk assessment.

3.2. Identification of factors that control the efficiency of sediment delivery from hillslopes to watercourses

A literature overview was undertaken to explore the concept of spatially explicit sediment delivery (SESD), to review the various measures for representing the efficiency of sediment delivery that are currently in use and to identify the factors that control the efficiency of sediment delivery and should therefore be taken into account by the procedure used to derive the connectivity index.

The diversity of existing approaches to representing sediment delivery efficiency (Appendix 2.2) and the uncertainties associated with these procedures largely reflect our limited understanding of sediment delivery processes, which represent a complex dynamic system characterised by a high degree of both temporal and spatial variability. The paucity of distributed datasets relating to terrain attributes also plays an important role in limiting the scope of existing SESD models. Nevertheless, some significant progress has been made in the development of the SESD concept, including the use of spatially distributed elevation data, the integration of SESD modelling with DEM based terrain analysis, and improvements in the representation of the transport capacity of surface runoff. The wider application of such models has,

however, been restricted by the underlying local variability, embedded empirical relationships, and, in some cases, arbitrary specification of parameters etc. As with most models, further calibration, validation and adjustment are necessary for any application outside the original environment.

Existing understanding indicates that the efficiency of sediment delivery from the land to watercourses is governed by three primary controls, namely, the transport capacity of surface runoff, the spatial distribution and density of the receiving watercourses, and the characteristics of the mobilised sediment. These primary controls can be represented by six factors, which should be incorporated into the algorithm used for deriving the connectivity index. The six factors are

1) A runoff potential factor
2) A slope steepness factor
3) A slope shape factor
4) A drainage pattern factor
5) A land use factor
6) A sediment characteristics factor

3.3 Parameterisation of the controlling factors

3.3.1 Selection and generation of relevant spatial datasets

As with any distributed modelling, the parameterisation of the controlling factors involves the acquisition, processing and integration of large amounts of spatial data and will therefore depend heavily on the availability of appropriate data sets. Following consultation with the project manager, the following spatial data sets were selected as base data layers:

1) A 50 m spatial resolution DEM (Ordnance survey)
2) Land cover data set for 1990 at a spatial resolution of 25 m, where land use has been grouped into 25 categories (CEH LCM, 1990)
3) Hydrological effective rainfall (HER) data derived from the ADAS MAGPIE database at a spatial resolution of 1 km
4) A 1: 50 000 river network coverage (CEH Wallingford)
5) 1 km grid soil data based on the 1: 250 000 map for England and Wales (NSRI), including texture and HOST classification from which storm runoff potential (the Standard Percentage Runoff, SPR) can be derived.

The cell-based modelling function from the GRID module of Arc/Info GIS was used to generate secondary data layers, to integrate different data layers, and to up-scale data to the required spatial resolution (1 km grid cells). Relevant functions will be referred to where appropriate in the following discussion. Several AML (Arc/Info Macro Language) routines were developed to facilitate data manipulation (Appendix 2.3).

3.3.2 Derivation of individual factors

The parameterisation of the controlling factors was constrained by the availability of relevant national datasets, and was based on established theoretical functions, empirical relationships, as well as expert judgement.

The slope steepness factor: The slope steepness factor is represented as $S^{1.4}$, where S is the sine of slope gradient. It can be calculated from a DEM using the 'slope' or 'curvature' functions available within the GRID module of Arc/Info GIS. The exponent (1.4) is based on the generally accepted relationship between overland flow transport capacity and slope gradient (cf. Prosser and Rustomji, 2000). To take account of the variability of the slope gradient within a 1 km cell, derivation of the slope steepness factor was based on a 50 m sub-grid. Values of slope gradient were derived for the individual 50 m grid cells and focal functions within the GRID module, including 'focalsum' and 'focalmajority' were employed to derive the slope gradient for the overall 1 km grid.

The slope shape factor: It is generally accepted that a surface with a convex profile is more efficient in terms of sediment delivery, because transport capacity increases downslope. In contrast, concave surfaces are commonly associated with deposition. A 50 m sub-grid was superimposed onto the DEM and the slope profile shape within each 50 m grid cell was characterised as either dominantly convex or dominantly concave. The proportion of convex elements (cells) within a 1 km grid square was used to represent the effect of slope shape on sediment delivery and to derive the slope shape factor. This involved use of the 'curvature', 'focalsum', and 'resample' functions of the GRID module.

The runoff potential factor: Surface runoff is the ultimate driver of sediment transfer. Its magnitude depends primarily on rainfall characteristics, surface condition, and soil properties. Two existing spatial data sets were combined to represent the potential for surface runoff generation, namely the hydrologically effective rainfall (HER) and the HOST soil classification. The latter is based on a number of conceptual models that describe the dominant pathways of water movement through the soil and, where appropriate, the substrate (Boorman *et al.,* 1995). As part of the HOST classification, there is an empirically derived base flow index (BFI) dataset from which the standard percentage runoff (SPR) can be estimated using established relationships (Boorman *et al.,* 1995). The estimated SPR for each 1 km grid cell is combined with the value of HER for the cell, in order to calculate the runoff potential factor using the following expression:

$$\text{Runoff potential factor} = (HER * SPR / 100)^{1.4} \qquad (3.1)$$

The exponent 1.4 conforms to the generally accepted relationship between sediment transport by surface runoff and runoff amount.

The drainage pattern factor: The drainage pattern reflects the spatial distribution and density of the drainage system. It has a direct effect on transfer distance. Although drainage density (km km^{-2}) is widely used to represent the drainage pattern, it only takes account of the total length of the drainage network within a cell and not its spatial configuration. An improved index is proposed. It is based on the integration of the higher resolution sub-grid (50 m) and the river network coverage (1: 50 000). The average distance (median value) from all land cells (50m) within a 1 km grid cell to the nearest river (D) is used to characterise the effects of drainage pattern on sediment delivery processes. An exponential decay relationship is used to derive the drainage pattern factor viz.

$$\text{Drainage pattern factor} = e^{-1 * k * D} \tag{3.2}$$

where k is a scaling constant depending on the units used. To avoid extreme values, k should be set to a value less than 3 / D_{max} where D_{max} is the maximum value of D expected.

The sediment characteristics factor: Sediment delivery is a size selective process. Fine particles are likely to be more easily transported and are therefore less prone to deposition. The particle size composition of an eroding soil can therefore be expected to exert a significant control on sediment delivery efficiency. Since most mobilised sediment results from interrill and rill erosion processes, the texture of the surface horizon is most relevant. A derived parameter, the d_{50} or median grain size, is frequently used to characterise the sediment size distribution in flume experiments (Govers, 1985) and this has also been incorporated into sediment transport equations for overland flow (Meyer and Monke, 1965; Everaert, 1991). It is an indicative particle size based on the cumulative size distribution curve.

Faced with a lack of detailed soil texture data, an estimate of d_{50} for the surface horizon was derived from available data on percentages of sand and silt. The relationship between cumulative mass coarser and particle size defined in φ-units was approximated using a second-order polynomial function viz:

$$y = a * x^2 + b * x + c \tag{3.3}$$

where y is the cumulative percent coarser by weight and x is the particle size.

For incorporation into the prediction model, the sediment characteristics factor was calculated as $d_{50}{}^{-0.5}$. The exponent of *–0.5* is used to account for the non-linear relationship between particle size and overland flow sediment transport capacity (Meyer and Monke, 1965; Everaert, 1991).

The land use factor: Land use is a highly dynamic factor. While land use can have a wide range of effects on environmental systems, surface roughness effects are likely to exert the key influence on the efficiency of sediment transfer. The surface roughness associated with a specific land use can be characterised by the Manning's roughness parameter (n). The parameter $n^{-0.6}$ has been used as the land use factor, where n is the Manning's surface roughness value and the exponent (0.6) is based on its commonly accepted relationship with overland flow transport capacity (cf. Moore and Burch, 1986). The land use data have been derived from the 1 km CEH land cover data set, based on dominant land use in the grid cell and a Manning's n data layer has been created using a look up table (Appendix 2.4). The specification of the Manning's n for each land use category was based on the documentation for several physically-based soil erosion and water quality models.

The relevant data layers were processed using the algorithms and the AML routines. As an example, the calculated average distance to watercourses is shown in Figure 3.1 (Maps of the other spatial datasets are provided in Appendix 2.1).

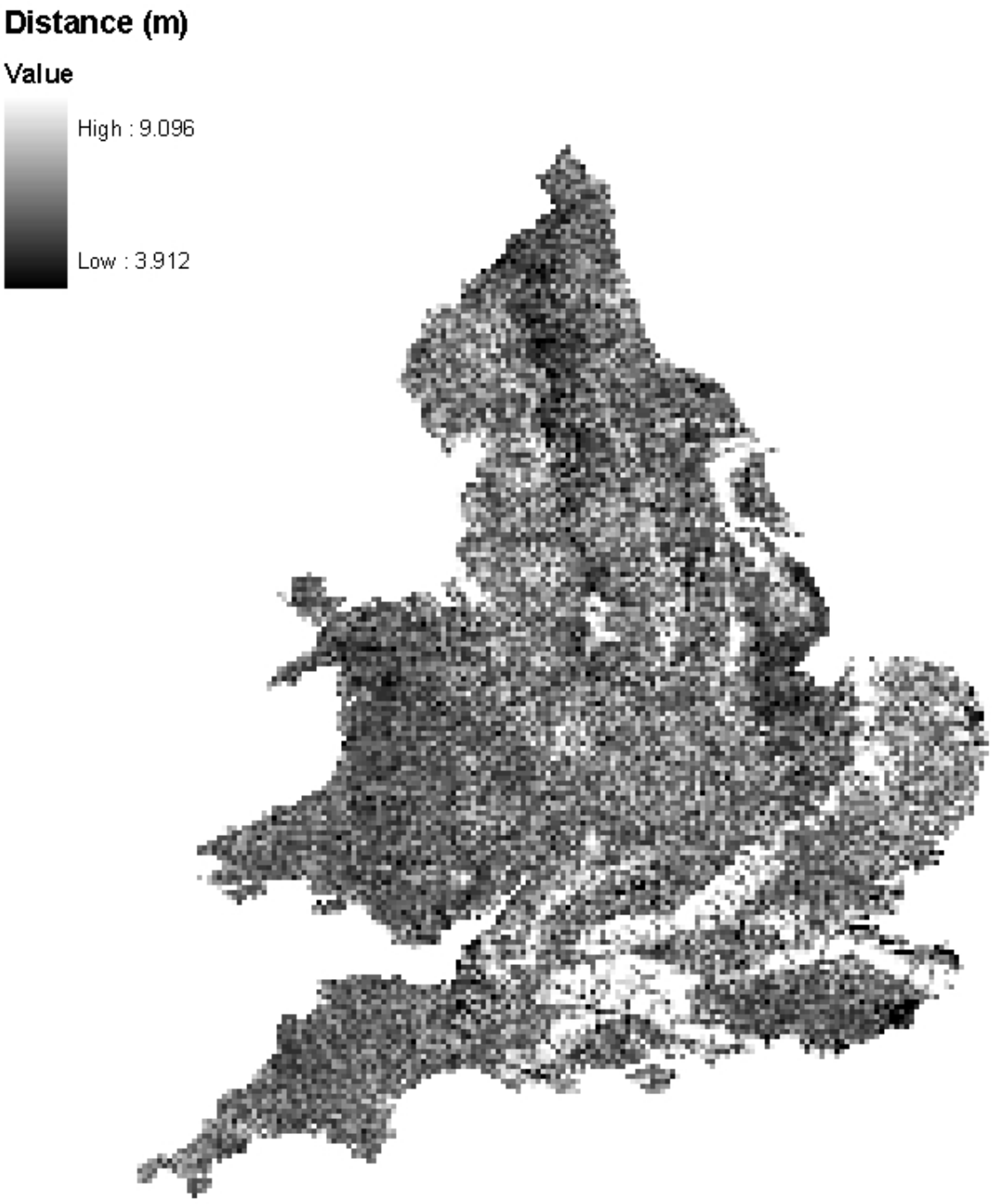

Figure 3.1. The spatial distribution of the average distance to watercourse after log transformation. The value for each 1 km grid cell represents the median value for the individual 50m subgrid cells. Based on the CEH 1: 50 000 river network.

3.4 Derivation of the connectivity index

In order to derive the final connectivity index, it is necessary to combine the values obtained for the six controlling factors into a single index. The process complexity associated with the temporal and spatial scales involved means that it is not possible to formulate a physically-based index that incorporates the influence of all the controlling factors identified. Instead, a conceptual formulation using a structure analogous to that employed by the Revised Universal Soil Loss Equation (cf. Renard *et al.*, 1991) has been employed.

The connectivity index (*CI*) is seen to be a function of the sediment transport capacity modified by slope shape and drainage pattern, with the effects of slope shape and drainage pattern being treated as multiplicative viz.

$$CI = f(TC * f_{sp} * f_{dp}) \tag{3.4}$$

where *TC* is the sediment transport capacity, f_{sp} is the slope shape factor, and f_{dp} is the drainage pattern factor. Although a positive relationship between the connectivity index and the modified sediment transport capacity is expected, the exact form of the functions embedded in Equation 3.4 should be calibrated, if possible, using empirical data. In the absence of empirical data to permit calibration, a simple logarithmic function has been assumed. Therefore, *CI* can be defined as follows:

$$CI = \log (f_{sp} * f_{dp} * TC) \tag{3.5}$$

where the log-transformation was employed to avoid potential distortion associated with the non-normal distribution of the spatial data sets.
To take account of the different magnitudes of the values obtained for the slope shape and drainage pattern factors, these values were scaled to a value between 0 and 1 using a simple linear stretch routine as represented by the following expression:

$$y = \frac{x - x_{\min}}{x_{\max} - x_{\min}} (x'_{\max} - x'_{\min}) + x'_{\min} \tag{3.6}$$

where y and x are the converted and original values, respectively; x_{max} and x_{min} are the maximum and minimum values of the original data set; and x_{max}' and x_{min}' are the maximum and minimum values of the derived range (i.e. 1 and 0).

The sediment transport capacity parameter *TC* incorporates the influence of surface runoff magnitude, slope gradient, surface roughness and sediment size. These variables can be represented by the generated runoff potential factor, the slope gradient factor, the land use factor and the sediment characteristics factor, respectively. The *TC* parameter can therefore be calculated as follows:

$$\begin{aligned} TC &= q^{1.4}\ S^{1.4}\ n^{-0.6}\ d_{50}{}^{-0.5} \\ &= runoff\ potential\ factor * slope\ gradient\ factor * land\ use\ factor \\ &\quad * sediment\ characteristic\ factor \end{aligned} \tag{3.7}$$

The resulting values of TC are shown in Figure 3.2. They were then combined with the scaled drainage pattern and slope shape factors to calculate CI. Finally, equation 3.6 was used to scale the final values CI within a pre-defined range (from 0 to1). The resulting values of CI are shown in Figure 3.3.

The connectivity index as defined by Equations 3.4, 3.5, and 3.7 incorporates a simplified representation of the key interactions among the controlling factors. The calculation of sediment transport capacity is based on established relationships for steady runoff on linear slopes obtained from laboratory experiments and field studies. Their use in this project is thought to be acceptable, since the final product is expressed as a dimensionless value between 0 and 1. As there are few documented relationships between sediment delivery and slope shape or drainage pattern, there is clearly more potential for improving their characterisation.

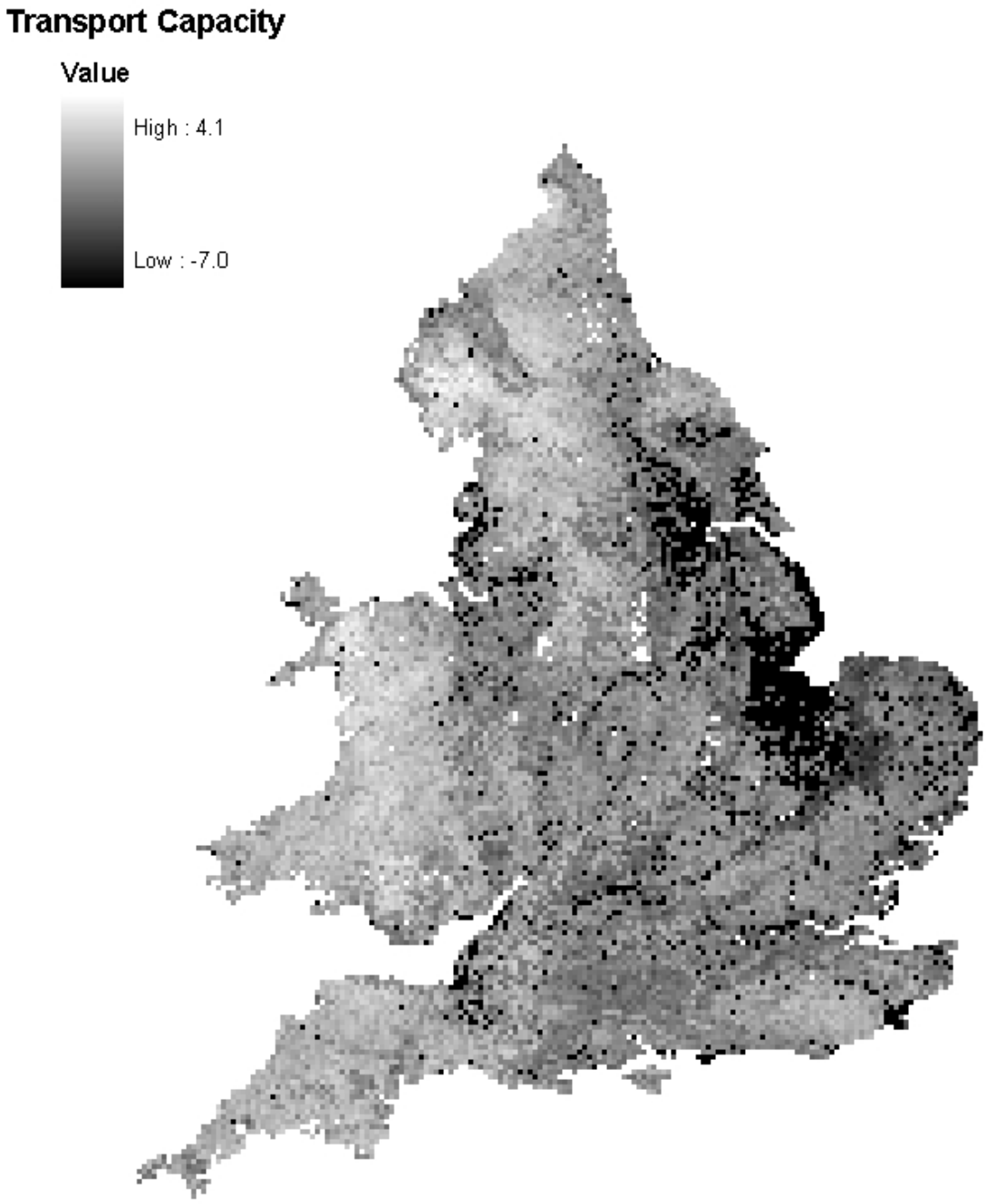

Figure 3.2 The spatial distribution of the sediment transport capacity of overland flow (log transformed).

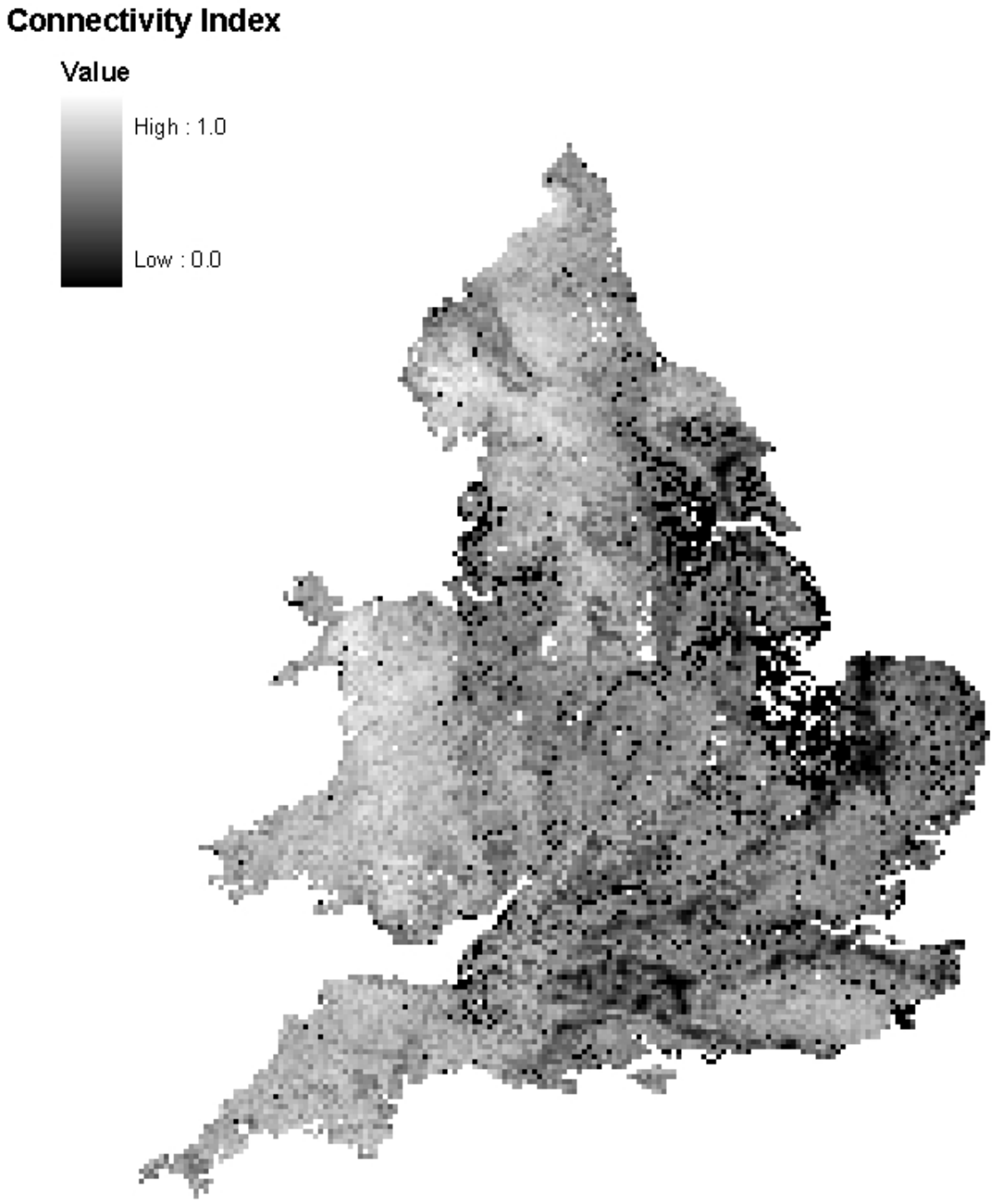

Figure 3.3. The spatial distribution of the connectivity index.

In order to provide some limited qualitative validation of the values of CI presented in Figure 3.3, cells representative of areas of arable land use in small catchments for which some evidence of the relative efficiency of sediment delivery was available were identified. The areas examined included catchments in Devon, Dorset, Wiltshire, Herefordshire and Derbyshire, characterised by contrasting landscapes and hydrological response. These areas were expected to exhibit different values for the connectivity index. Preliminary examination of the values obtained confirmed their relative ranking and thus the general acceptability of the data presented in Figure 3.3 as representing broad national scale contrasts in sediment delivery efficiency.

3.5 Derivation of the Connectivity Ratio

In order to derive values for the connectivity ratio, which represents the fraction of the soil mobilised by erosion from the land surface within a grid cell that will reach the stream channels within, or adjacent to, that cell, it is necessary to calibrate or scale the values obtained for the connectivity index (0-1). In the case of a grid cell characterised by a maximum value for the connectivity index (i.e. 1), it is unlikely that all the sediment will reach the stream network, and thus the value for the connectivity ratio is likely to be <1. Equally, for a cell characterised by a very low value for the connectivity index (i.e. ≈ 0), it is unlikely that none of the sediment will reach the stream network and the value of the connectivity ratio is likely to be >0.

A detailed calibration exercise would be required to produce the required scaling, but this was beyond the scope of the current study, due to both the limited time available and the general lack of empirical data on which to base such calibration. One approach would be to take a number of small catchments for which quantitative data on both soil erosion rates and sediment yield were available and to derive estimates of the sediment delivery ratio for these catchments which could be compared with the values of the connectivity index obtained for representative grid cells within these catchments by the present study. To be meaningful, such comparisons would need to assume that the estimates of sediment delivery ratio were essentially equivalent to values of the connectivity ratio for the land surface of the catchments. This assumption would not be unreasonable for most small catchments where channel erosion is unlikely to represent a major sediment source and where only limited conveyance losses would be expected to occur within the channel system. However, the absence of reliable quantitative erosion rate data for the land surface of such catchments currently precludes such an approach.

In the absence of such direct calibration, preliminary estimates of the connectivity ratio values have been derived by applying the linear stretch function given in Equation 3.6 to rescale the connectivity index values to the range 0.2 - 0.7. This range was selected using subjective judgement as being consistent with existing understanding and knowledge, albeit limited, of the efficiency of sediment delivery within small catchments in the UK. The national distribution of the resulting connectivity ratio values is shown in Figure 3.4.

3.6 The final products: their use and limitations

The primary products of this component of the project are the national maps and associated spatial data bases for the ***connectivity index*** and the ***connectivity ratio***

represented in Figures 3.3 and 3.4. A flow chart of the procedure used to derive these two measures and their associated data bases is provided in Figure 3.5.

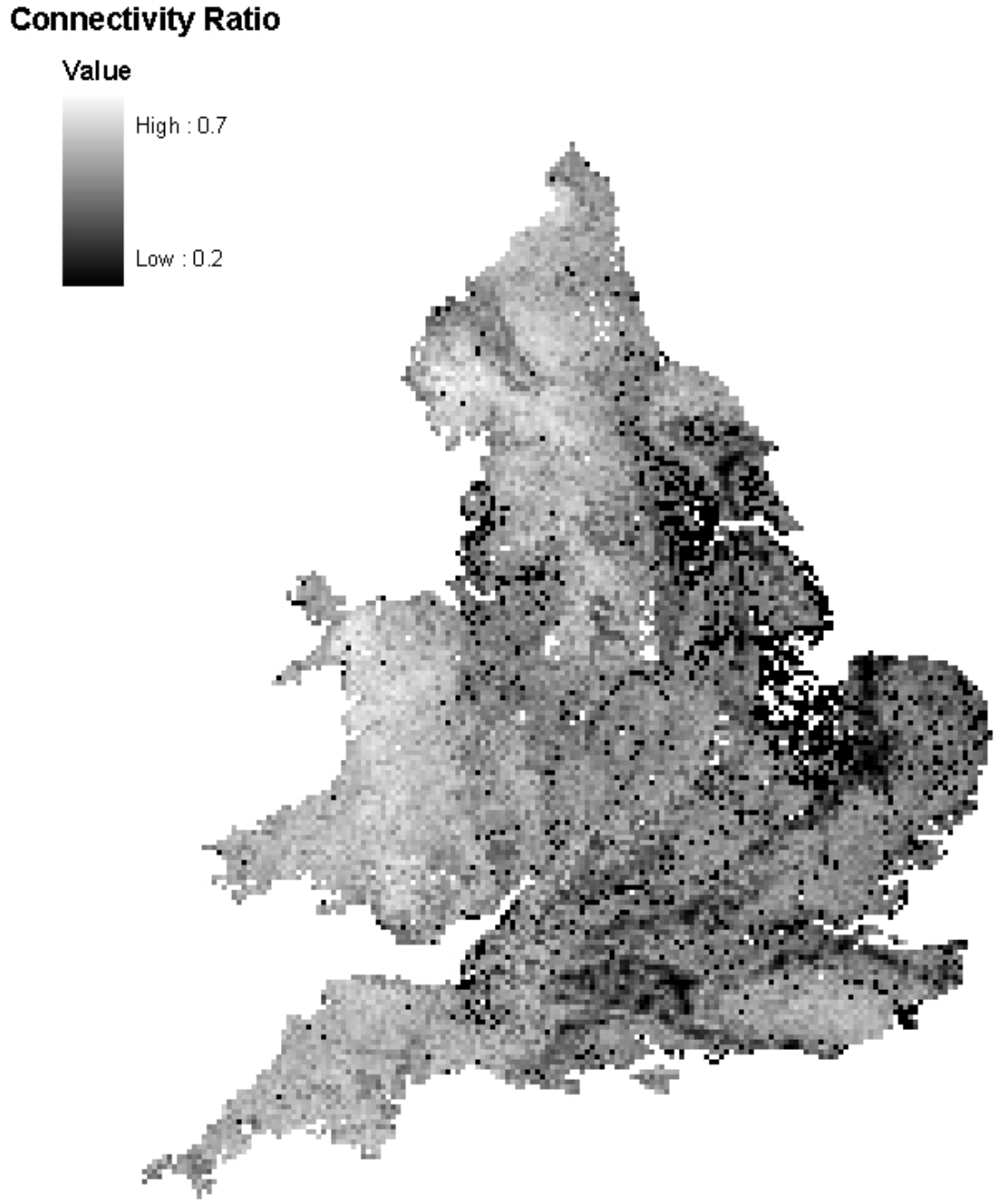

Figure 3.4. The spatial distribution of the connectivity ratio.

The national data base for the ***connectivity index*** affords a means of assessing the risk of sediment transfer from the land surface to the stream network in different parts of a catchment and identifying spatial variability and contrasts in the magnitude of this risk. Due to its non-quantitative basis, the connectivity index provides only a relative measure of slope-channel connectivity, and it will generally be useful to relate the values found within a particular study area or catchment to those in the overall national data base, in order to place them in a wider context. It is important to recognise that the connectivity index refers only to the *efficiency* of sediment transfer and does not itself provide a direct indication of the *amount* of sediment being supplied to the channel network. Interpretation of the connectivity index data must also take account of the rate of gross or on-site soil loss within the grid square. Even if the slope-channel connectivity is high, only small amounts of sediment will reach the channel system, if the gross erosion rates are low. Equally, the amounts of sediment supplied to the stream network in areas of low connectivity could exceed those in areas of high connectivity, if the gross erosion rates in the former areas are substantially greater than those in the latter areas.

The data base for the ***connectivity ratio*** could also be used in an essentially non-quantitative manner to assess the risk of sediment transfer within a study area or catchment, by relating the values obtained for a particular area and the variability of these values to the overall range associated with the national dataset. However, the primary value of the connectivity ratio is that it affords a quantitative estimate of the fraction of the sediment mobilised by water erosion from the land surface or slopes within a grid cell that reaches the streams within or adjacent to the grid square. Thus, if estimates of the gross or on-site soil loss are available for the grid cell, it is possible to estimate the rate of sediment supply to the stream system (t ha^{-1} $year^{-1}$) as the product of the rate of soil loss and the connectivity ratio.

The data sets for the connectivity index and the connectivity ratio presented in Figures 3.3 and 3.4 possess a number of constraints and limitations and it is important that these should be recognised viz.

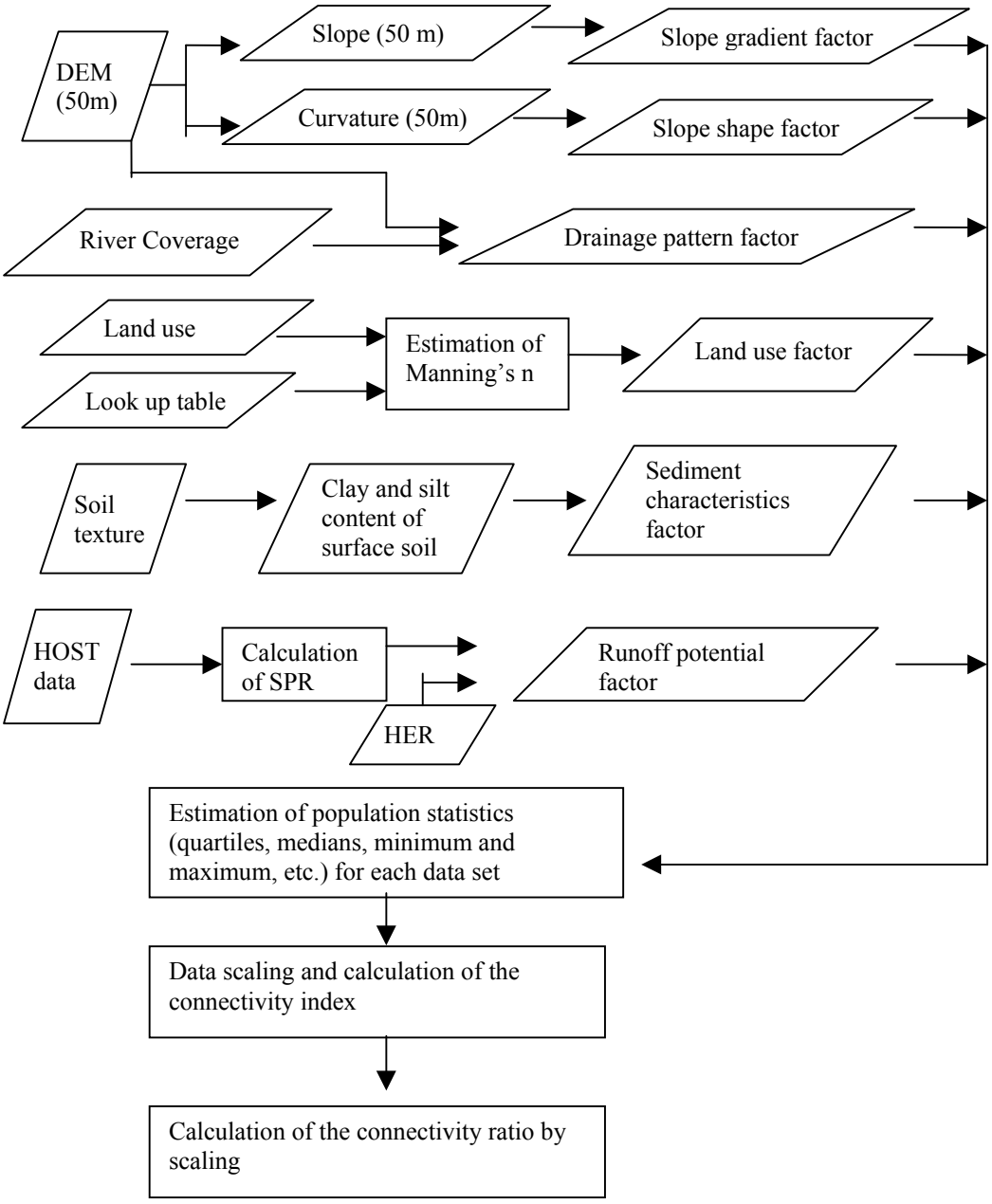

Figure 3.5. Flow chart of the GIS-based procedure used for the estimation of the connectivity index and ratio.

1) Data from many sources with different levels of precision and quality assurance have been used to derive these measures of slope-channel connectivity and it must be accepted that the quality of the generated secondary data layers and the final results cannot be better than that of the data used.
2) The procedure used to derive the connectivity index involved a number of simplifying assumptions. For example, the connectivity index only takes account of transfer of sediment from the land surface to the stream network by surface

runoff. No account is taken of the potential for transfer through subsurface drains. In areas of clay soils with underdrains, some of the mobilised sediment may be transferred through fissures to the drainage network and thence to the stream system (cf. Russell *et al.,* 2001). Such transfer is likely to be highly efficient, since there is little opportunity for deposition within the drains. The values for the connectivity index and connectivity ratio obtained for such areas using the current procedure are there likely to be underestimates. Similarly, the current procedure takes no account of the influence of what might be termed adventitious effects on the efficiency of sediment transfer which include the spatial topology and linkage of hedges, the location of field gateways and the role of other field boundaries, road networks, man-made drainage systems etc in routing sediment from the land surface to the channel network. These may both increase and decrease the 'inherent' connectivity of a landscape, as represented by the six key factors used in this study, and thus cause the values obtained in this study to both overestimate and underestimate the true values, according to the local influence of these adventitious effects.

3) It must be emphasised that estimates of sediment input to the stream network, derived as the product of the on-site erosion rate and the connectivity ratio, relate only to sediment supply from the land surface or catchment slopes. Bank erosion may result in additional inputs of sediment, causing the sediment loads passing through the channel system to exceed the calculated inputs. Equally, it should be appreciated that a significant proportion of the sediment entering the stream network from the adjacent slopes may be deposited either in the channel or on the floodplain as it is transported through the channel system. It is therefore not possible to sum the sediment inputs to the stream network from individual grid cells within a catchment and thereby estimate the sediment yield at the catchment outlet. Conveyance losses will cause the sediment yield at the catchment outlet to be less than the sum of the inputs, although, where bank erosion is significant, the additional inputs from this source could exceed the conveyance losses, causing the sediment yield at the catchment outlet to exceed the sum of the inputs to the channel network from the catchment surface.
4) The procedure outlined in Figure 3.4 has been designed to be applied to 1 km grid cells. The values for the connectivity index and connectivity ratio obtained will necessarily involve a degree of spatial averaging and it is likely that areas with both higher and lower connectivity will occur within a specific grid cell. The approach developed here was designed to provide a broad-scale assessment of the risk of sediment transfer to the stream network. A finer scale approach would be necessary to assess the connectivity of individual fields.

The present study has been limited by both the time and resources available. The results must, therefore, be seen as a first attempt to produce a national scale assessment of the risk of sediment transfer to the stream network. Considerable scope exists for further improvement and refinement. More particularly, further work is required to explore the potential to include additional controlling factors, and to refine the parameterisation of the existing factors and their incorporation into the final equation used to estimate CI. Although limited in both nature and extent, the available empirical information related to the soil erosion rates, sediment yields and sediment delivery efficiency should be utilised to assist in such work. Additional work is also required to inform the calibration of the connectivity index used to produce estimates of the connectivity ratio and to validate the resulting values. Again, the available

empirical information need to be exploited for this purpose. In the longer-term, however, there is an important need to undertake further field-based and experimental investigations to improve existing understanding of sediment delivery and the factors controlling slope-channel connectivity. This improved understanding is likely to lead to the incorporation of further controlling factors into the procedure used to estimate the connectivity index, particularly factors related to adventitious effects on slope-channel connectivity, such as field boundaries, the position of gateways and the role of tracks and roads in routing water and sediment.

4 SPATIAL DATA PROCESSING AND MAPPING

4.1 Introduction

In Phase I, a GIS-based approach was used to extrapolate the results of an extensive soil erosion survey of arable land in England and Wales (Fraser *et. al.,* 2000). A classification was developed for erosion vulnerability on lowland arable soils based on five classes of topsoil texture and five slope gradient groups. The former was derived from the NSRI's digitised National Soil Map data (NatMap) and the latter was derived from the Ordnance Survey 50 m *PANORAMA* digital elevation model (DEM). The data were manipulated in ESRI's *ArcView GIS*© using the *Spatial Analyst*© extension software.

In this second phase, the erosion data have been re-analysed to determine the probability of erosion of a given magnitude occurring for different soil-slope combinations. The reasons for this and the methodology used have been discussed (Section 2). The approach to implementing the erosion vulnerability estimation within the GIS has been altered accordingly.

Considerable improvements to the Phase I GIS processing procedures have been made, still within ESRI's *ArcView GIS*©. The exact procedures are outlined in a separate document, "Sediment delivery handbook – GIS methods", available from the project manager on request. One of the main underlying assumptions – that using only the most dominant soil type within each 1 km pixel is satisfactory – is proven to be invalid, and a solution to characterising all the soil information is given. In addition, a more accurate approach to characterising slope gradient is used, moving away from a single mean value within each 1 km pixel to a representation of the *distribution* of slope gradients. Finally, areas of 'arable land', 'lowland grassland' and 'upland' are identified based on the Centre for Ecology and Hydrology's Landcover map of Great Britain. Its use is considered in relation to the inherent level of mapping uncertainty and the impact on model output.

4.2 Characterisation of slope gradient distribution

4.2.1 Introduction

The steepest slopes often represent a small proportion of the total distribution of slope gradients within a landscape. It was acknowledged in Phase I that simple averaging of slope gradient derived from a 50 m DEM to the 1 km resolution would lead to a loss of important data and possibly lead to a misrepresentative estimate of erosion potential. This is because greater erosion is typically associated with increasing slope gradient. The approach outlined here moves away from a single summary value of slope to a representation of the slope distribution.

4.2.2 Slope distribution

Figure 4.1 shows the result of spatial averaging slope values from 50 m to 1 km pixels. It is visually evident that within each 1 km pixel, the slope distribution is complex and an erosion model that ignores this detail may produce erroneous

estimates of potential sediment generation. However, the application of even the simplest of erosion models at a 50 m resolution would raise both data processing and data management issues.

The retention of the general nature of slope distribution is achieved by storing a histogram of the slope gradient *distribution* for each 1 km pixel, as shown in Figure 4.2. Although the spatial information within each 1 km pixel is lost, the information content should suffice for modelling erosion at the national scale and represents a considerable improvement on using simple average slope values for each 1 km pixel. In estimating sediment generation for arable and lowland grassland areas, the distribution of three slopes classes (0-3°, 3-7° and >7°) were computed (Figure 4.3). For upland areas, only two slope classes were required (<12° and >12°). The GIS approach to generating these data is outlined in the accompanying handbook.

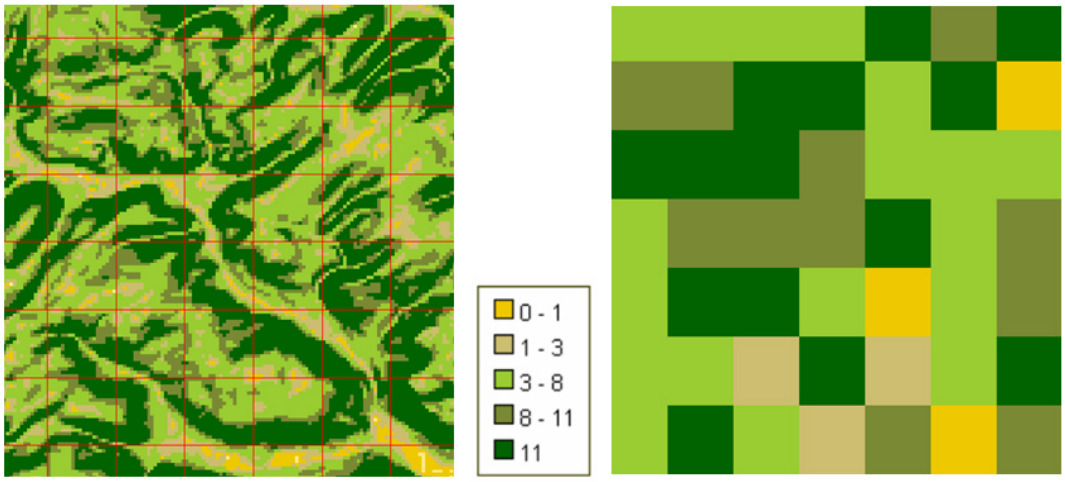

Figure 4.1. 7 km x 7 km area indicating slope gradient classes derived from the Ordnance Survey 50 m PANORAMA DEM. Left: the original 50 m slope classes with red lines representing a 1 km grid. Right: how slope classes might be represented if simply averaged.

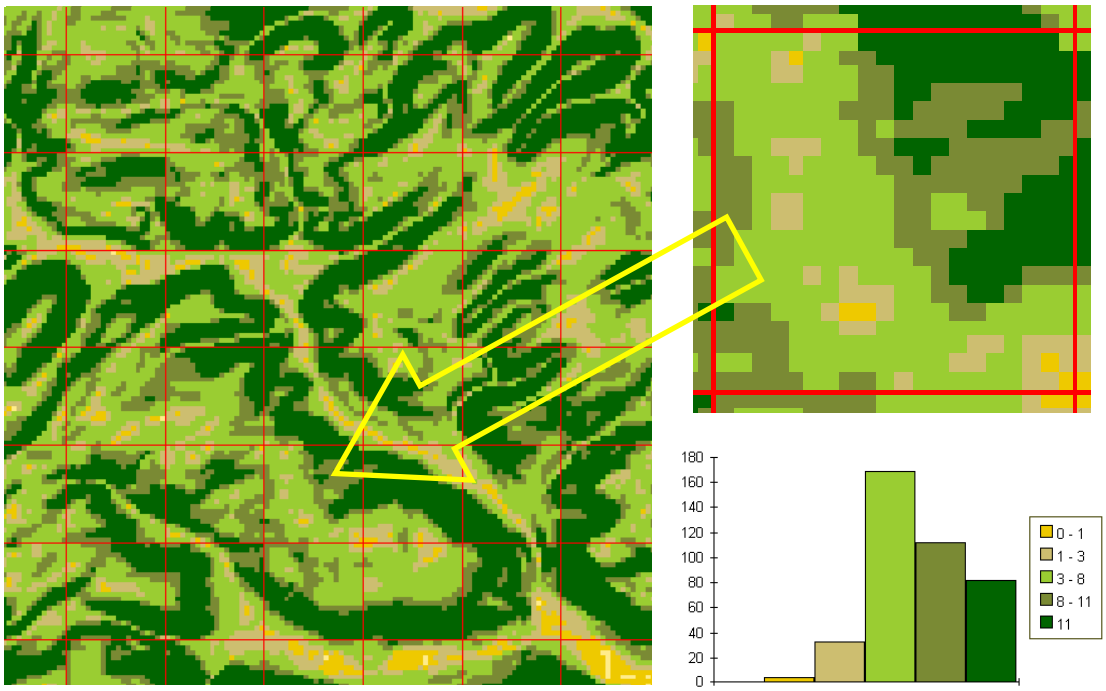

Figure 4.2 – Characterisation of slope distribution within each 1 km pixel. The inset shows a 1 km x 1 km area with its respective slope distribution histogram indicating the frequency of each slope class.

a. Distribution of 0-3° slopes **b. 3-7° slopes** **c. >7° slopes**

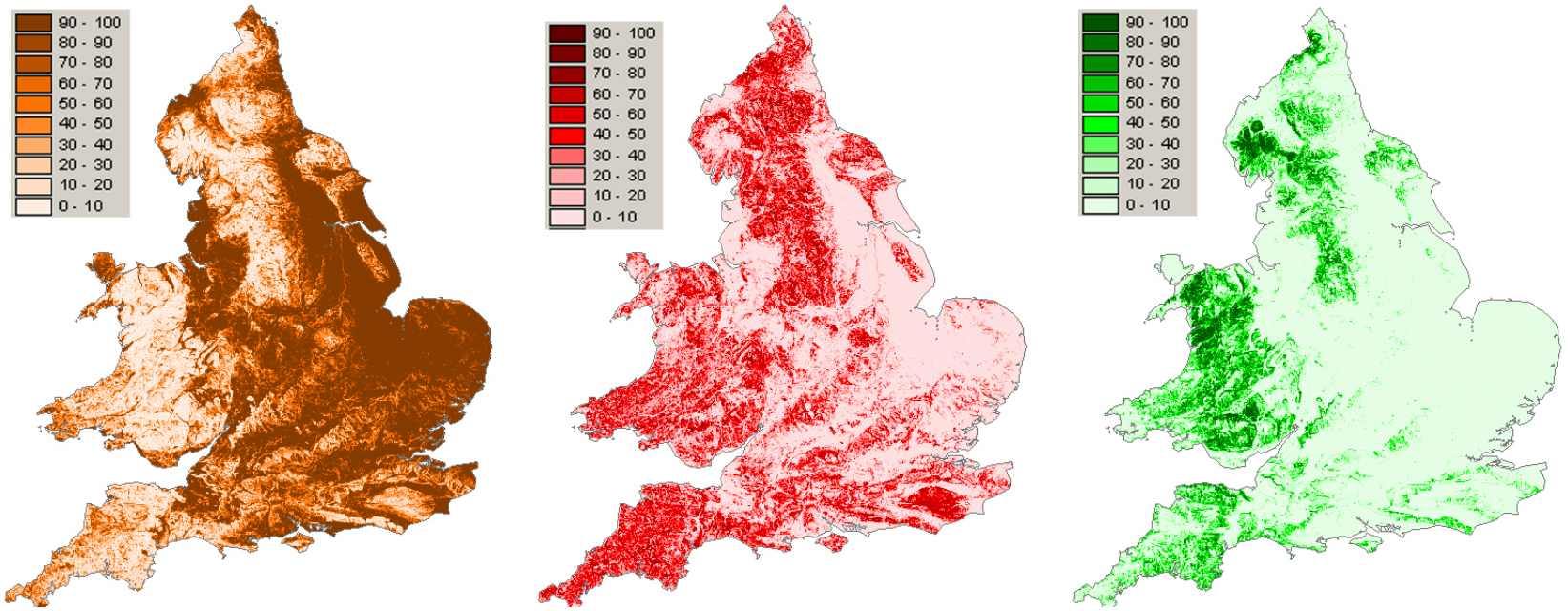

Figure 4.3 Example of the slope classes used to determine sediment generation rates on arable and lowland grassland soils. The maps show the distribution of slope classes and their percentage proportions occurring in each 1 km pixel.

4.3 Soil distribution

The NSRI's National Soil Map (NatMap) provides a summary of the soil series in England and Wales and is produced on a regular 1 km grid. Within each of the 1 km squares, the area proportions within each Map Unit are represented in decreasing order of dominance, as indicated in Table 4.1. In Phase I, only a single attribute of the soil database was utilised, which was the most dominant soil series in the predominant Map Unit 1 (i.e. Unit 1 in Table 4.1). This was assumed to provide a representative soil type for each 1 km map-unit. The assumption that this is valid is challenged here.

A simple review of the NatMap data will reveal that only 17% of all 1 km pixels in England and Wales have are represented by one single Map Unit. Only one quarter of all 1 km pixels have 95% or more of their area represented by one single Map Unit (Table 4.2). In most cases, the number of individual Map Units making up each 1 km pixel can be numerous – up to the first eleven are stored in the NatMap database. In extreme cases, the percentage area of the predominant Map Unit is as low as 40%. It is, therefore, important to consider more of the data within the NatMap than was first proposed. In order to take into account 95% of the all soils in each 1 km pixel, only the first three most dominant Map Units are required (this is true for 95% of the area of England and Wales).

If the Map Unit (Unit 1, Table 4.1) has similar characteristics, in relation to erosion vulnerability, to the second and third most dominant units, then it would be sufficient to use only Unit 1 in the GIS modelling. However, this is not the case. In this erosion study, the soil series have been aggregated to the soil subgroup level. One might expect a significant number of the soil series in each 1 km pixel to share the same subgroup. A pixel-by-pixel comparison of the dominant soil series in the first three most predominant Map Units shows that this is only true in 10% of all cases. It is concluded, therefore, that using only the most dominant Map Unit is insufficient and misrepresentative of the soils in each 1 km pixel. It is necessary to use the first three most dominant Map Units in the NatMap to account for 95% of all the area in each 1 km pixel. The first three Map Units will be used in this study. This approach does not explicitly take into account that within each Map Unit there are a number of individual soil series. A full investigation of this approach is required and extends beyond the scope of this project.

Table 4.1. Extract from the NatMap attribute table, indicating soil composition within each 1 km pixel in decreasing order of dominance. Each row represents a single 1 km pixel and is interpreted as follows: in the first 1 km pixel there is 73.86% of Map Unit 1, with a predominant Flint Soil Series (7.11m) and the remaining 26.14% is comprised if Map Unit 2, which is predominantly Altcar Series (1024a).

East_1k	North_1k	Unit1	Urban1	Unit1_pc	Unit2	Urban2	Unit2_pc	Unit3	Urban3	Unit3_pc	Unit4	Urban4	Unit4_pc	…	…	Unit11
365000	318000	0711m		73.86	1024a		26.14									
365000	319000	0551a		66.39	0711m		33.61									
365000	321000	0541r		61.96	0711m		32.51	0551d		2.77	0551a		2.76			
365000	323000	0541r		72.76	0551d		16.56	0551a		6.46	0711m		4.22			
365000	327000	0711n		45.16	0572f		28.75	0551d		18.81	0631b		7.26			
365000	328000	0631b		71.8	0711n		28.2									
365000	329000	0631b		99.87	lake		0.13									
365000	335000	0711m		51.01	0541r		23.64	0813e		21.36	1024a		3.8			
365000	336000	0541r		35.9	0813e		32.57	0711m		31.53						
368000	515000	0711n		100												

Table 4.2. Frequency histogram of the proportion of individual 1 km pixels represented by their dominant Map Unit within England and Wales.

Area proportion of the most dominant Map Unit in each 1km pixel	Proportion of England and Wales (%)
100	17.1
95 - 99	9.8
90 - 95	6.2
85 - 90	5.9
80 - 85	6.2
75 - 80	6.3
70 - 75	6.8
65 - 70	7.3
60 - 65	7.7
55 - 60	8.4
50 - 55	8.7
45 - 50	4.3
40 - 45	3.0
35 - 40	1.7
30 - 35	0.6
25 - 30	0.1
20 - 25	0.0
15 - 20	0.0
10 - 15	0.0
5 - 10	0.0
0 - 5	0.0

4.4 Landcover mapping

4.4.1 Introduction

The Land Cover Map of Great Britain (LCMGB) was produced by the Centre for Ecology and Hydrology (CEH) using a supervised classification of Landsat Thematic Mapper (TM), which provides 30 m resolution satellite images. The LCMGB map, resampled to 25 m, records 25 cover types consisting of sea and inland water, beaches and bare ground, developed and arable land and 18 types of semi-natural vegetation (Appendix 3).

4.4.2 Classification accuracy

Accuracy assessment determines the quality of the information derived from remotely sensed data. The purpose is the identification of mapping errors and involves the comparison of landcover classes assigned to an individual pixel with verified reference information recorded on the ground, so-called 'ground truthing'. CEH classification accuracy assessment of the 1990 data showed an overall mapping accuracy of 67% (http://www.ceh.ac.uk/data/lcm/index.htm). This is consistent with known mapping accuracies of satellite-image-derived thematic maps (Richards and Jia, 1999).

In addition to the intrinsic accuracy of the original classification, a user's own classification scheme may not fit easily into the satellite image classification. For example, the NSRI erosion surveys were carried out in areas of England and Wales broadly grouped into arable, lowland grassland and upland landcover categories. Within the uplands, the original data contained subclasses of heath, grassland, grassland/heath, bracken and bog. Difficulties arise when relating the CEH classification of landcover to the landcover types identified in the NSRI erosion surveys. Discrepancies in class matching will introduce more uncertainty to the final maps. These factors are inherent in both 1990 and 2000 LCMGB.

The reclassification scheme of the LCMGB data into the broader arable, lowland grassland and upland landcovers is given in Table 4.3. A comparison was made of all the points used in the original NSRI soil erosion survey with the coincident locations in the LCMGB 1990 map (at 25 m resolution). A cross tabulation between the two datasets is given in Table 4.4. Although not taken from a random sample of observations, Table 4.4 provides a useful indication of the likely level of class agreement and disagreement for the map in Figure 4.5.

Table 4.4 indicates that the LCMGB arable class is in agreement with 89% of the 211 arable field sites visited during the NSRI erosion survey. Of the remaining 11%, 10% were classed as grassland and 1% as upland. The estimated accuracy of lowland grassland was very low (44%) with considerable confusion between arable and lowland-grassland classes. Upland areas had an accuracy of 81% with the remaining areas equally confused between grassland and arable classes. This is likely to be due, in part, to difficulties in classifying transitional areas in the upland/lowland fringes, and, possibly to a lesser extent, due to *real* landcover changes between the dates of the erosion surveys and the LCMGB surveys. This level of uncertainty will have a

direct impact on the landcover masks used in the GIS to isolate the arable, lowland grassland and upland areas and will, therefore, have an impact on the final estimates of sediment generation potential and sediment delivery to watercourses.

Although beyond the original scope of this project, if the original ground data used to classify the CEH data were made available, there are recognised methodologies for correcting area-estimates which could be used to adjust the estimated erosion output from the type of modelling approach used here. These methods have been used to correct the use of satellite data used by the European Statistical Office when supporting the management of the Common Agricultural Policy (Taylor *et al.*, 1997).

For this project, the landcover maps should be treated with due caution, with attention to the information provided in Table 4.4.

Table 4.3. Classification scheme relating the CEH landcover subgroups to the NSRI erosion survey landcover groups.

Broad Landcover	CEH Key	CEH sub-class names
Arable	18	Tilled Land
Lowland grassland	5	Grass Heath
	6	Mown / Grazed Turf
	7	Meadow / Verge / Semi-natural
	8	Rough / Marsh Grass
	25	Open Shrub Heath
Upland	9	Moorland Grass
	10	Open Shrub Moor
	11	Dense Shrub Moor
	12	Bracken
	13	Dense Shrub Heath
	14	Scrub / Orchard
	15	Deciduous Woodland
	16	Coniferous Woodland
	17	Upland Bog
	19	Ruderal Weed
	23	Felled Forest
Other	1	Sea / Estuary
	2	Inland Water
	3	Beach and Coastal Bare
	4	Saltmarsh
	20	Suburban / Rural Development
	21	Continuous Urban
	22	Inland Bare Ground
	24	Lowland Bog
	0	Unclassified

Table 4.4. Cross-tabulation matrix indicating landcover class mapping accuracy. Diagonal values indicate agreement between NRSI and CEH classification.

		NSI erosion surveys				
		Arable	Grassland	Upland	Total	Accuracy
CEH LCMGB 1990	Arable	187	21	3	*211*	*89%*
	Grassland	92	94	27	*213*	*44%*
	Upland	11	10	88	*109*	*81%*
	Unclassified	26	4	4	*34*	-

4.4.3 Landcover masks

Whilst bearing in mind the cautionary use of the reclassified LCMGB 1990 map, these data are used to mask areas of arable, lowland grassland, and upland. A set of binary maps (0 or 1) was produced at 1 km pixel resolution for each of the three landcover types. The value assigned to each 1 km pixel, from the 25 m LCMGB data, is that of the most dominant landcover class (see handbook for details). Once created, the resulting map will appear noisy (Figure 4.4a). This could be a true reflection of the heterogeneous composition of the landscape at this scale, although it might be expected that adjacent pixels have a higher degree of spatial correlation. It was decided to remove this noise by smoothing the map using a majority filter (Schowengerdt, 1997). The result of the smoothing is illustrated in Figure 4.4b and 4.5.

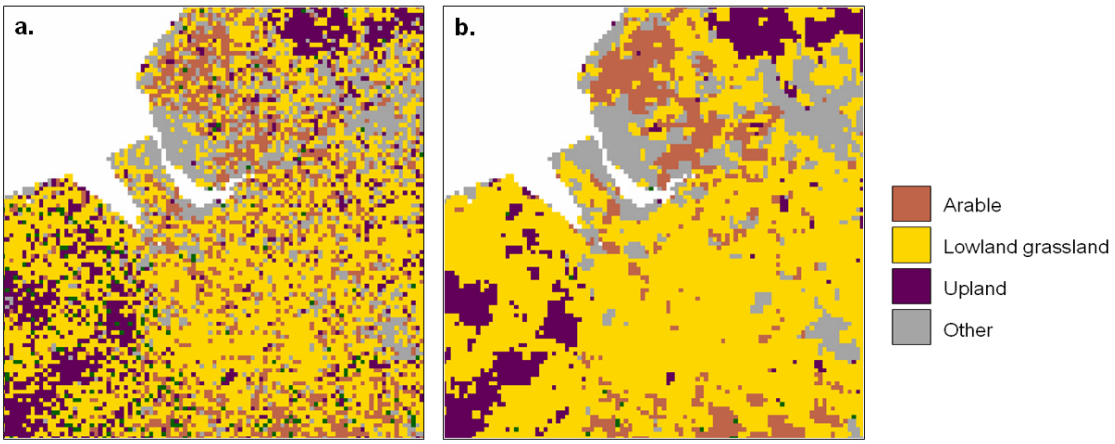

Figure 4.4. The effect of a 3x3 majority filter on the 1 km pixel landcover map.

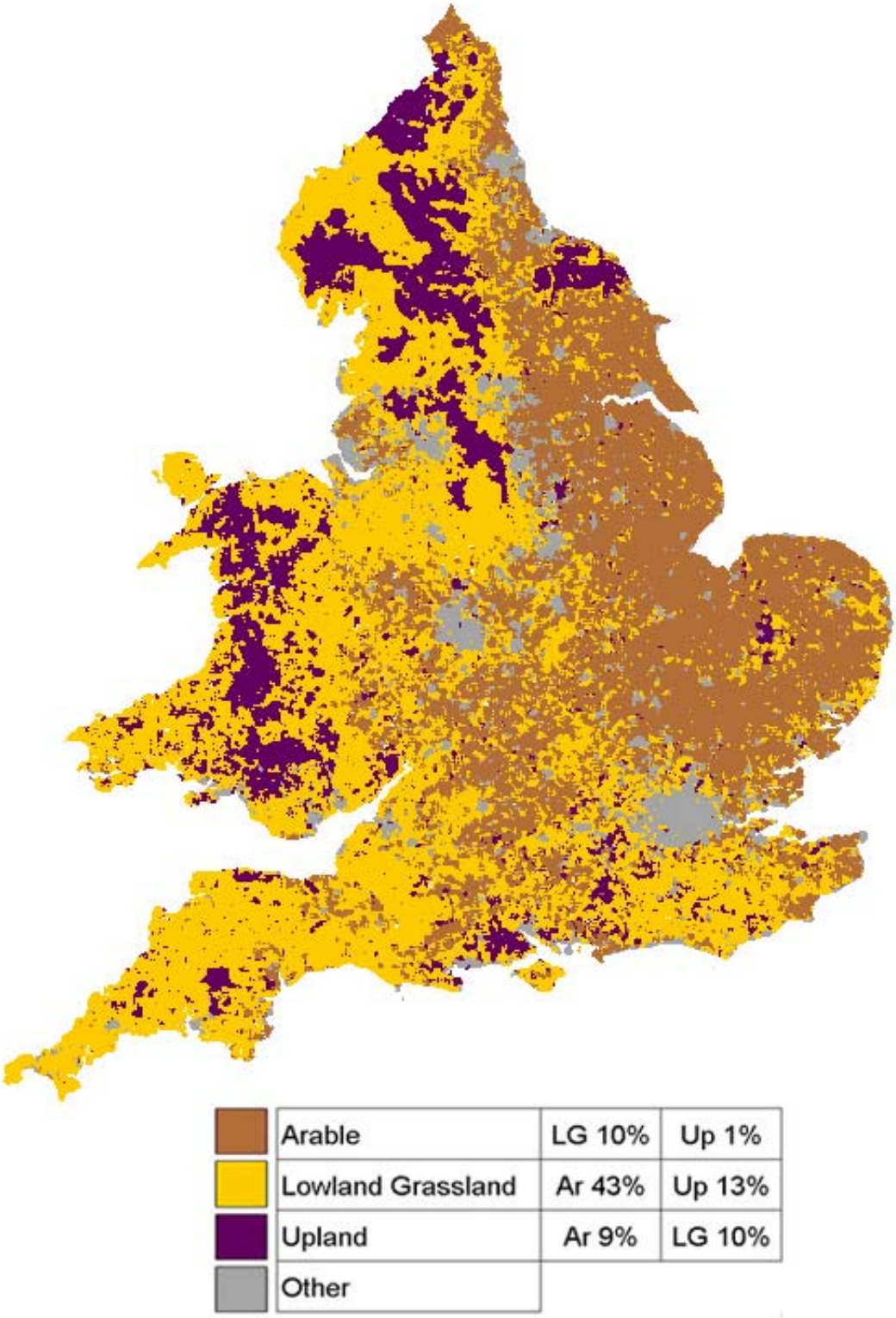

Figure 4.5. Landcover mask for England and Wales, produced at 1 km pixel resolution from LCMGB 1990. Landcover classes are given along with the percentage probability of misclassification in relation to the other landcover classes; Ar – arable, LG – lowland grassland, and Up – upland.

4.5 Erosion modelling

Analysis of the erosion survey data provided a series of tables that represented the probable rate of erosion over given return periods for different soil-slope combinations. These tables form the basis of a classification model for erosion vulnerability. For any one combination of soil subgroup and slope class, an erosion rate (m^3 ha^{-1}) can be determined, which represents the expected annual rate of sediment generated. The 1-in-1 year tables will be used to determine an estimate of potential sediment generated each year in m^3 ha^{-1} yr^{-1}.

Within any single 1-km pixel a combination of different soil-slope classes will occur in varying proportions, as illustrated in Figure 4.6. When summarised as 1 km pixels, only the relative proportions of each slope and soil class are known, and it can only be assumed that each subgroup contains slope classes in proportion to their weighted averages within the 1 km pixel[1]. The total erosion for each 1 km pixel can be estimated using Equation 4.1.

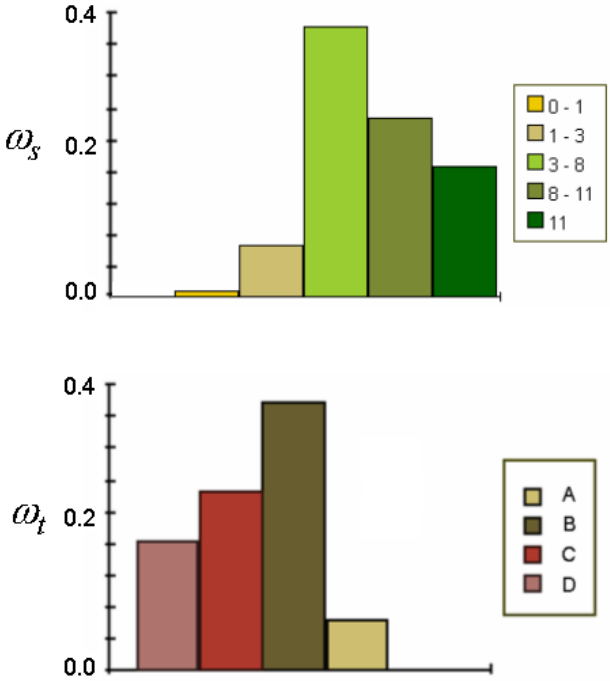

Figure 4.6. Class distributions in a single 1 km pixel used to determine class weightings, ω. Top: slope classes. Bottom: four soil classes. Sum of weightings ω of each histogram equals 1.0.

$$R = \sum_{t=1}^{m} \omega_t . \sum_{s=1}^{n} \omega_s . E_{ts} \qquad (4.1)$$

where R is the estimate of total channelled erosion; ω_s is the slope-area weighting factor; ω_t is the soil group area weighting factor and E is the estimated erosion rate in association with slope class s and soil group t as presented in the erosion tables.

[1] Soil subgroups will occur within associated topographic zones of a landscape due to their pedogenic origins and may be expected, therefore, to have an orderly spatial relationship to different slope classes.

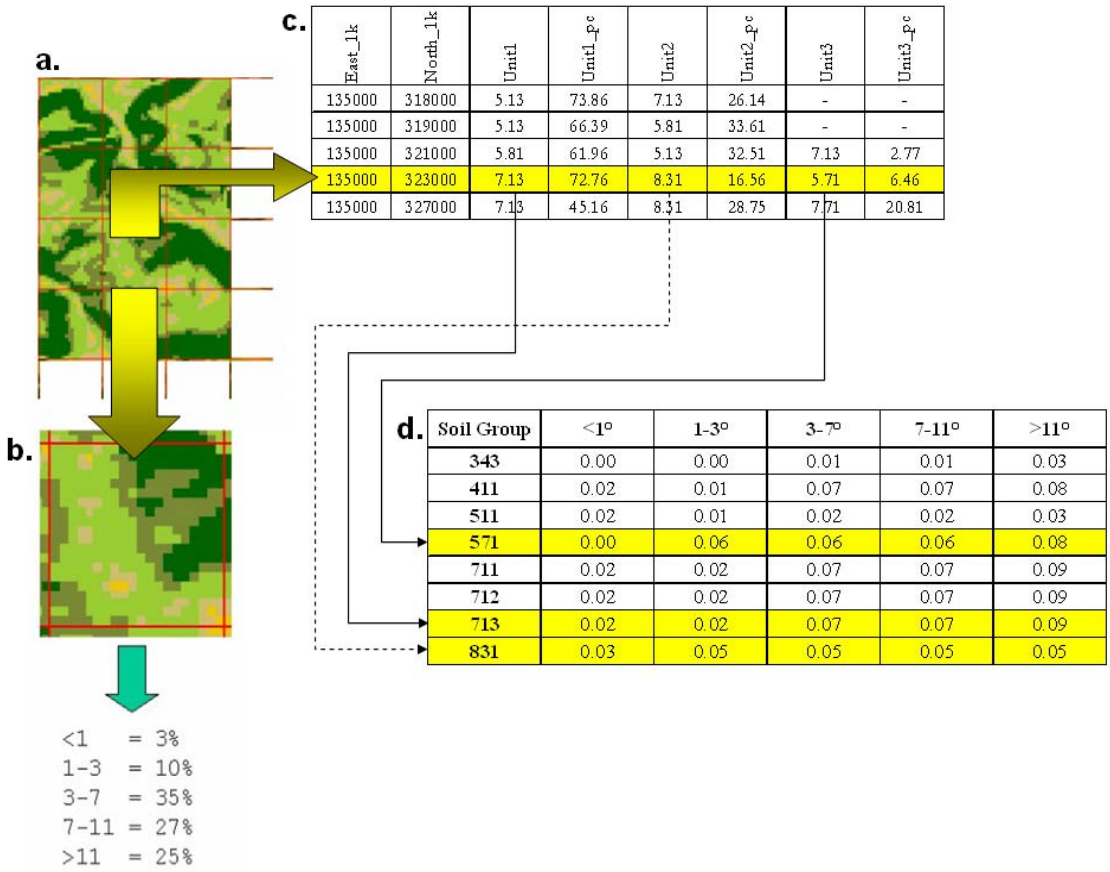

East_1k	North_1k	Unit1	Unit1_pc	Unit2	Unit2_pc	Unit3	Unit3_pc
135000	318000	5.13	73.86	7.13	26.14	-	-
135000	319000	5.13	66.39	5.81	33.61	-	-
135000	321000	5.81	61.96	5.13	32.51	7.13	2.77
135000	323000	7.13	72.76	8.31	16.56	5.71	6.46
135000	327000	7.13	45.16	8.31	28.75	7.71	20.81

Soil Group	<1°	1-3°	3-7°	7-11°	>11°
343	0.00	0.00	0.01	0.01	0.03
411	0.02	0.01	0.07	0.07	0.08
511	0.02	0.01	0.02	0.02	0.03
571	0.00	0.06	0.06	0.06	0.08
711	0.02	0.02	0.07	0.07	0.09
712	0.02	0.02	0.07	0.07	0.09
713	0.02	0.02	0.07	0.07	0.09
831	0.03	0.05	0.05	0.05	0.05

Figure 4.7. Schematic diagram indicating the use of soil and slope gradient data within the GIS.

For each 1 km pixel in England and Wales an estimate of total erosion was calculated using Equation 4.1. In this example, there are five slope classes (n=5) and the first three most dominant soil subgroups are used (m=3). In the example pixel (b), the increasing slope classes have respective proportions ω_s of 3%, 10%, 35%, 27% and 25%. The corresponding pixel in the NatMap database (an extract is shown in Figure 4.7c) has a dominant soil of 7.31 (a cambic stagnogley) making up 72.8% of the 1 km pixel area and for which ω_t equals 0.728. The second most dominant soil is a typical cambic gley (8.31), for which ω_t equals 0.166. The third most dominant soil is a typical argillic brown earth (7.71) for which ω_t equals 0.065. The slope-soil data is used to cross reference to the erosion table (d) to determine the total estimated erosion potential: for example, soil subgroup 7.13 on a 3-7° slope will have an erosion rate of 0.07 m^3 ha^{-1}.

Example calculation (based on Figure 4.7)

Step 1 calculating the erosion rate based on soil-slope combinations, according to the slope proportions in each 1 km pixel – three calculations, one for each soil subgroup.

Dominant soil (m=1): Unit1 = 7.31;

$$\sum_{s=1}^{n} \omega_s . E_{ts} = \begin{matrix} s=1; & <1 \\ s=2; & 1-3 \\ s=3; & 3-7 \\ s=4; & 7-11 \\ s=5; & >7 \end{matrix} \begin{bmatrix} 0.03 & \text{x} & 0.02 \\ 0.10 & \text{x} & 0.02 \\ 0.35 & \text{x} & 0.07 \\ 0.27 & \text{x} & 0.07 \\ 0.25 & \text{x} & 0.07 \end{bmatrix} = 0.0685$$

2nd dominant soil (m=2): Unit2 = 8.31;

$$\sum_{s=1}^{n} \omega_s . E_{ts} = \begin{matrix} s=1; & <1 \\ s=2; & 1-3 \\ s=3; & 3-7 \\ s=4; & 7-11 \\ s=5; & >7 \end{matrix} \begin{bmatrix} 0.03 & \text{x} & 0.03 \\ 0.10 & \text{x} & 0.05 \\ 0.35 & \text{x} & 0.05 \\ 0.27 & \text{x} & 0.05 \\ 0.25 & \text{x} & 0.05 \end{bmatrix} = 0.0494$$

3rd dominant soil (m=3): Unit3 = 5.71;

$$\sum_{s=1}^{n} \omega_s . E_{ts} = \begin{matrix} s=1; & <1 \\ s=2; & 1-3 \\ s=3; & 3-7 \\ s=4; & 7-11 \\ s=5; & >7 \end{matrix} \begin{bmatrix} 0.03 & \text{x} & 0.00 \\ 0.10 & \text{x} & 0.06 \\ 0.35 & \text{x} & 0.06 \\ 0.27 & \text{x} & 0.08 \\ 0.25 & \text{x} & 0.08 \end{bmatrix} = 0.0686$$

Step 2 calculating total erosion according to the proportion of soil in each 1 km pixel.

$$R = \begin{bmatrix} \omega_1 & \text{x} & \sum_{s=1}^{n} \omega_s . E_{ts} \\ \omega_2 & \text{x} & \sum_{s=1}^{n} \omega_s . E_{ts} \\ \omega_3 & \text{x} & \sum_{s=1}^{n} \omega_s . E_{ts} \end{bmatrix} = \begin{bmatrix} 0.728 & \text{x} & 0.0685 \\ 0.166 & \text{x} & 0.0494 \\ 0.065 & \text{x} & 0.0686 \end{bmatrix} = 0.06 m^3 / ha \quad (2dp.)$$

4.6 Erosion vulnerability mapped output

In the following, maps representing the distributions of arable, lowland grassland and upland land in England and Wales are presented (Figures 4.8, 4.10 and 4.12). The vulnerability to erosion of each of these landcovers under 1-in-1 year ($p = 0.99$) events is presented in Figures 4.9, 4.11 and 4.13 respectively.

In Figure 4.14, the individual erosion vulnerabilities of arable, grassland and upland areas under 1-in-1 year events are combined. The resultant map represents the distribution of erosion vulnerability estimates expected to occur annually in England and Wales.

In Figure 4.15, the individual erosion vulnerabilities of arable, grassland and upland areas are again represented in combination, but this time for 1-in-10 year ($p = 0.999$) erosion events. Figure 4.16 juxtaposes the maps of erosion vulnerability under 1-in-1 year and 1-in-10 year events for comparison. Note, therefore, that the legend for erosion under 1-in-1 year has been modified to conform to that on the 1-in-10 year map.

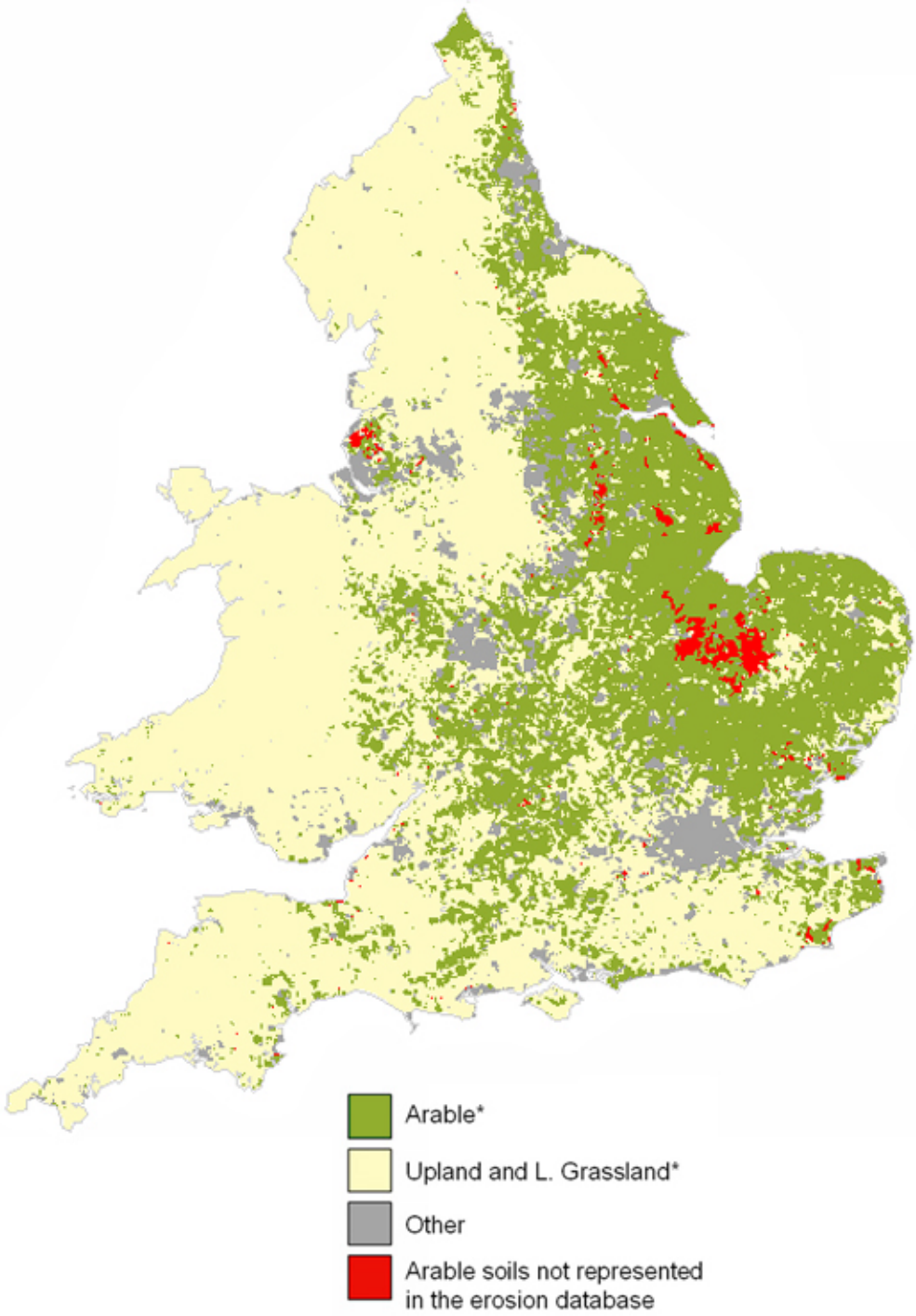

Figure 4.8. Arable areas as determined from the CEH LCMGB 1990. Red areas refer to arable areas where the majority of soil (>95%) was not represented in the soil erosion database. *Refer to Section 4.4.2 (classification accuracy).

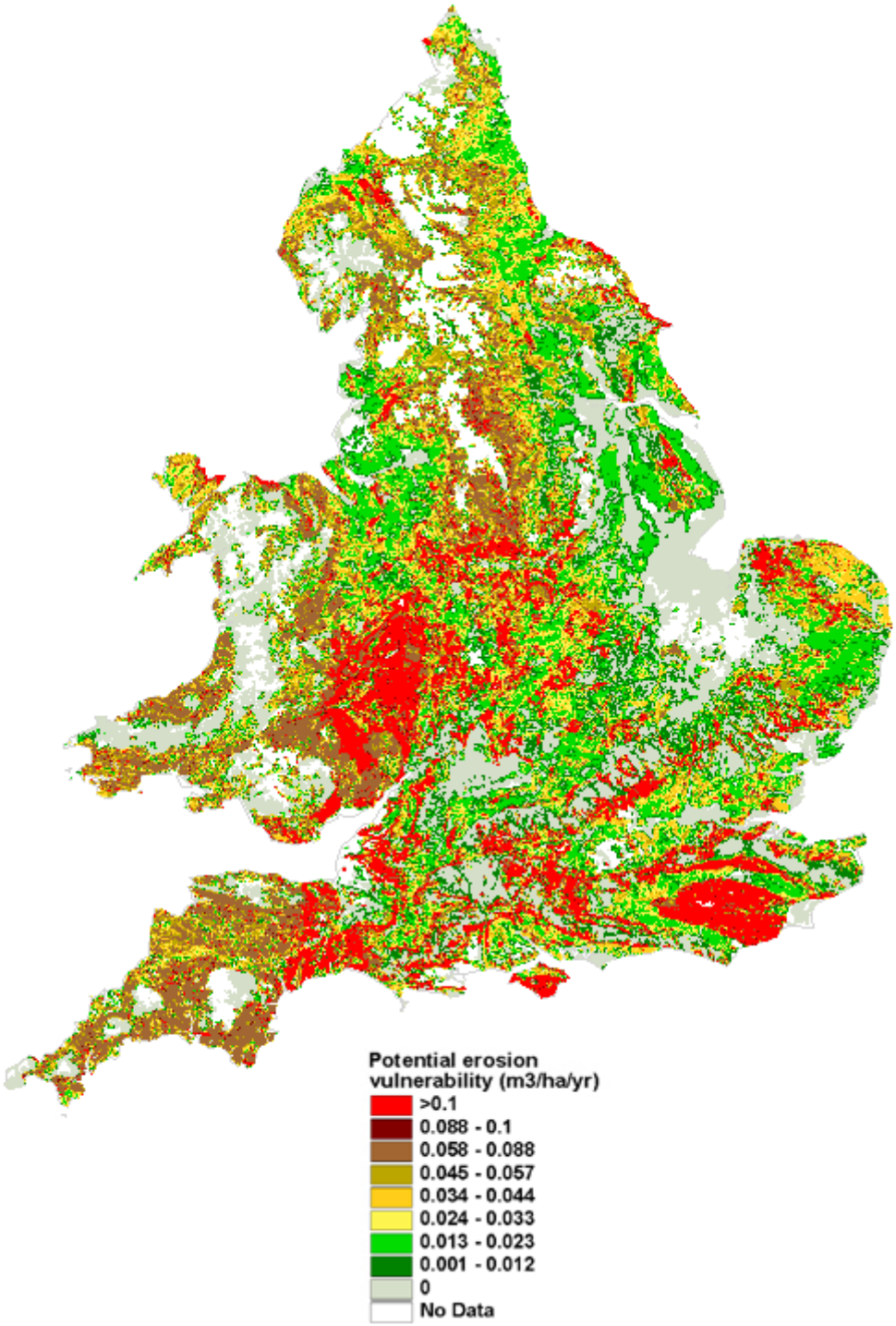

Figure 4.9. Distribution of estimated erosion vulnerability (1-in-1 year events) on soils associated with arable land use in England and Wales. N.B. the map assumes all areas are under arable land use. No Data relates to areas whose soils are not in the arable erosion database.

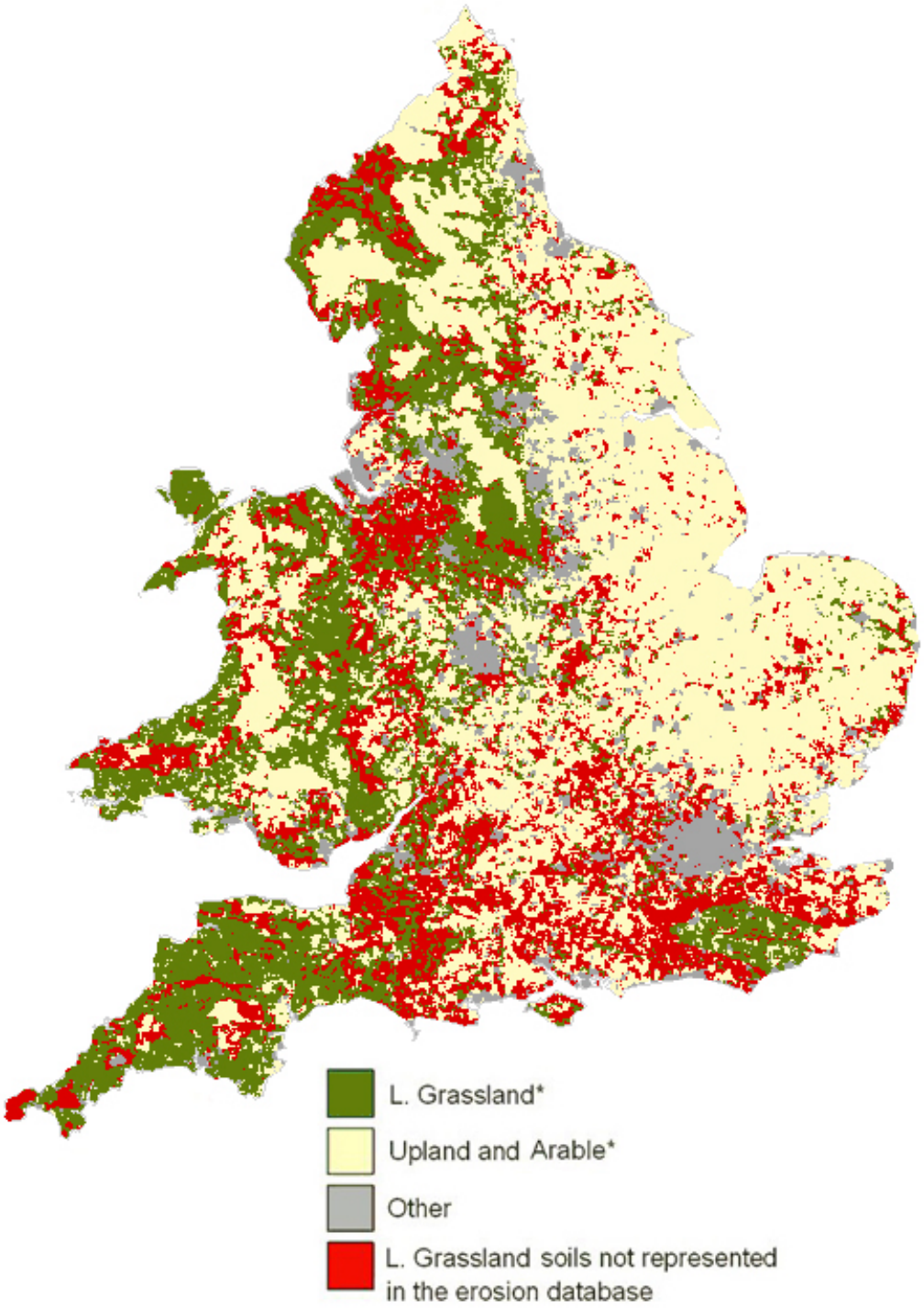

Figure 4.10. Lowland grassland areas as determined from the CEH LCMGB 1990. The red areas refer to grassland areas where the majority of soil (>95%) was not represented in the soil erosion database. *Refer to Section 4.4.2 (Classification accuracy).

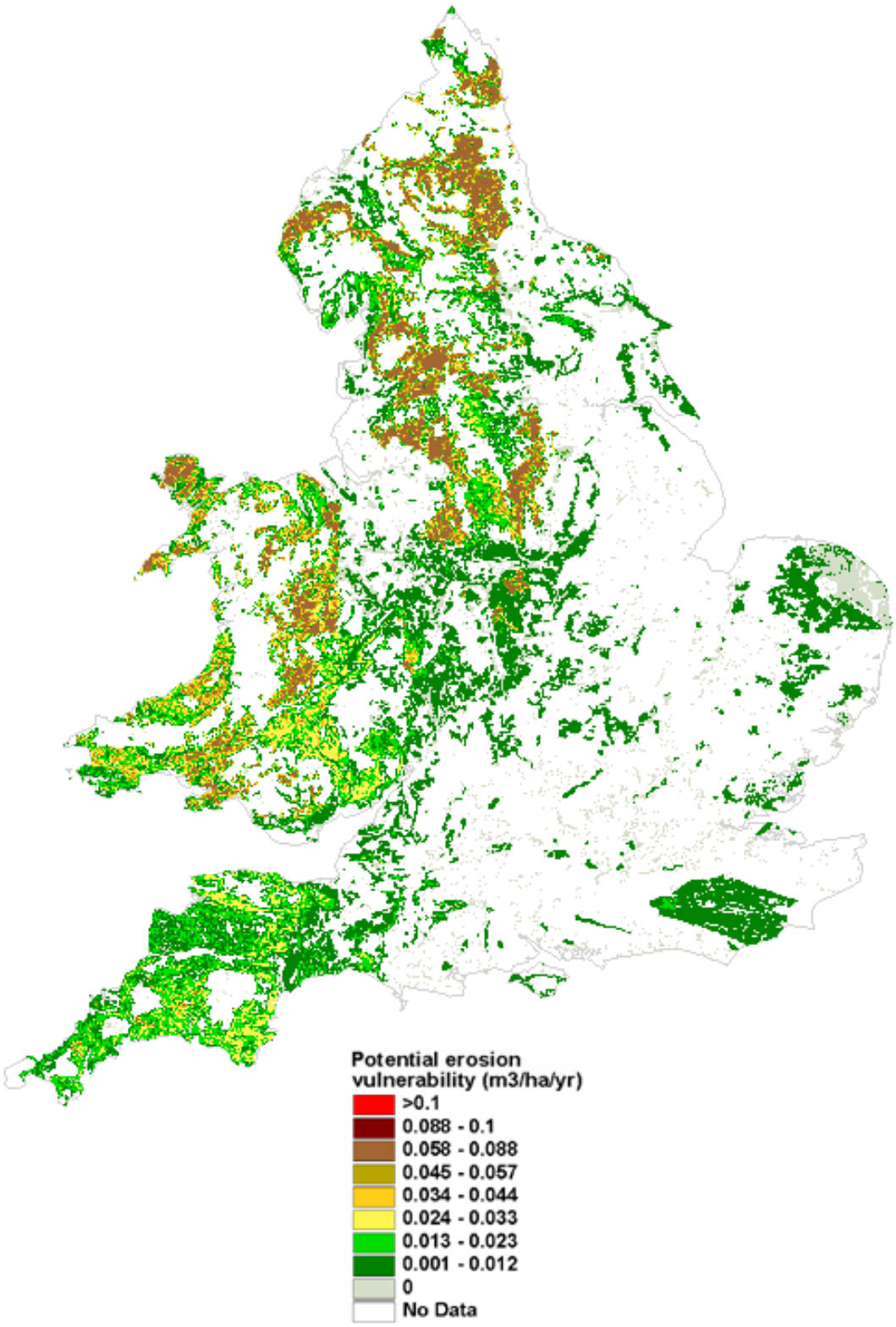

Figure 4.11. Distribution of estimated erosion vulnerability on soils associated with lowland grassland production in England and Wales (1-in-1 year events). N.B. the map assumes all areas are lowland grassland land use. No Data relates to areas whose soils are not in the lowland grassland erosion database.

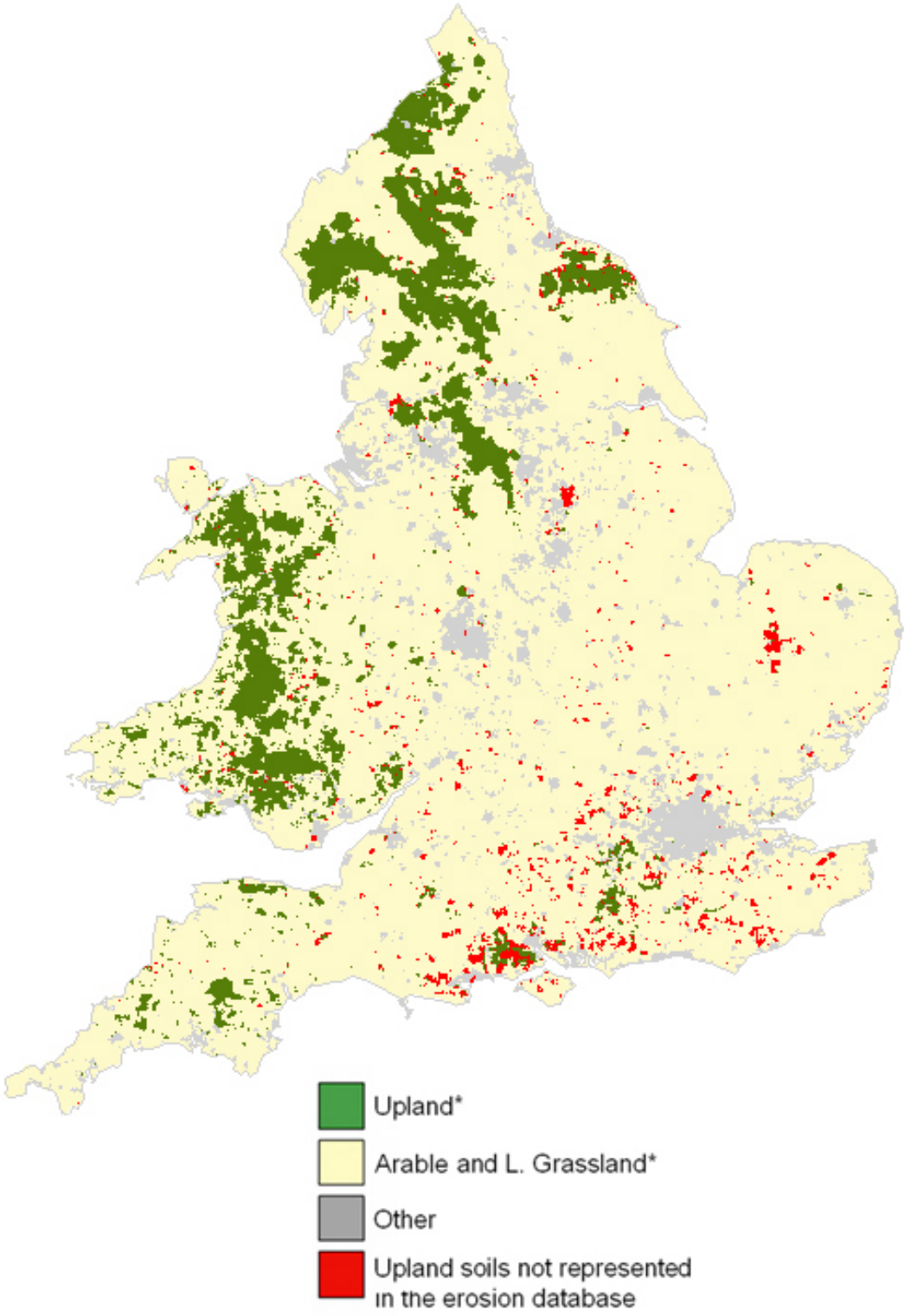

Figure 4.12. Upland areas as determined from the CEH LCMGB 1990. The red areas refer to upland areas where the majority of soil (>95%) was not represented in the soil erosion database. *Refer to Section 4.4.2 (Classification accuracy).

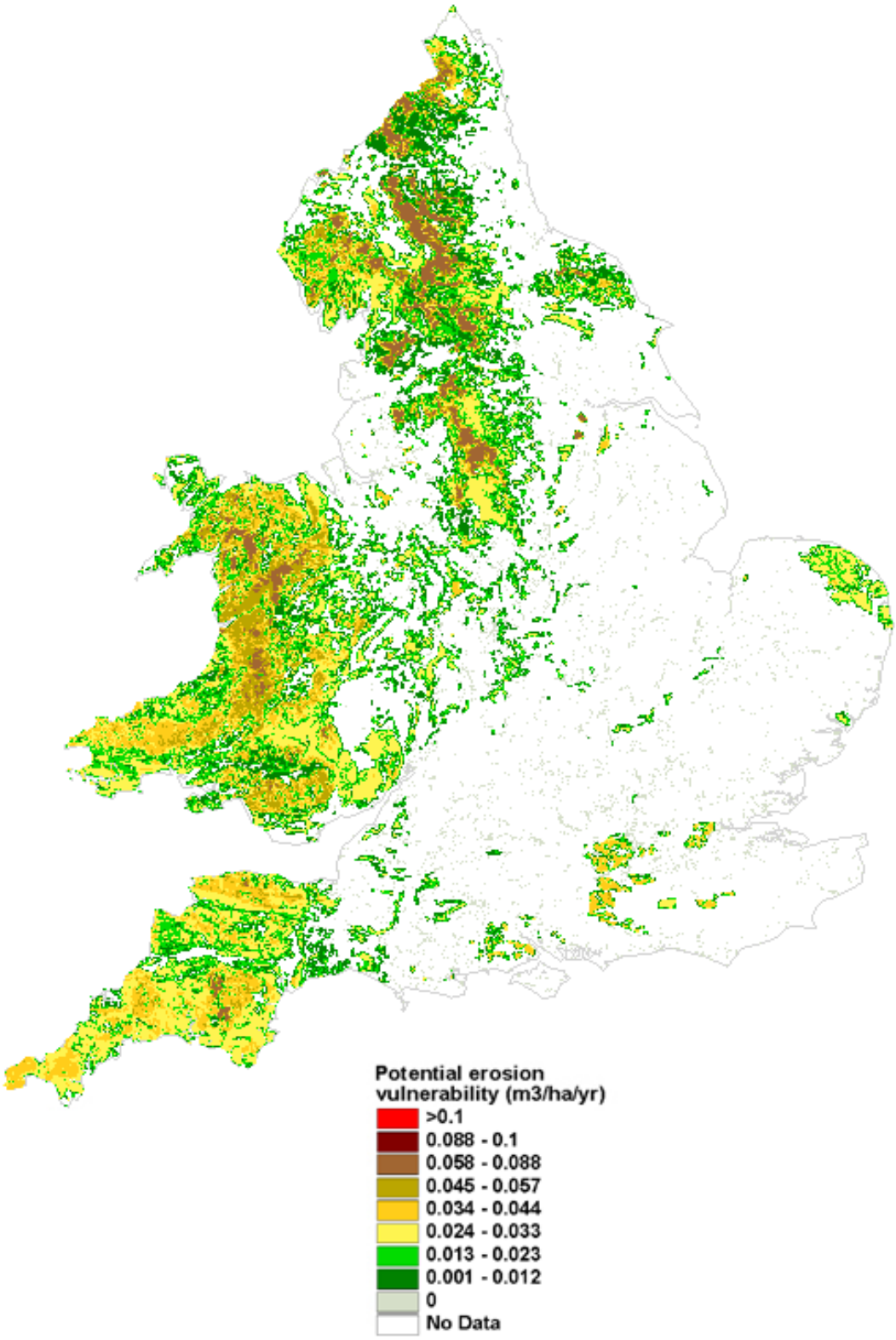

Figure 4.13. Distribution of estimated erosion vulnerability on soils associated with upland land use in England and Wales (1-in-1 year events). N.B. the map assumes all areas are upland land use. No Data relates to areas whose soils are not in the upland erosion database.

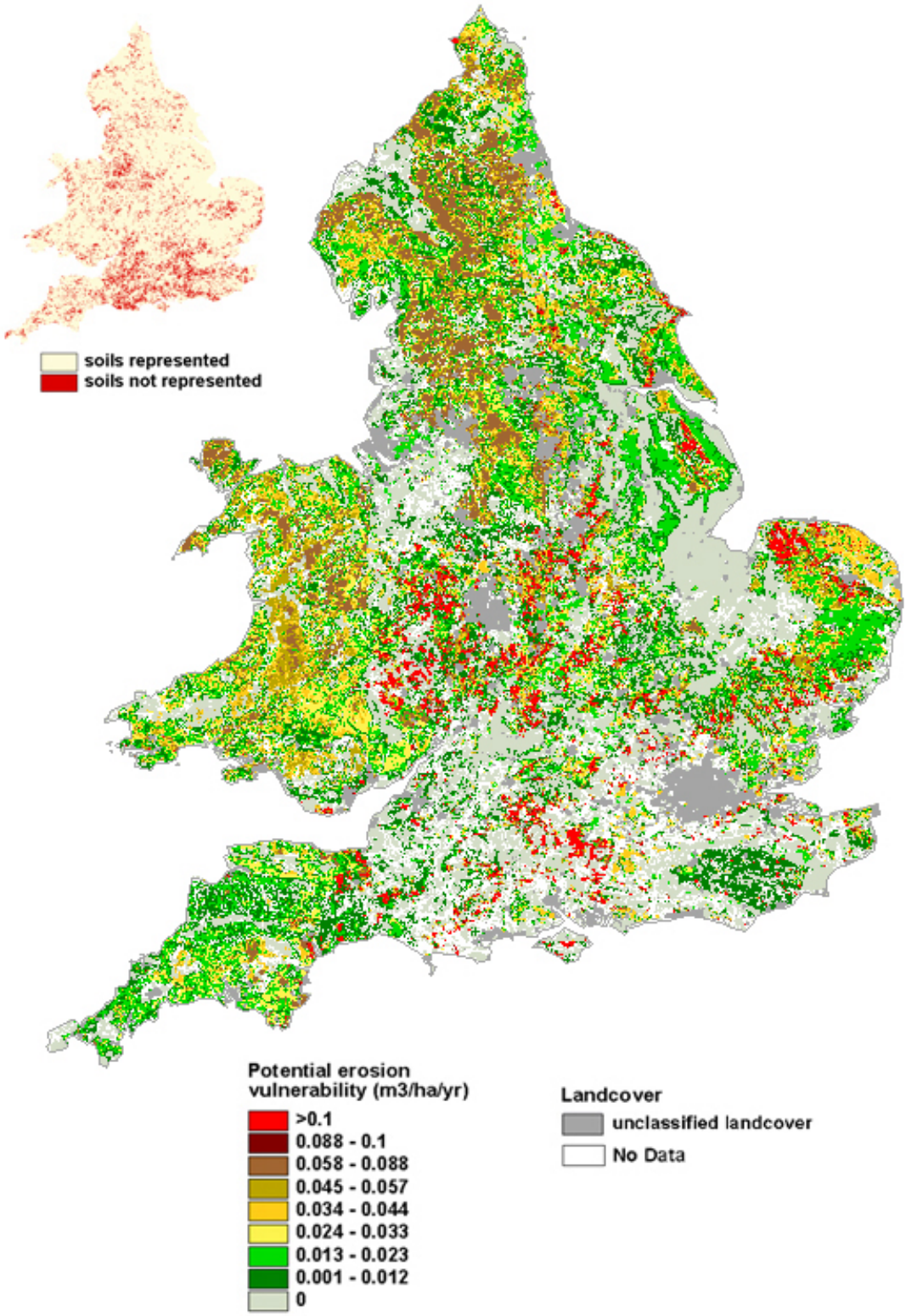

Figure 4.14. Combined map showing the distribution of erosion vulnerability estimates expected to occur annually in England and Wales (1-in-1 year erosion events). *Inset:* areas where the majority of soil (>95%) is not represented in the soil erosion database, represented as 'No Data' in the main map.

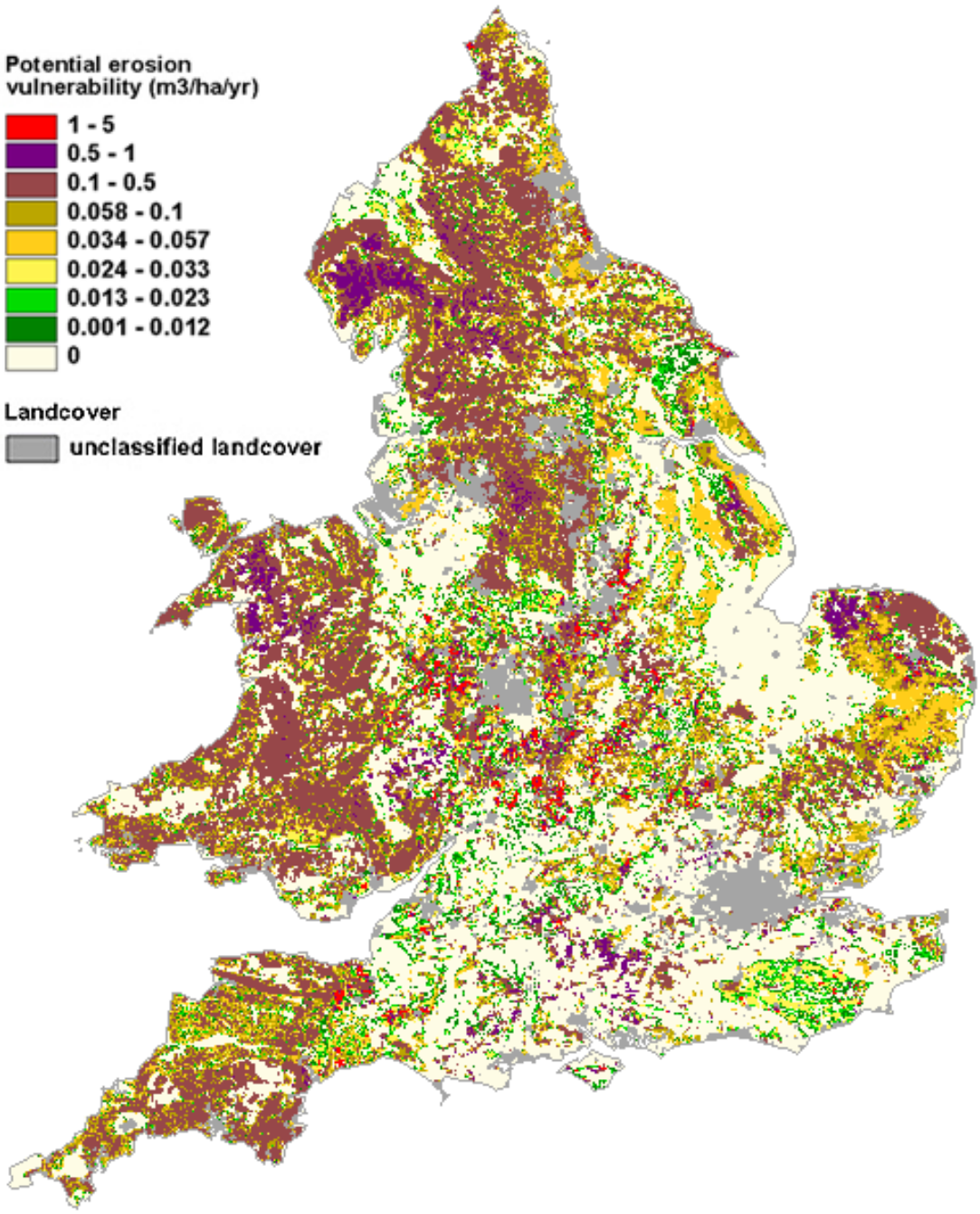

Figure 4.15. Combined map showing the distribution of erosion vulnerability estimates expected to occur annually in England and Wales (1-in-10 year erosion events). *Inset:* areas where the majority of soil (>95%) is not represented in the soil erosion database, represented as 'No Data' in the main map.

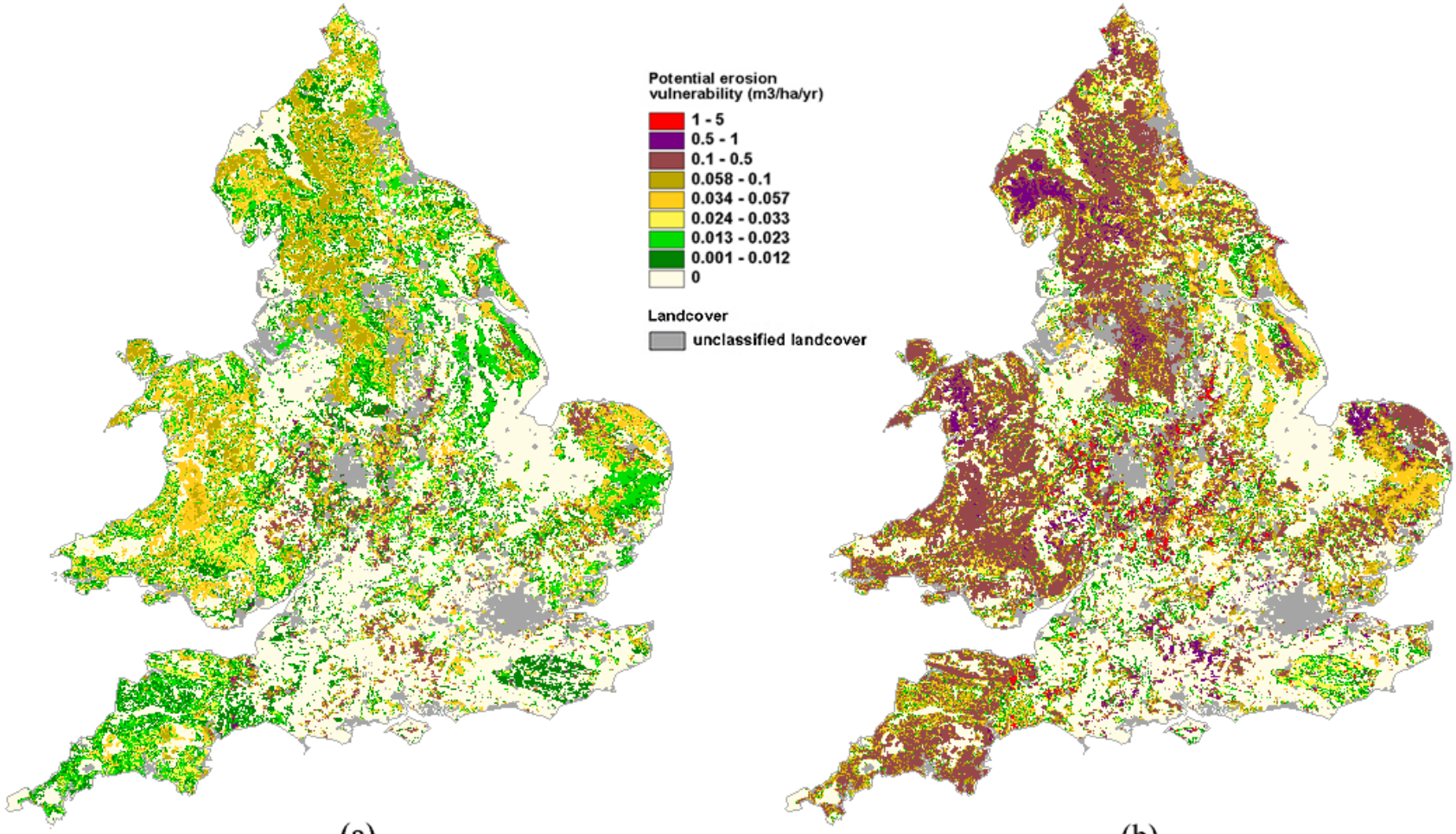

Figure 4.16 Erosion vulnerability for (a) 1-in-1 year erosion events and (b) for 1-in-10 year erosion events, with shared legend.

5 FINAL PROJECT OUTPUT: SEDIMENT DELIVERY TO WATERCOURSES

In this section, the final project output is presented, comprising consolidated maps of sediment delivery to watercourses in England and Wales for arable, lowland grassland and upland soils. The maps represent the linking, through modelling within a GIS environment, of the estimates of sediment generation (Section 4) with the quantitative estimate of the fraction of the sediment mobilised within each 1 km grid-cell that reaches the stream provided by the connectivity ratio (Section 3). The rate of sediment supply to the river system (in m^3 ha^{-1} yr^{-1}) was determined by calculating the product of the rate of sediment generation and the connectivity ratio.

The following figures address the main project objective of estimating annual delivery rates of sediment to watercourses in England and Wales. In Figure 5.1, sediment delivery for the 1-in-1 year return period (p = 0.99) for England and Wales combining all three land uses is shown. In Figure 5.2, sediment delivery for 1-in-10 year (p = 0.999) events is presented and in Figure 5.3, both 1-in-1 year and 1-in-10 year maps are presented together to allow comparison. As before, the legend for the 1-in-1 year map has been modified to conform to that of the 1-in-10 year map.

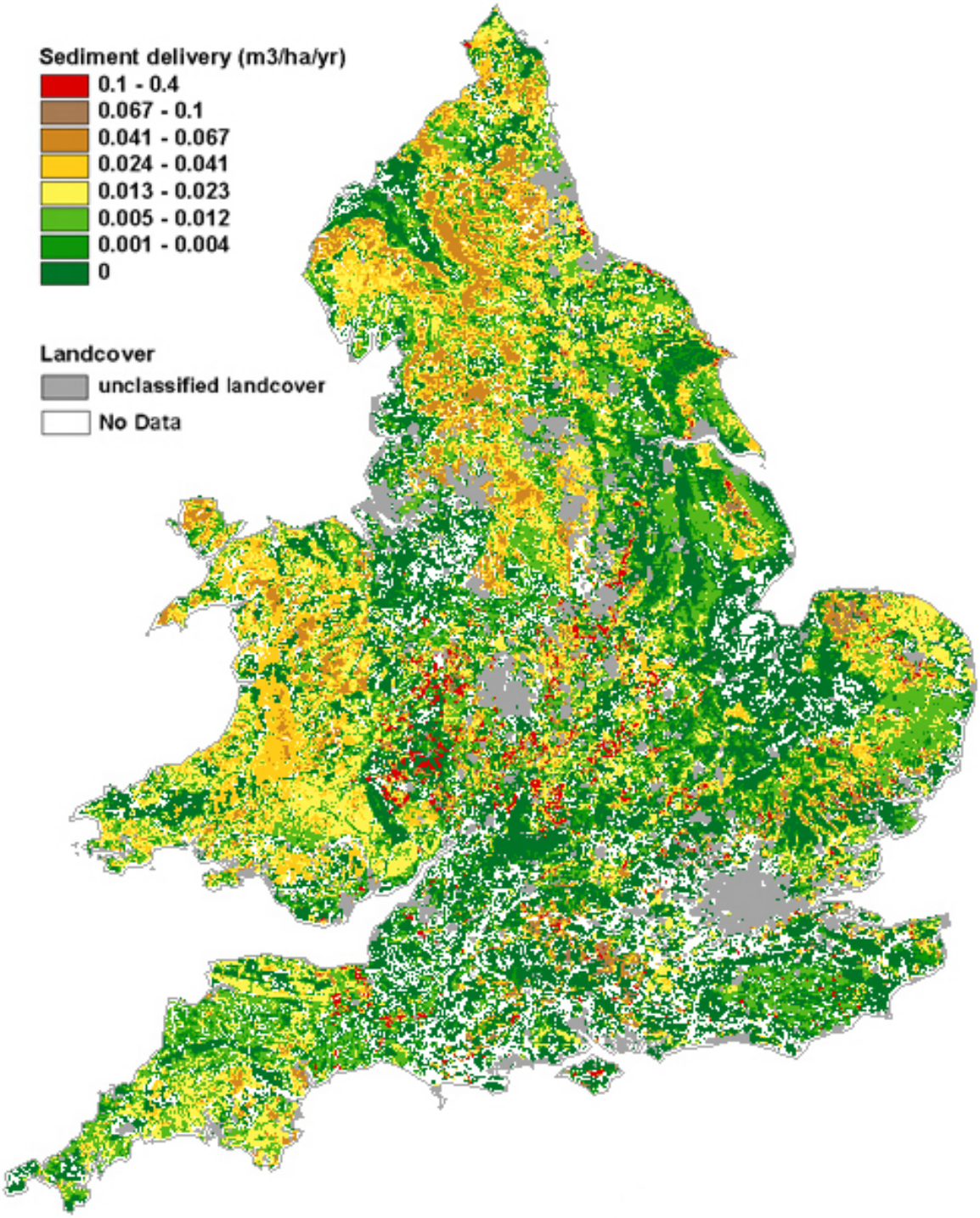

Figure 5.1. Combined map showing the distribution of estimated sediment delivery to watercourses (1-in-1 year) in England and Wales expected to occur annually. 'No Data' indicates where >95% of soil is not represented in the erosion database.

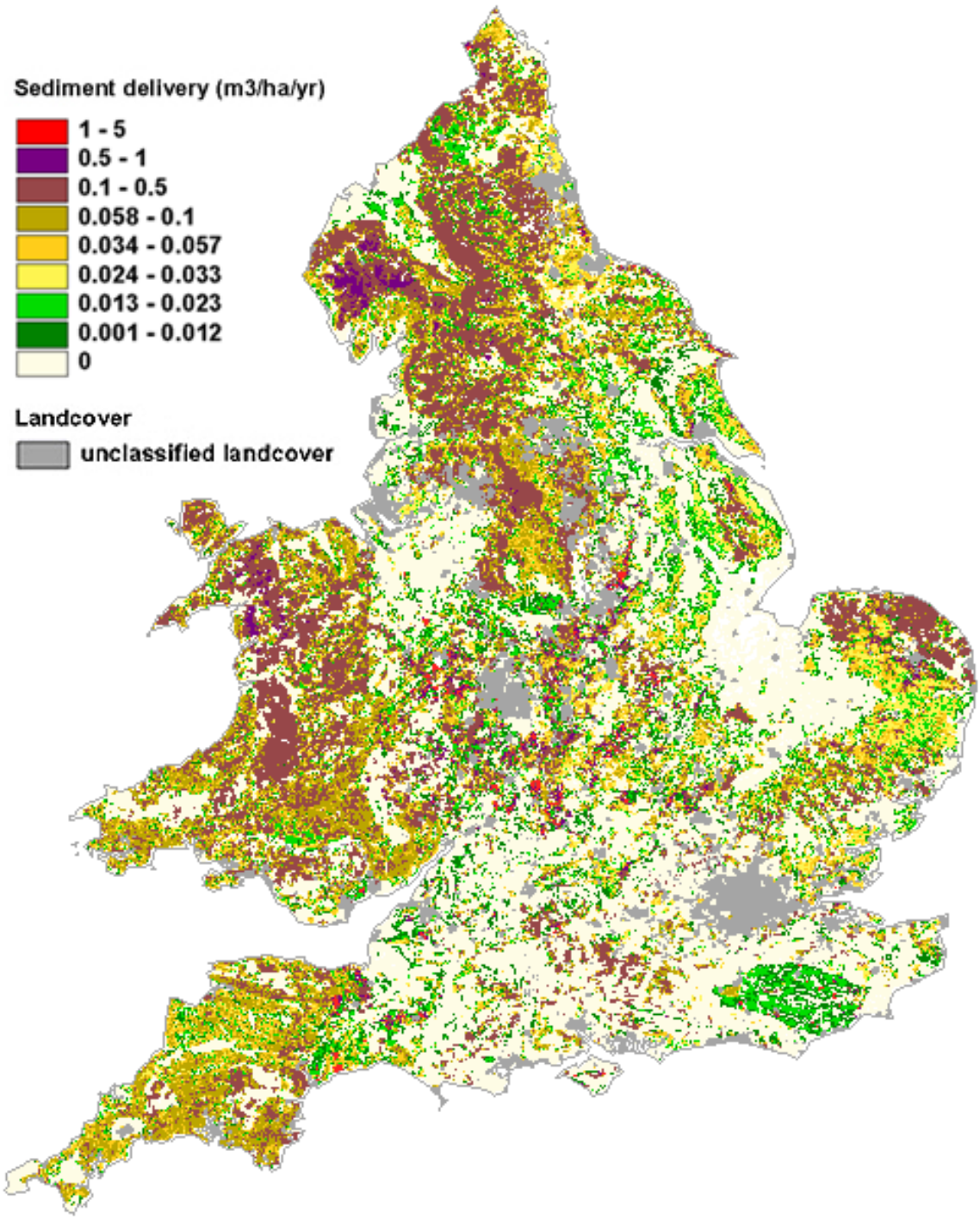

Figure 5.2. Combined map showing the distribution of estimated sediment delivery to watercourses (1-in-10 year) in England and Wales expected to occur annually. 'No Data' indicates where >95% of soil is not represented in the erosion database.

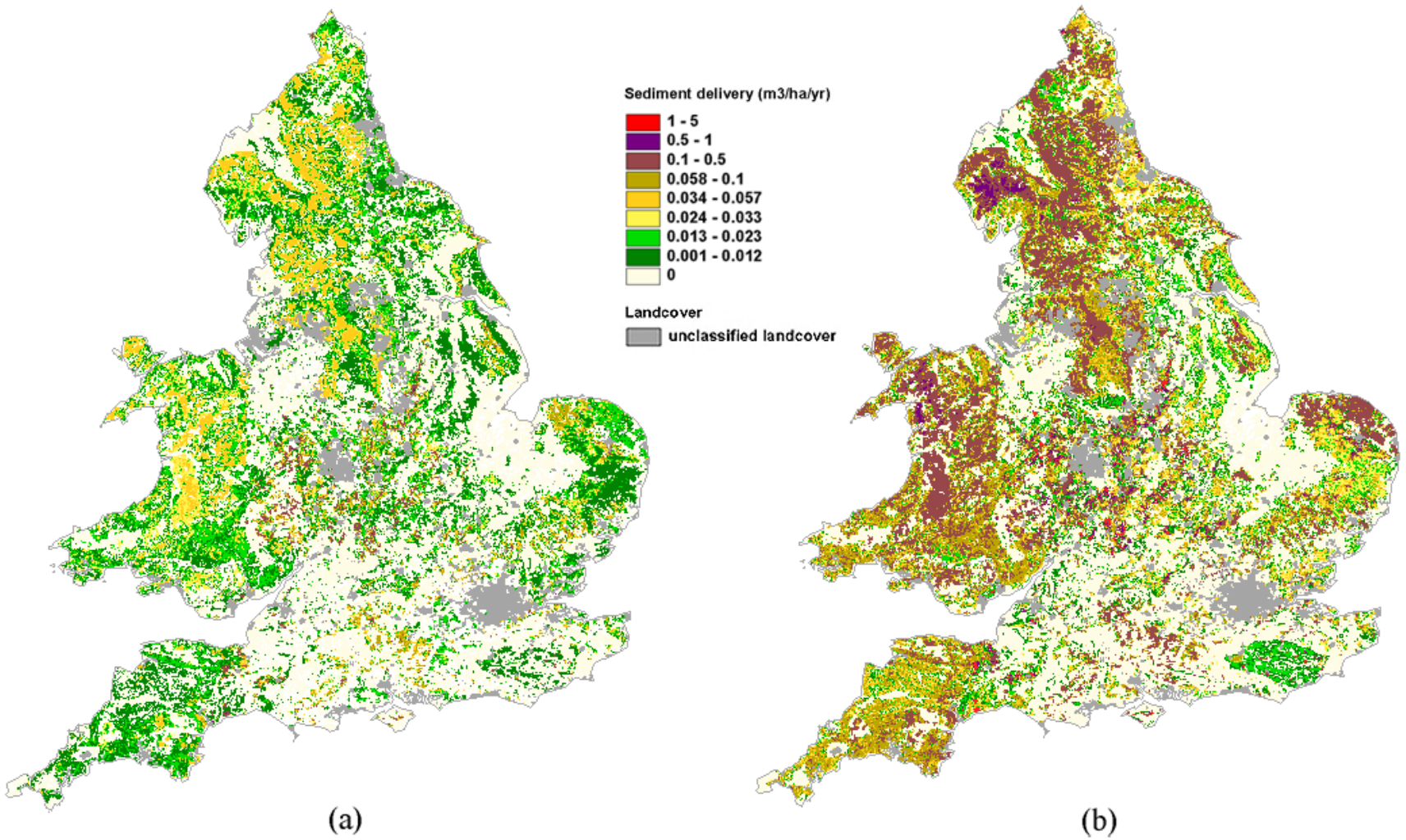

Figure 5.3 Annual sediment delivery rates to watercourses for (a) 1-in-1 year erosion events and (b) 1-in-10 year erosion events, with shared legend.

6 DISCUSSION

This section reviews the mapped output, previous comments on its appropriate use and its limitations, and presents recommendations for future work.

6.1 Sediment generation

The modelling procedure developed in Section 4 has provided a means of estimating sediment delivery to watercourses as a set of mapped outputs in two stages. The first stage provides an estimate of the quantity of annual hillslope erosion based on expected erosion events taking place over specific return periods. The generation of erosion risk tables for 1-in-1 year, 1-in-5 year, and 1-in-10 year probabilities was discussed in Section 2. The mapped output provides a means of assessing the spatial distribution of erosion vulnerability and its estimated magnitude in terms of the volume of generated sediment (m^3 ha^{-1}). Maps of both the 1-in-1 year and 1-in-10 year erosion events are given in Figure 4.16.

The maps for the 1-in-1 year probability show erosion rates that are extremely low. In contrast, the rates shown for the 1-in-10 year probability indicate parts of England and Wales where the erosion exceeds 1.0 m^3 ha^{-1} y^{-1}, equivalent to 1.4 t ha^{-1} y^{-1} on the assumption that the bulk density of the soil is 1.4 Mg m^{-3}. It is generally recognised that annual erosion rates in excess of 1 t ha^{-1} can give rise to unacceptable problems of diffuse pollution and sedimentation (Moldenhauer and Onstad, 1975; Morgan, 1995). The marked differences in rates between the 1-in-1 year and 1-in-10 year probabilities are expected, given the typical characteristics of erosion data obtained over periods of only one to three years. Data on rates of erosion for individual events or individual years are strongly negatively skewed, indicating that rates in very frequent events, such as 1-in-1 year, are low. Serious erosion events, defined as >10 m^3 ha^{-1}, have return periods of 1-in-25 years or more. When such events are sampled within short-term monitoring periods, calculations of the mean annual erosion are biased by the occurrence of these events (see Boardman, 1998; Evans, 1998), causing mean annual values to be unrealistically high. The use of probability analysis helps to reduce this bias. It should be noted, however, that some of the datasets were small and not ideally suited to fitting a probability distribution because of gaps (zeros or lack of occurrences) in moderate to high erosion events (see Figure 2.1). Notwithstanding this reservation, probability analysis provided an effective and convenient way of analysing the data.

The 1-in-10 year probability is proposed as a reasonable indicator of events that are likely to cause environmental problems. Although the rates shown on the map for erodible areas concur with both mean and median rates measured by Evans (1998) and Boardman (1998), they do not contain any occurrences of rates >10 m^3 ha^{-1} yr^{-1}. The reasons for this are, firstly, that such rates have a longer return period and, secondly, the map relates to data averaged over 1 x 1 km squares whereas the field observations of erosion were for fields generally one to three hectares in size.

Although the maps have not been validated, overall they confirm the observations of Evans (1998) that erosion in lowland arable areas is associated with soil associations 3.43, 5.41, 5.51 and 5.71 and that there is an erosion problem in Somerset, the Isle of Wight, Norfolk, the West Midlands and Nottinghamshire. Somewhat surprisingly, the

area of the South Downs, shown by Boardman (1990) to be subject to serious erosion, is not clearly represented on the map, although some individual grid squares designated in the third highest category of erosion probably contain many of his eroded sites.

The probability analysis enabled comparable data on erosion rates to be obtained for lowland arable, upland and lowland grassland soils. It is thus a major improvement on the original methodology, which was based on calculations of erosion rates over variable time periods. This has provided the potential to integrate the three broad landcover types into a single map of continuous estimates of annual erosion rates for England and Wales, allowing subsequent production of continuous estimates of sediment delivery. However, this presumes that landcover can be objectively mapped with an acceptable level of accuracy. In this work, it was not, for two broad reasons

1) The only national coverage of landcover available to this project was the CEH Landcover Map Great Britain (LCMGB) based on 1990 data. More recent data exist (2000), but both datasets have a mapping accuracy of *c*.65%. The accuracy at which lowland grassland can be distinguished from lowland arable is a particular problem.
2) Land use is temporally dynamic (although it may follow a pattern of land management). Hence, if accurately mapped for one date, these maps will not represent the situation at later dates. The degree of this discrepancy is unknown.

Although the LCMGB 1990 data were used for this work, the final composite maps are presented on the assumption that the landcover categories mapped are 100% accurate. This limits the usefulness of the composite maps. The following examples demonstrate the consequential effects of misclassification of land cover type on erosion estimates.

In some cases, it is possible to partly determine landcover (suitability) from soil type since specific soil subgroups are inappropriate for certain land cover practices. For example, there are clearly no lowland grassland or arable practices on peat soils. However, not all soils are exclusive in this way, which means that in some 1 km squares the same soils could be managed in different ways leading to contrasting erosion risks. The effect of land cover misclassification has implications for the accuracy of the final map output.

The preliminary scoping analysis presented in Table 4.4 highlighted the potential class confusion between grassland and arable land cover maps. The implications of this are highlighted using the example in Figure 6.1, which represents the two alternative estimated sediment generation rates if under (a) arable or (b) lowland grassland management, as extracted from Figures 4.9 and 4.11. It highlights three points

1) Mis-labelling a 1 km square's landcover type will lead to systematic errors in estimates of erosion risk and, consequently, sediment delivery. Consider the area around Hereford and Worcester – the visually dominating (red) high erosion class (>0.1 m^3 ha^{-1} yr^{-1}) in Figure 6.1

2) As, in some cases, the erosion risk under arable is an order of magnitude greater than that under grassland management, the errors have significant practical implications
3) There are areas where the soils in the arable erosion table (Table 2.8) are not represented in the grassland erosion table (Tables 2.10), and landcover confusion (between arable and grassland in this case) is, therefore, not an issue. Compare the white areas (no data) in Figure 6.1a with those in 6.1b.

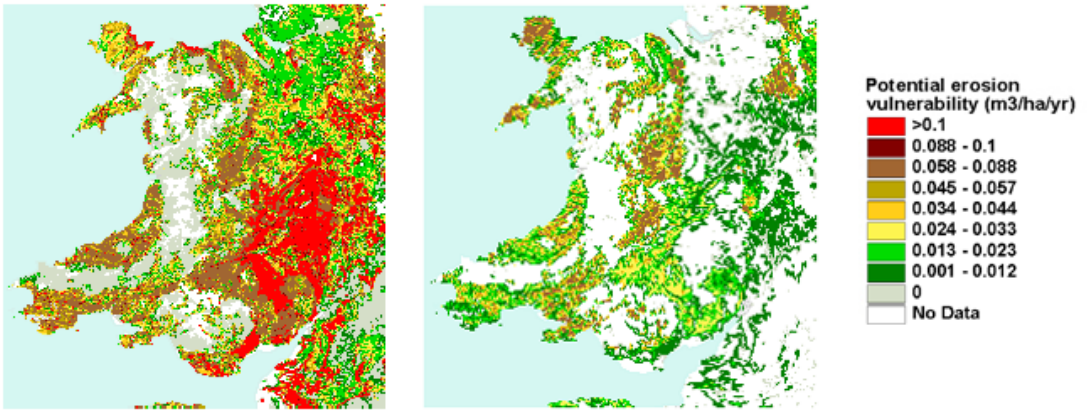

Figure 6.1. Estimated erosion rates for 1-in-10 year erosion events under (a) arable landcover, for soils in the arable erosion database and (b) lowland grassland cover, for soils in the lowland grassland erosion database.

It must be remembered that the composite maps are only as accurate as the land cover maps from which they are referenced. It is recommended, therefore, that the maps generated in the earlier processing step are used instead of the composite maps, *i.e.*, the individual maps (Figures 4.9, 4.11 and 4.13) produced before map integration. In this way, at any given point, the estimated sediment generation for a given 1 km pixel will have three possible values, related to arable, upland or lowland grassland erosion. The appropriate value is then the choice of the user who may have better local knowledge of land cover type.

Several key points relating to data quality, modelling assumptions and mapping accuracy have been made in earlier sections. The main points are drawn together here.

1) The erosion model is based erosion data from the most comprehensive available for England and Wales.
2) The form of the model is founded on sound reasoning and is expected to reflect the real situation very well. However, the data are not validated, and so no statement of model accuracy can be made.
3) Erosion rates are likely to be underestimates because the methodology used to measure soil loss only includes visually evident erosion features, and does not take account of erosion rain-splash and shallow unchannelled flow.
4) The erosion analysis in Section 2 is based on the assumption that spatial probabilities can be used to approximate temporal probabilities.
5) The probability of erosion may be overestimated for soil subgroups 5.13, 5.47 and 5.81.

6.2 Sediment connectivity

The final stage of the spatial data processing procedure linked sediment generation with the connectivity ratio, where the latter provides a quantitative estimate of the fraction of the sediment generated within each 1 km grid-cell that reaches the stream. It was possible to estimate the rate of sediment supply to the river system (m^3 ha^{-1} yr^{-1}) by calculating the product of the rate of sediment generation and the connectivity ratio. Figure 5.3 presents the estimated sediment delivery for 1-in-1 year and 1-in-10 year erosion events. It is this figure that addresses the main project objective of estimating annual delivery rates of sediment to watercourses in England and Wales and identifying those areas most at risk of increased sediment inputs to the watercourses. The main points relating to the estimates of connectivity are

1) The data used to derive measures of slope-channel connectivity are derived from many sources with different levels of precision and quality assurance. It must be accepted that the quality of the generated secondary data layers and the final results cannot be better than that of the data used.
2) The procedure used to derive the connectivity index involved a number of simplifying assumptions. The current procedure takes no account of the influence on sediment transfer efficiency of the spatial topology and linkage of hedges, the location of field gateways and the role of other field boundaries, road networks or man-made drainage systems.
3) It must be emphasised that estimates of sediment input to the stream network, derived as the product of the on-site erosion rate and the connectivity ratio, relate only to sediment supply from the land surface or catchment slopes. Bank erosion may result in additional inputs of sediment, causing the sediment loads passing through the channel system to exceed the calculated inputs.
4) Equally, it should be appreciated that a significant proportion of the sediment entering the stream network from the adjacent slopes may be deposited either in the channel or on the floodplain as it is transported through the channel system. It is therefore not possible to sum the sediment inputs to the stream network from individual grid cells within a catchment and thereby estimate the sediment yield at the catchment outlet.
5) The procedure outlined in Figure 3.5 has been designed to be applied to 1 km grid cells. The values for the connectivity index and connectivity ratio obtained will necessarily involve a degree of spatial averaging and it is likely that areas with both higher and lower connectivity will occur within a specific grid cell. The approach developed here was designed to provide a broad-scale assessment of the risk of sediment transfer to the stream network. A finer scale approach would be necessary to assess the connectivity of individual fields.

6.3 Sediment delivery

This section considers the composite sediment delivery maps presented in Figure 5.3. The divisions in the legend key have been chosen to highlight the most detail in the spatial pattern of sediment delivery rates. Because the distribution of erosion rates is negatively skewed, the class intervals are narrower at the low erosion rates. A cut-off of over 1 m^3 ha^{-1} yr^{-1} was chosen at the upper limit, since, as indicated in Section 6.1, this is considered to be a threshold above which delivery rates have significant management implications.

The best form in which to consider all the output maps is digitally, and on-screen. To facilitate easier interpretation in printed form, Figure 5.3 has been reproduced in Figure 6.2 with only the two highest sediment delivery classes shown. This map identifies more clearly the hotspot areas of highest sediment delivery. Taking the highest value class, i.e. >1 m^3 ha^{-1} yr^{-1}, the main area of high delivery rates is concentrated around the West Midlands, extending down to small areas in East Devon, near to Sidmouth and Taunton. Additional hotspots occur on the East Sussex / Kent border, the north-east coast between Whitby and Redcar, west of Hartlepool and in isolated areas to the west of Norwich. Hotspots also occur on the Scottish border near to Coldstream, on the Tweed and on the Isle of Wight in the west, and also to the east of Newport. For sediment delivery rates of 0.5 to 1 m^3 ha^{-1} yr^{-1}, there are more extensive, contiguous areas in the Gwynedd region of North Wales and in the Lake District.

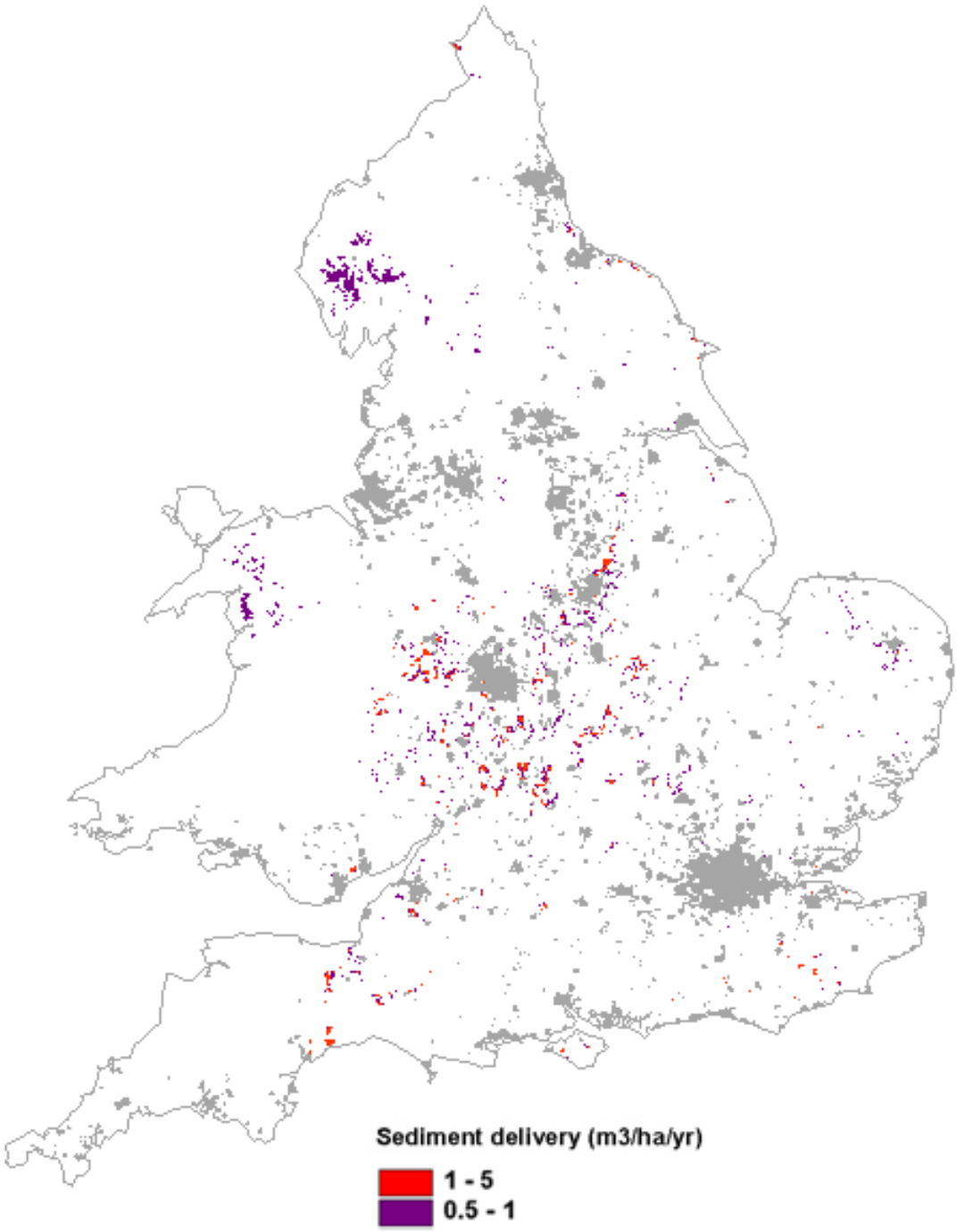

Figure 6.2. Annual sediment delivery rates to watercourses for 1-in-10 year erosion events with only the areas at risk of extreme sediment delivery to watercourses indicated.

7 CONCLUSIONS AND RECOMMENDATIONS

A map estimating the annual sediment delivery rates to watercourses in England and Wales has been produced, based on a 1 km grid. The order of magnitude of the output values is broadly consistent with what is known about suspended sediment loads in UK streams (Walling and Webb, 1987). However, there was no scope in this study for validation and so no statement on accuracy can be made. Whilst the broad distribution appears sensible, it must be reiterated that the erosion rates are likely to be underestimates of total sediment yields because the methodology used only measures of visible, channelled erosion features. The reader is also reminded of the comments made earlier relating to the varying degrees of uncertainty in some of the supporting input mapped data.

It would be possible to do a limited scoping validation exercise, which might inform how a more detailed validation survey could be carried out. This might involve referring to published erosion studies and comparing erosion figures in those same geographic regions, with the output values from this project. The output could be further improved by considering the effect on risk of different crop cover. Simply labelling a land parcel as arable masks the range in erosion risk that is possible when the land is managed under different cover crops. There is some scope to consider using the current arable erosion data to produce maps showing erosion at different levels of probability if the arable area was under winter cereals or sugar beet, i.e. the crops most frequently associated with serious erosion (Evans, 1998). There may also be a possibility of using the upland data set to consider scenarios with different grazing intensities. There is little scope with the current data for further work on lowland grassland erosion.

The need for validation and improvement extends to the estimates of connectivity, for which a key deficiency relates to the present limited understanding of sediment delivery processes and thus of the factors influencing the efficiency of slope-channel sediment transfer. To a large extent, this reflects the lack of detailed field investigations of sediment delivery and related experimental investigations and thus the paucity of empirical data for use in developing, calibrating and validating models. There is therefore a clear need for further field-based and empirical investigations to remedy these deficiencies. Such work should focus on both the more traditional representation of sediment delivery and its controlling factors, such as that employed in this study, as well as the need to incorporate what have been termed adventitious effects, and which include the role of field boundaries, field gates, unmetalled tracks, and roads and road drains. It should involve both direct monitoring, as well as the use of sediment tracers, including Cs-137, Pb-210 and Be-7, which permit retrospective assessment and interpretation of soil and sediment redistribution and delivery processes. This work could usefully subdivide the delivery processes operating in agricultural landscapes into three components related to the movement of sediment from within a field to the field boundary, the transfer of sediment along and through the field boundaries and the routing of the sediment leaving the field to the stream channel. Field investigations should be coupled with experimental studies of aspects such as the size selectivity of sediment

transfer and improved characterisation of surface roughness, to take account of both the microtopography and the vegetation cover.

The empirical data assembled could be used to improve and refine each of the key components of the existing procedure and for calibration purposes. Key aspects to be addressed would include:

1) Specification and parameterisation of the controlling factors.
2) Formulation of the numerical procedure used to derive the estimate of the connectivity index from values for the controlling factors.
3) Calibration of the relationship between the connectivity ratio and the connectivity index.

These objectives should be used to guide and focus the data collection programme, in order to ensure that it met the requirements of the study.

In addition, there remains an important need to validate the current procedure for estimating the connectivity index and any further refinement of that procedure that might be developed. This should involve a targeted programme of data collection aimed at assembling information on soil erosion rates and sediment yields from a representative selection of small catchments in order test the model in those catchments. Some of these data could be derived from existing studies, although there would be a need to undertake additional monitoring and field sampling to complete the datasets.

8 REFERENCES

Avery, B.W. (1980). Soil Classification for England and Wales (Higher Categories). Soil Survey Technical Monograph No. 14. Harpenden.

Bibby, J.S. and Mackney, D. (1969). Land use capability classification. Soil Survey Technical Monograph No. 1, Harpenden.

Boardman, J. (1990). Soil erosion on the South Downs: a review. In Boardman, J., Foster, I.D.L. and Dearing, J.A. (eds), Soil erosion on agricultural land. Wiley, Chichester, 87-105.

Boardman, J. (1998.) Modelling soil erosion in real landscapes: a Western European perspective. In Boardman, J. and Favis-Mortlock, D. (eds), Modelling soil erosion by water. Springer-Verlag, Berlin, 17-29.

Boorman, D.B., Hollis J.M. and Lilly, A. (1995). Hydrology of soil types: a hydrologically-based classification of the soils of the United Kingdom (Report No.126). Institute of Hydrology, Crowmarsh Gifford, Wallingford, Oxfordshire, OX10 8BB.

Bower, M.M. (1962). The cause of erosion in blanket peat bogs. A review of evidence in the light of recent work in the Pennines. Scottish Geographical Magazine 78, 33-43.

Bunce, R.G.H. (1987). The extent and composition of upland areas in Great Britain. *In* Agriculture and Conservation in the Hills and Uplands. (M. Bell and R. G. H. Bunce, eds.), pp. 19-21. Institute of Terrestrial Ecology, Grange-over-Sands, Cumbria.

Butcher, D.P., Claydon, J., Labdaz, J.C., Pattinson, V.A., Potter A.W.R. and White, P. (1992). Reservoir sedimentation and colour problems in Southern Pennine reservoirs. IWEM 1991 Conference.

De Ploey, J. (1984). Hydraulics of runoff and loess loam deposition. Earth Surface Processes and Landforms 9: 533-539.

Evans, E. and Skinner, D. (1987). A survey of soil erosion. Soil and Water 15 (1-2), 28-31.

Evans, R. (1990). Erosion studies in the Dark Peat. Journal of Northern Soils Discussion Group 24, 39-61.

Evans, R. (1990a). Soils at risk of accelerated erosion in England Wales. Soil Use and Management 6: 125-131.

Evans, R. (1990b). Erosion studies in the Dark Peak. Journal of Northern Soils Discussion Group 24: 39-61.

Evans, R. (1996) Soil erosion and its impacts in England and Wales. Friends of the Earth Trust, London.

Evans, R. (1998). Field data and erosion models. In Boardman, J. and Favis-Mortlock, D. (eds), Modelling soil erosion by water. Springer-Verlag, Berlin, 313-327.

Everaert, W. (1991). Empirical relations for the sediment transport capacity of interrill flow. Earth surface processes and landforms. Vol. 16, 513-532.

Fraser, A.I., Harrod, T.R. and Walling, D.E. (2000). Sediment Delivery from arable land and delivery to Surface Waters. Phase I: A Pilot GIS Feasibility Study. Final Report to the Environment Agency.

Govers, G. (1985). Selectivity and transport capacity of thin flows in relation to soil erosion. Catena, Vol.12, 35-49.

Hall, D.G.M., Reeve, M.J., Thomasson, A.J. and Wright, V.F. (1977). Water retention, porosity and density of field soils. Soil Survey Technical Monograph No. 9.

Harrod, T. R. (1979). Soil suitability for grassland. Soil Survey Applications. Eds: M. G. Jarvis and D. Mackney. Soil Survey Technical Monograph No. 13: 51-70.

Harrod T.R. (1998). A systematic approach to national budgets of Phosphorus loss through soil erosion and surface runoff at National Soil Inventory (NSI) nodes. Final Report to MAFF. MAFF project NT1014, SSLRC Project JF3818.

Harrod T.R., McHugh, M., Appleby, P.G., Evans, R., George, D.G., Haworth, E.Y., Hewitt, D., Hornung, M., Housen, G. Leeks, G. Morgan, R.P.C., Tipping, E. (2000). Research on the quantification and causes of upland erosion. Final report to MAFF (Project SP0402).

Heathwaite, A.L., Burt, T.P. and Trudgill, S.T. (1990a). The effect of land use on nitrogen, phosphorus and suspended sediment delivery to streams in a small catchment in Southwest England. *In* Thornes, J.B. (ed), Vegetation and erosion. Wiley, Chichester, 161-177.

Heathwaite, A.L., Burt, T.P. and Trudgill, S.T. (1990b). Land-use controls on sediment production in a lowland catchment, south-west England. *In* Boardman, J., Foster, I.D.L. and Dearing, J.A. (eds), Soil erosion on agricultural land. Wiley, Chichester, 69-86.

Higgitt D.L. and Lu X.X. (2001). Sediment delivery to the three gorges: 1. Catchment controls. Geomorphology, 41 (2-3): 143-156.

Hodgson, J. M. (1997). Soil Survey Handbook. SSLRC Technical Monograph No.5. Soil Survey and Land Research Centre (Cranfield University), Silsoe, Bedfordshire, UK.

Hudson, N.W. (1981). Soil conservation. Batsford, London.

Lea, J.W. (1979). Slurry acceptance. Soil Survey Applications. Eds: M. G. Jarvis and D. Mackney. Soil Survey Technical Monograph No. 13: 83-100. Soil Survey of England and Wales, Harpenden, Herts.

McGrath, S.P. and Loveland, P.J. (1992). The Soil Geochemical Atlas of England and Wales. 101 pp. Blackie.

McHugh, M. (2000). Extent, causes and rates of upland soil erosion in England and Wales. PhD Thesis, Cranfield University.

McHugh, M**.** (2002). NSI erosion resurvey. DEFRA Project SP0407, 2002.

McHugh, M., Harrod, T.R. and Morgan, R.P.C. (2002). The extent of soil erosion in upland England and Wales. Earth Surface Processes and Landforms 27: 99-107.

Meyer, L.D. and Monke, E.J. (1965). Mechanics of soil erosion by rainfall and overland flow. Transactions of ASAE, 8, 572-577, 580.

Moldenhauer, W.C. and Onstad, C.A. (1975). Achieving specified soil loss levels. Journal of Soil and Water Conservation 30:166-168.

Moore, I.D. and Burch, G.J. (1986). Modelling erosion and deposition: topographic effects. Transactions of the ASAE, Vol. 29(6), 1624-1630.

Morgan, R.P.C. (1985). Assessment of soil erosion risk in England and Wales. Soil Use and Management, 1, 127-131.

Morgan, R.P.C. (1985). Assessment of soil erosion risk in England and Wales. Soil Use and Management 1: 127-131.

Morgan, R.P.C. (1995). Soil erosion and conservation. Second edition, Longman,

Paine, A.D.M. (1985). 'Ergodic' reasoning in geomorphology: time for a review of the term. Progress in Physical Geography 9: 1-15.

Phillips, J., Yalden, D. and Tallis, J. (1981). Moorland Erosion Project, Phase 1 Report. Bakewell, Peak Park Planning Board.

Proctor, M.E., Siddons, P.A., Jones, R.J.A., Bellamy, P.H. and Keay, C.A. (1998). LandIS - a Land Information System for the UK. European Soil Bureau Research Report No. 4 EUR 17729 EN.

Prosser, I.P. and P. Rustomji (2000). Sediment transport capacity relations for overland flow. Progress in Physical Geography, Vol. 24(2), 179-193.

Renard, K.G., Foster, G.R., Weesies, G.A., Porter, J.P, (1991). RUSLE: Revised Universal Soil Loss Equation. Journal of Soil and Water Conservation, Vol. 40 (1): 30- 33.

Richards J A, Jia X (1999) Remote Sensing Digital Image Analysis – An introduction. 3rd edition, Springer, pp 259-290.

Robinson, D.A. and Blackman, J.D. (1990). Some costs and consequences of soil erosion and flooding around Brighton and Hove, Autumn 1987. In Soil Erosion on Agricultural Land (edited by J. Boardman, I.D.L. Foster and J.A. Dearing). John Wiley and Sons, Chichester.

Rudeforth, C.C., Hartnup, R., Lea, J.W., Thompson, T.R.E., Wright, P.S. (1984). Soils and their use in Wales. Soil Survey of England and Wales Bulletin No. 11. Harpenden.

Russell, M.A., Walling, D.E. and Hodkinson, R. (2001). Suspended sediment sources in two small lowland agricultural catchments in the UK. Journal of Hydrology 252, 1-24.

Scheidegger, A.E. (1970). Theoretical geomorphology. Springer-Verlag, New York.

Scheidegger, A.E. and Langbein, W.B. (1966). Probability concepts in geomorphology. United States Geological Survey Professional Paper No. 500-C.

Schowengerdt, R.A. (1997) Techniques for Image Processing and Classification in Remote Sensing, Academic Press, pp249.

Soil Survey of England and Wales, (1983). Legend for the 1:250,000 Soil Map of England and Wales. Harpenden.

Tallis, J.H. (1987). Fire and flood at Holme Moss: erosion processes in an upland blanket mire. Journal of Ecology 75, 1099-1129.

Tallis, J.H. (1994). Pool-and-hummock patterning in a Southern Pennine blanket mire II. The formation and erosion of the pool system. Journal of Ecology 82, 789-803.

Taylor, J.C., Sannier, C., Delince J and Gallego, F.J. (1997). Regional crop inventories in Europe assisted by remote sensing: 1988 – 1993. Synthesis report of the MARS Project – Action 1, Joint Research centre, Ispra, EUR 17319, pp71.

Theurer, F.D., Harrod, T.R., Theurer, M. (1998). Sedimentation and Salmonids in England and Wales. Environment Agency Technical Report P194.

Thomasson, A.J. (1982). Soil and climatic aspects of workability and trafficability. Proceedings of the 9th Conference of the International Soil Tillage Research Organisation, Osijek, Yugoslavia.

Walling D.E., Collins A.L., Sichingabula H.M. and Leeks, G.J.L. (2001). Integrated assessment of catchment suspended sediment budgets: a Zambian example. Land Degradation and Development 12 (5): 387-415.

Walling, D.E. (1983). The sediment delivery problem. Journal of Hydrology, Vol. 65, 209-237.

Walling, D.E. and Webb, B.W. (1987). Suspended load in gravel-bed rivers: UK experience. *In* C.R. Thorne, J.C. Bathurst and R.D. Hey (eds) Sediment Transport in Gravel-Bed Rivers, Wiley, Chichester, pp 691-732.

Young, A. (1972). Slopes. Oliver & Boyd, Edinburgh.

9 LIST OF FIGURES

Figure ES1. The distribution of (a) of erosion vulnerability estimates and (b) estimated sediment delivery to watercourses expected to occur annually in England and Wales under 1-in-10 year events. 'No Data' indicates where >95% of soil is not represented in the erosion database.

Figure 2.1 Frequency of erosion classes for soil subgroups 5.71 and 5.72 under lowland arable on slopes ≥3°.

Figure 3.1. The spatial distribution of the average distance to watercourse after log transformation. The value for each 1 km grid cell represents the median value for the individual 50m subgrid cells. Based on the CEH 1: 50 000 river network.

Figure 3.2 The spatial distribution of the sediment transport capacity of overland flow (log transformed).

Figure 3.3. The spatial distribution of the connectivity index.

Figure 3.4. The spatial distribution of the connectivity ratio.

Figure 3.5. Flow chart of the GIS-based procedure used for the estimation of the connectivity index and ratio.

Figure 4.1. 7 km x 7 km area indicating slope gradient classes derived from the Ordnance Survey 50 m PANORAMA DEM. Left: the original 50 m slope classes with red lines representing a 1 km grid. Right: how slope classes might be represented if simply averaged.

Figure 4.2 – Characterisation of slope distribution within each 1 km pixel. The inset shows a 1 km x 1 km area with its respective slope distribution histogram indicating the frequency of each slope class.

Figure 4.3 Example of the slope classes used to determine sediment generation rates on arable and lowland grassland soils. The maps show the distribution of slope classes and their percentage proportions occurring in each 1 km pixel.

Figure 4.4. The effect of a 3x3 majority filter on the 1 km pixel landcover map.

Figure 4.5. Landcover mask for England and Wales, produced at 1 km pixel resolution from LCMGB 1990. Landcover classes are given along with the percentage probability of misclassification in relation to the other landcover classes; Ar – arable, LG – lowland grassland, and Up – upland.

Figure 4.6. Class distributions in a single 1 km pixel used to determine class weightings, ω. Top: slope classes. Bottom: four soil classes. Sum of weightings ω of each histogram equals 1.0.

Figure 4.7. Schematic diagram indicating the use of soil and slope gradient data within the GIS.

Figure 4.8. Arable areas as determined from the CEH LCMGB 1990. Red areas refer to arable areas where the majority of soil (>95%) was not represented in the soil erosion database. *Refer to Section 4.4.2 (classification accuracy).

Figure 4.9. Distribution of estimated erosion vulnerability (1-in-1 year events) on soils associated with arable land use in England and Wales. N.B. the map assumes all areas are under arable land use. No Data relates to areas whose soils are not in the arable erosion database.

Figure 4.10. Lowland grassland areas as determined from the CEH LCMGB 1990. The red areas refer to grassland areas where the majority of soil (>95%) was not represented in the soil erosion database. *Refer to Section 4.4.2 (Classification accuracy).

Figure 4.11. Distribution of estimated erosion vulnerability on soils associated with lowland grassland production in England and Wales (1-in-1 year events). N.B. the map assumes all areas are lowland grassland land use. No Data relates to areas whose soils are not in the lowland grassland erosion database.

Figure 4.12. Upland areas as determined from the CEH LCMGB 1990. The red areas refer to upland areas where the majority of soil (>95%) was not represented in the soil erosion database. *Refer to Section 4.4.2 (Classification accuracy).

Figure 4.13. Distribution of estimated erosion vulnerability on soils associated with upland land use in England and Wales (1-in-1 year events). N.B. the map assumes all areas are upland land use. No Data relates to areas whose soils are not in the upland erosion database.

Figure 4.14. Combined map showing the distribution of erosion vulnerability estimates expected to occur annually in England and Wales (1-in-1 year erosion events). *Inset:* areas where the majority of soil (>95%) is not represented in the soil erosion database, represented as 'No Data' in the main map.

Figure 4.15. Combined map showing the distribution of erosion vulnerability estimates expected to occur annually in England and Wales (1-in-10 year erosion events). *Inset:* areas where the majority of soil (>95%) is not represented in the soil erosion database, represented as 'No Data' in the main map.

Figure 4.16 Erosion vulnerability for (a) 1-in-1 year erosion events and (b) for 1-in-10 year erosion events, with shared legend.

Figure 5.1. Combined map showing the distribution of estimated sediment delivery to watercourses (1-in-1 year) in England and Wales expected to occur annually. 'No Data' indicates where >95% of soil is not represented in the erosion database.

Figure 5.2. Combined map showing the distribution of estimated sediment delivery to watercourses (1-in-10 year) in England and Wales expected to occur annually. 'No Data' indicates where >95% of soil is not represented in the erosion database.

Figure 5.3 Annual sediment delivery rates to watercourses for (a) 1-in-1 year erosion events and (b) 1-in-10 year erosion events, with shared legend.

Figure 6.1. Estimated erosion rates for 1-in-10 year erosion events under (a) arable landcover, for soils in the arable erosion database and (b) lowland grassland cover, for soils in the lowland grassland erosion database.

Figure 6.2. Annual sediment delivery rates to watercourses for 1-in-10 year erosion events with only the areas at risk of extreme sediment delivery to watercourses indicated.

10 LIST OF TABLES

Table 2.1 Vulnerability of lowland arable soils to soil erosion based on texture and calcareous nature of the topsoil (after Evans, 1990; Harrod, 1998)

Table 2.2 Slope gradients proposed for assessment of vulnerability of lowland arable soils to soil erosion

Table 2.3 Mean annual soil erosion (m^3 ha^{-1}) for lowland arable soils according to topsoil texture classes (A-E) and slope classes (I-V) (Harrod, 1998). Blanks represent classes for which no data exist.

Table 2.4 Classification of upland soils into HOST classes (Boorman *et al.,*1995)

Table 2.5 Amounts of soil loss (m^3 ha^{-1}) for upland soils (Harrod *et al.,* 2000). Values relate to variable and unspecified time periods.

Table 2.6 Vulnerability of lowland grassland soils to erosion based on HOST poach classes.

Table 2.7 Cumulative probability distributions based on Poisson distribution for selected soil subgroups under lowland arable.

Table 2.8 Estimated annual soil erosion (m^3 ha^{-1}) for lowland arable soils with given return periods.

Table 2.9 Estimated annual soil erosion (m^3 ha^{-1}) for upland soils with given return periods.

Table 2.10 Estimated annual soil erosion (m^3 ha^{-1}) for lowland grassland soils with given return periods.

Table 2.31a Vulnerability of soil subgroups (3.11 to 5.83) to erosion under different land uses. Shading denotes vulnerable soils; n/a = conditions do not exist in surveyed data.

Table 2.41b Vulnerability of soil subgroups (6.11 to 10.13) to erosion under different land uses. Shading denotes vulnerable soils; n/a = conditions do not exist in surveyed data.

Table 4.1. Extract from the NatMap attribute table, indicating soil composition within each 1 km pixel in decreasing order of dominance.

Table 4.2. Frequency histogram of the proportion of individual 1 km pixels represented by their dominant soil series within England and Wales.

Table 4.3. Classification scheme relating the CEH landcover subgroups to the NSRI erosion survey landcover groups.

Table 4.4. Cross-tabulation matrix indicating landcover class mapping accuracy. Diagonal values indicate agreement between NRSI and CEH classification.

APPENDIX 1

DATA FOR CLASSIFICATION OF EROSION VULNERABILITY ON ARABLE, GRASSLAND AND UPLAND SOILS

Table 1.1 Quantitative erosion on arable field sites, classified according to topsoil texture groups (A – E) and slope (Harrod, 1998).

	Topsoil texture group					
	Slope	A	B	C	D	E
Number of field sites	<1	9	48	51	12	0
	1-2.99	9	93	63	36	3
	3-6.99	3	81	99	69	6
	7-11	3	27	36	27	9
	>11	0	3	0	9	0
	Total	24	252	249	153	18

		A	B	C	D	E
Total erosion (m^3/ha)	<1	0.00	1.21	0.12	0.00	0.00
	1-2.99	0.00	4.83	6.24	0.30	0.00
	3-6.99	0.14	39.47	6.32	4.50	0.00
	7-11	0.00	9.71	0.38	1.31	2.50
	>11	0.00	0.00	0.00	1.11	0.00

		A	B	C	D	E
Mean erosion (m^3/ha)	<1	0.00	0.03	0.00	0.00	0.00
	1-2.99	0.00	0.05	0.10	0.01	0.00
	3-6.99	0.05	0.49	0.06	0.07	0.00
	7-11	0.00	0.36	0.01	0.05	0.28
	>11	0.00	0.00	0.00	0.12	0.00

		A	B	C	D	E
Median erosion (m^3/ha)	<1	0.00	0.00	0.00	0.00	0.00
	1-2.99	0.00	0.05	0.00	0.00	0.00
	3-6.99	0.07	0.49	0.00	0.00	0.00
	7-11	0.00	0.36	0.00	0.00	0.00
	>11	0.00	0.00	0.00	0.00	0.00
		0.00	0.00	0.00	0.00	0.00

Table 1.2 HOST classes and their descriptions (from Boorman *et al.*, 1995 and Procter *et al.*, 1998). Underlined HOST classes are represented by upland National Soil Inventory field sites, and therefore have associated soil erosion data.

HOST	DESCRIPTION
1	Free draining permeable soils on chalk and chalky substrates with relatively high permeability and moderate storage capacity.
2	Free draining permeable soils on 'brashy' or dolomitic limestone substrates with high permeability and moderate storage capacity.
3	Free draining permeable soils on soft sandstone substrates with relatively high permeability and high storage capacity.
4	Free draining permeable soils on hard but fissured rocks with high permeability but low to moderate storage capacity.
5	Free draining permeable soils in unconsolidated sands or gravels with relatively high permeability and high storage capacity.
6	Free draining permeable soils in unconsolidated loams or clays with low permeability and storage capacity.
7	Free draining permeable soils in unconsolidated sands or gravels with groundwater at less than 2m from the surface.
8	Free draining permeable soils in unconsolidated loams or clays with groundwater at less than 2m from the surface.
9	Soils seasonally waterlogged by fluctuating groundwater and with relatively slow lateral saturated conductivity.
10	Soils seasonally waterlogged by fluctuating groundwater and with relatively rapid lateral saturated conductivity.
11	Drained lowland peaty soils with groundwater controlled by pumping.
12	Undrained lowland peaty soils waterlogged by groundwater.
13	Soils with slight seasonal waterlogging from transient perched water tables caused by slowly permeable subsoil or substrate layers.
14	Soils seasonally waterlogged by perched water tables caused by impermeable subsoil or substrate layers.
15	Permanently wet, peaty topped upland soils over relatively free draining permeable rocks.
16	Relatively free draining soils with a moderate storage capacity over slowly permeable substrates with negligible storage capacity.
17	Relatively free draining soils with a large storage capacity over hard impermeable rocks with no storage capacity.
18	Slowly permeable soils with slight seasonal waterlogging and moderate storage capacity over slowly permeable substrates with negligible storage.
19	Relatively free draining soils with a moderate storage capacity over hard impermeable rocks with no storage capacity.
20	Slowly permeable soils with slight seasonal waterlogging and moderate storage capacity over impermeable clay substrates with no storage capacity.
21	Slowly permeable soils with slight seasonal waterlogging and low storage capacity over slowly permeable substrates with negligible storage capacity.
22	Relatively free draining soils with low storage capacity over hard impermeable rocks with no storage capacity.
23	Slowly permeable soils with slight seasonal waterlogging and low storage capacity over impermeable clay substrates with no storage capacity.
24	Slowly permeable, seasonally waterlogged soils over slowly permeable substrates with negligible storage capacity.
25	Slowly permeable, seasonally waterlogged soils over impermeable clay substrates with no storage capacity.
26	Permanently wet, peaty topped upland soils over slowly permeable substrates with negligible storage capacity.
27	Permanently wet, peaty topped upland soils over hard impermeable rocks with no storage capacity.
28	This soils type, eroded peat, is not mapped separately in England & Wales.
29	Permanently wet upland blanket peat.
98	Lake
99	Sea

Table 1.3 Summary data for gross erosion on upland field sites, measured in 1999 (Harrod *et al.*, 2000).

		HOST group			
	Slope	A	B	C	D
Total number of sites	0-3	4	7	1	69
	4-6	3	2	3	65
	7-12	6	5	1	56
	>12	11	15	2	43

	Slope	A	B	C	D
Total eroded volume (m^3/ha)	0-3	351.00	3.40	0.00	16442.00
	4-6	0.00	0.00	578.00	26139.00
	7-12	418.00	25.40	1.43	13560.00
	>12	53.00	216.00	4.73	15297.00

	Slope	A	B	C	D
Mean eroded volume (m^3/ha)	0-3	87.75	0.49	0.00	238.29
	4-6	0.00	0.00	192.67	402.14
	7-12	69.67	5.08	1.43	242.14
	>12	4.82	14.40	2.37	355.74

Table 1.4 Data on eroded grassland field sites from visits in 1997 (Harrod, 1998)

NSI reference	HOST poach	Eroded area (m^2)	Eroded volume (m^3)	Field area (ha)	Area over which erosion was measured (ha)	Eroded area (m^2/ha	Eroded volume (m^3/ha)
NU00/1010	2	20	2	3	3	6.67	0.67
NU01/6010	4	6	3	12	4	1.50	0.75
NU01/6060	4	5	1.25	4	4	1.25	0.31
NU11/6010	4	8	2	6	4	2.00	0.50
SH46/6060	4	120	1.2	6	4	30.00	0.30
SJ07/1010	2	50	0.5	4.8	4	12.50	0.13
SJ53/6010	3	0.15	0.015	2	2	0.08	0.01
SN24/1060	2	25	0.5	4	4	6.25	0.13
SN56/1060	4	100	5	1.6	1.6	62.50	3.13
SN72/1060	1	33	2.3	5	4	8.25	0.58
SS63/6010	3	150	45	1.8	1.8	83.33	25.00

APPENDIX 2

DATA ASSOCIATED WITH SLOPE-CHANNEL COUPLING

2.1 Maps of relevant spatial datasets

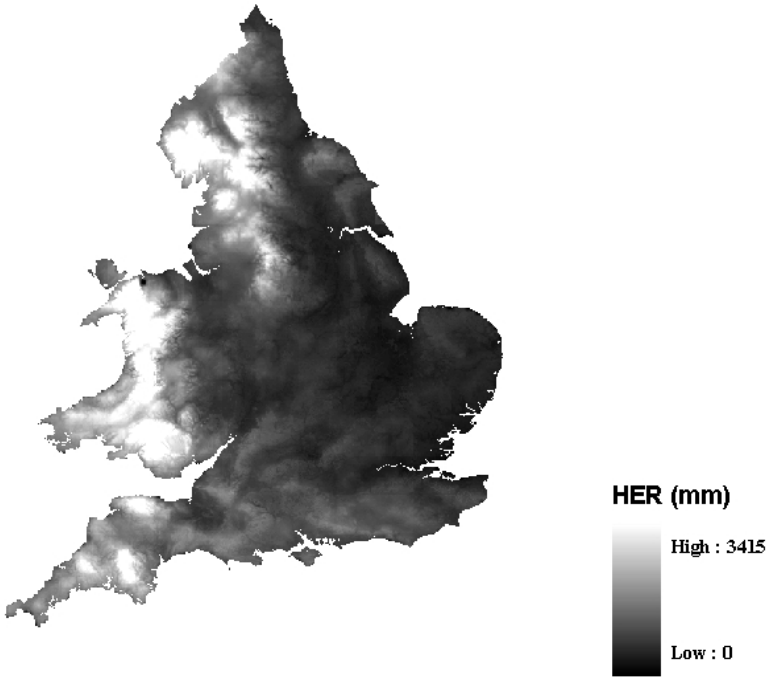

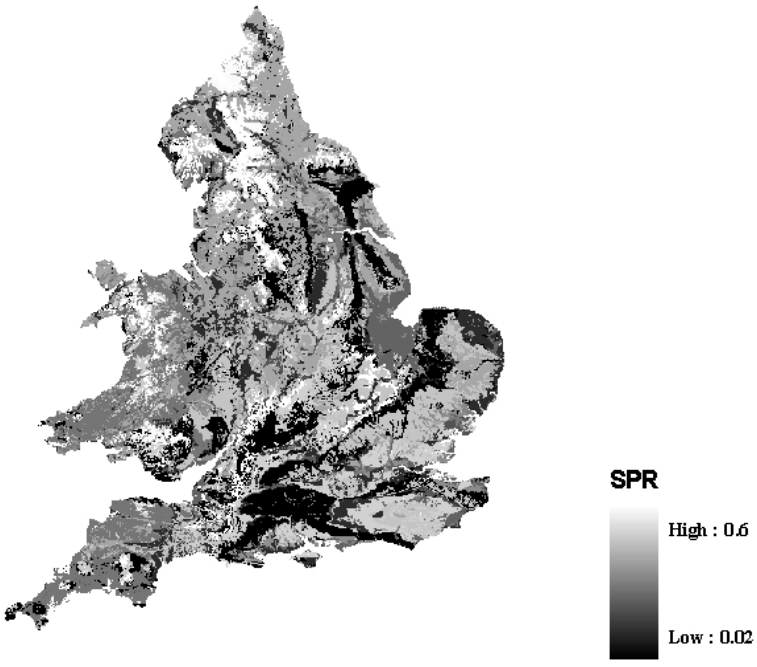

Data used for the estimation of the runoff potential factor. HER (mean annual hydrologically effective rainfall) data was taken from ADAS MAGPIE dataset and SPR data was derived from NSRI HOST classification database

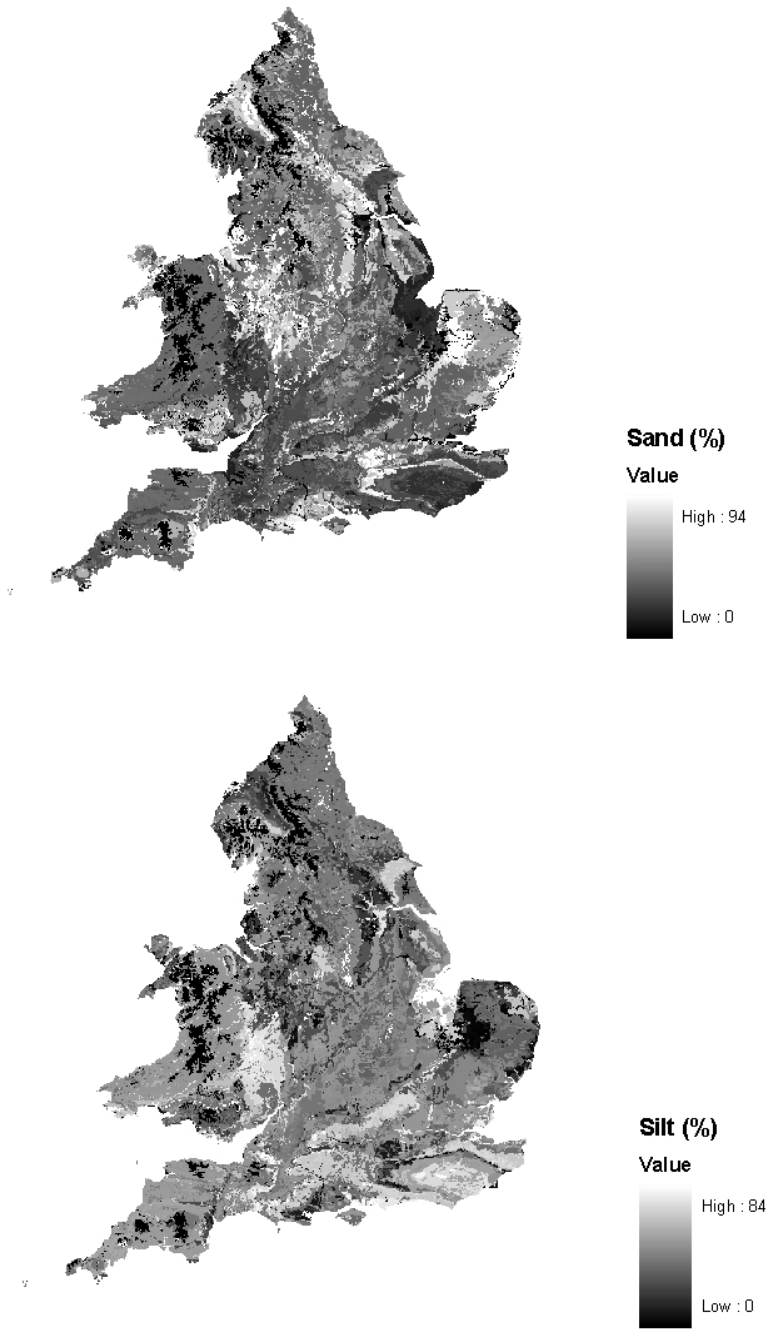

Data used for the estimation of the sediment characteristic factor. Derived from NSRI soil dataset.

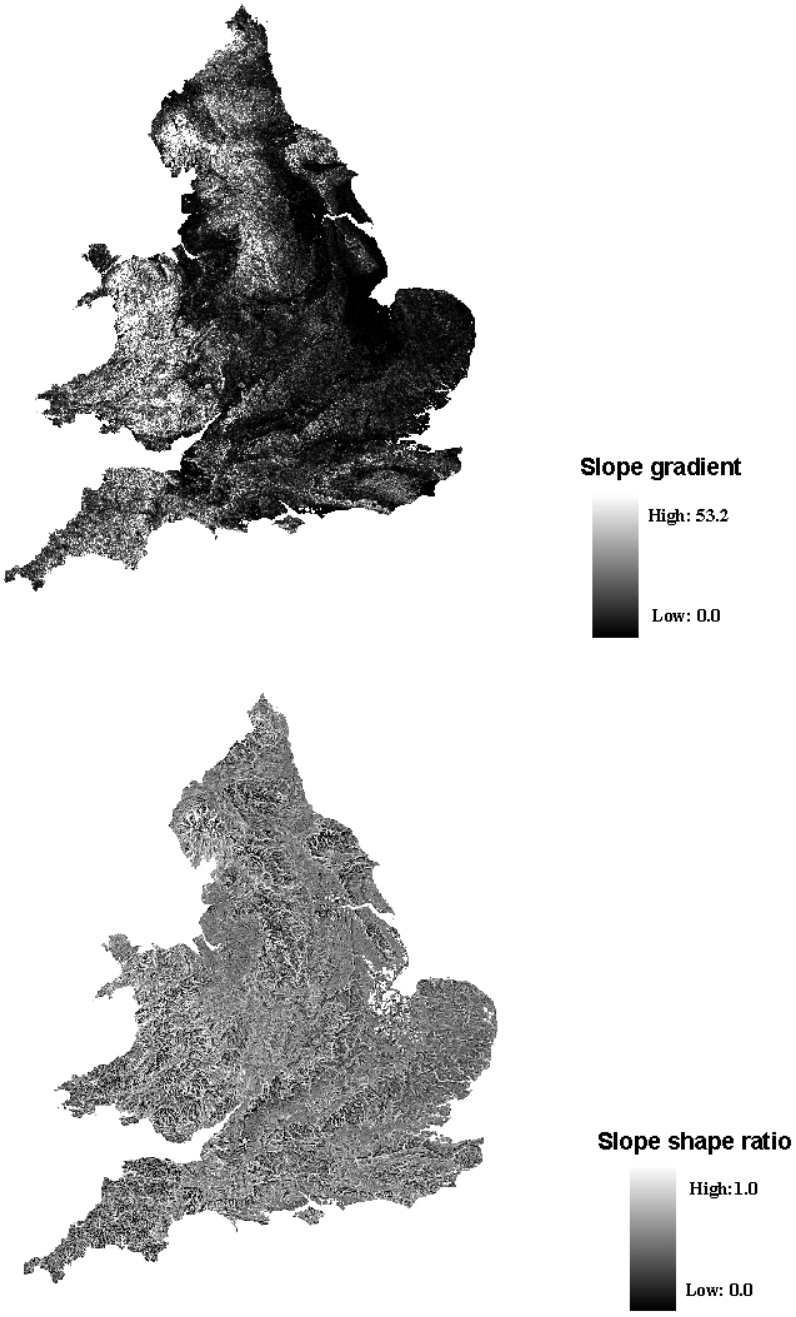

Generated data for the estimation of the slope steepness factor (top) and the slope shape factor (bottom). Based on Ordnance Survey 50 m DEM. The value of slope gradient for each 1 km grid cell represents value for the individual 50 m subgrid cells. The slope shape ratio represents the proportion of the 50m subgrid cells with convex slope profiles.

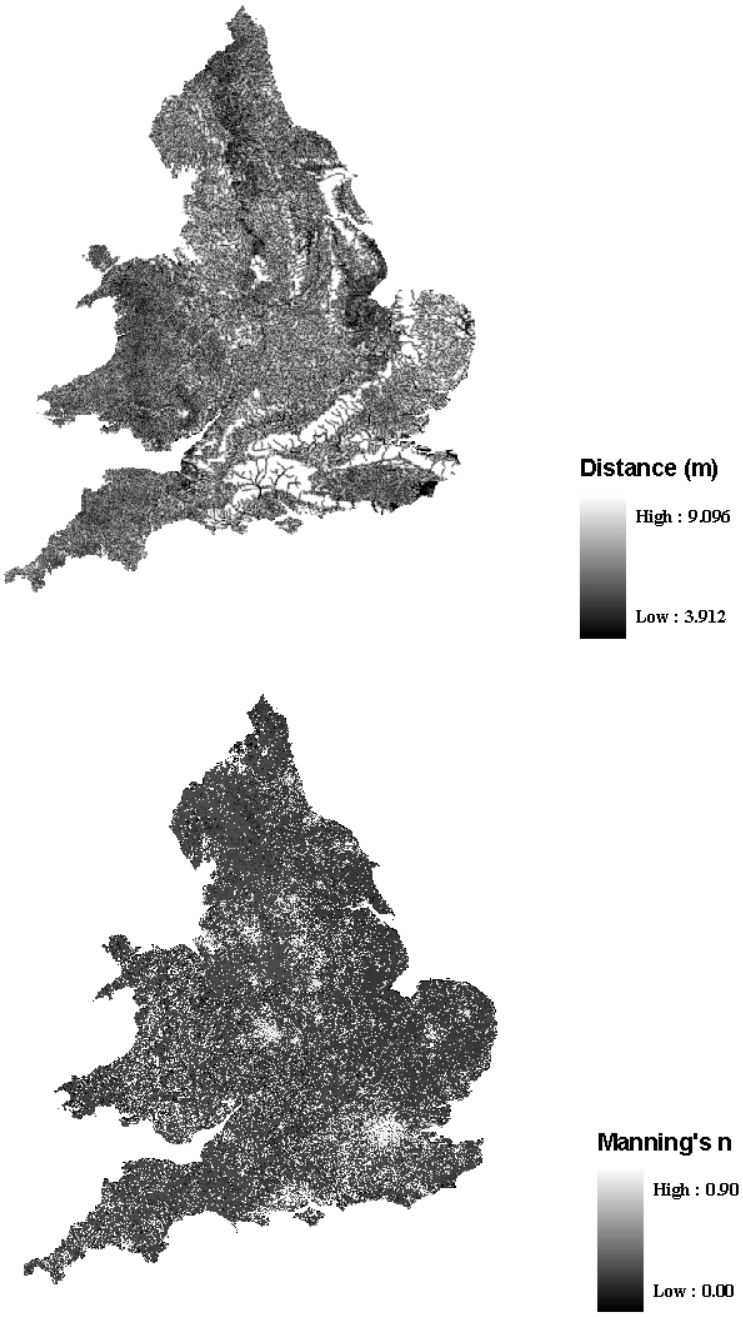

Generated data for the estimation of the drainage pattern factor (top, log transformed average distance to watercourse) and the land use factor (bottom). Average distance to watercourse was derived from the CEH 1: 50000 river network. Manning's *n* was derived from the CEH LCM 1990 dataset using the look up table provided in Appendix 2.4

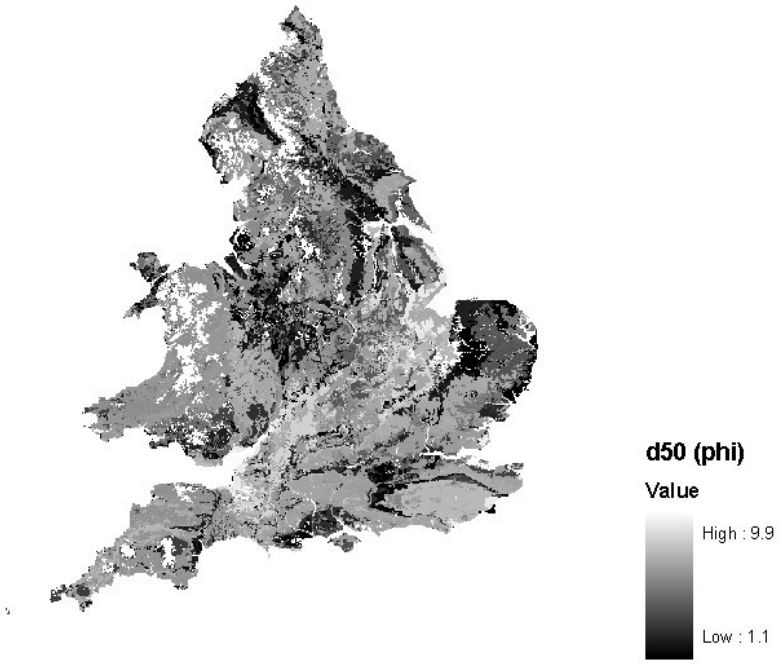

Generated data for the estimation of the sediment characteristic factor. The d_{50} or median grain size in φ-units was derived from the percentages of sand and silt.

2.2 Review of representative spatial explicit sediment delivery (SESD) models

2.2.1 USEPA (1980)

Because of the lack of a reliable sediment delivery model, an index approach was recommended to estimate how much sediment reaches a stream channel from eroding sites. Eight factors were deduced as being important in the proposed procedure (Table 1).

Table 1 Controlling factors and their parameterisation in the EPA, USA Procedure*

Factor	**Estimation procedure**
Transport agent (e.g. water availability)	Multiplication of maximum anticipated rainfall and slope length of the site
Texture of eroded material	Percentage of eroded material that is finer than 0.05 mm
Ground cover	Percent
Slope shape	0 for extremely concavity or 4 for extremely convexity
Slope gradient	Relief between the site and the stream is divided by horizontal distance and expressed in percent
Delivery distance	Log_{10} of the distance between the source area and a stream channel.
Surface roughness	0 for extremely smooth forest floor surface and 4 for very rough surface
Site specific factors	A value between 0 and 100

* Compiled from the USEPA (1980)

To calculate the sediment delivery index for a particular site, each factor is firstly scaled using empirical relationships drawn from the literature or theoretical relationships with delivery potential. Then, a STIFF diagram is drawn to produce an irregular polygon, the shape of which is determined by the values of scaled variables. The higher the values, the larger the area of the closed polygon. The area of the polygon as a percentage of the maximum polygon area possible can then be calculated. Finally, a S-shaped curve is used to derive the spatially explicit sediment delivery ratio (*SESDR*, %). A curve-fitting exercise undertaken at Exeter shows that this curve can be best described using the following formula:

$$SESDR = \frac{104.52031}{(1+\exp(2.608612 - 0.06942621 * X)^{\frac{1}{0.49750546}}} \qquad (1)$$

where X is the percentage derived from STIFF diagram.

2.2.2 Clark and Waldo (1986)

Slope angle, surface roughness, and flow depth were identified as the principal factors influencing the velocity of overland flow which in turn, controls the transport and deposition of sediment. It was assumed that a downslope reduction in slope angle, or in the C or P value in the USLE would be accompanied by a proportionate reduction in transport capacity, and that deposition is inversely proportional to transport capacity.

The procedure evaluates cumulative changes along the overland flow path (profiles) which are selected to represent geomorphic zones or watershed sub-areas. In order to estimate the SESDR, the slope profile under examination should be divided into sections based on the spatial distribution of slope gradient, and the P and C values in the USLE. Then, the SESDR for each section can be estimated as follow:

$$SESDR_i = \prod_{i=1}^{m} P_i \qquad (2)$$

where P is the transport efficiency defined as the downslope change in slope gradient and roughness and m is the number of deposition points occurring between the segment and a channel. The changes of individual factors were expressed as ratios and multiple factors were combined through multiplication. No attempt was made to account for flow convergence because of the profile-based spatial representation.

The SDR for the whole profile was estimated using following equation:

$$SDR = 1/A_w * \sum_{i=1}^{n} (A_i * L_{ui} / L_t * SESDR_i) \qquad (3)$$

where A_w is the weighted average annual soil loss for the overall slope profile (tons/acre/year), A_i is the soil loss rate for a given slope segment (tons/acre/year), L_{ui} is the segment length along the profile occurring upslope from a section (ft), and L_t is the total length of the slope profile (ft).

2.2.3 Ferro and Minacapilli (1995)

In this study, the SESDR of each morphological unit was considered to be dependent on travel time from the unit to the nearest stream reach. The travel time was related to the length of the hydraulic path and to the square root of the slope of the hydraulic path. The SESDR is perceived to be proportional to the probability of non-exceedence of the travel time. Based on examination of empirical cumulative frequency distributions of the travel time in seven Sicilian catchments, the following relationship was proposed:

$$SESDR = \exp\left[-k \left[\sum_{j=1}^{m} \frac{L_j}{\sqrt{S_j}} \right] \right] \qquad (4)$$

where k is a coefficient which is assumed constant for a given basin, m is the number of morphological units located along the hydraulic paths and L and S are the length and slope of each of the j morphological areas.

The theoretical basis of this proposed SESDR was tested and verified in five Apulian and four Calabrian catchments. The application of the SESDR for the prediction of sediment

yield at the catchment was deemed to be successful. A flow-tube approach was advocated for its implementation in a catchment with complex topography.

2.2.4 Cell based SESDRs

With a cell-based spatial data structure, two kinds of SESDR can be calculated. One predicts the SESDR of a cell in terms of delivery to the next receiving cell and the other in terms of delivery from the cell to targeted watercourse cells. As an example for the former, Kothyari and Jain (1997) used the following equation for sediment routing

$$SESDR = k * (1 - F) \tag{5}$$

where F is the fraction of the area of the cell covered by forest.

As an example of the latter, Hession and Shanholtz (1988) proposed the equation shown below

$$SESDR = 10 * R / L \tag{6}$$

where R and L are the relief and flow length between an agricultural cell and a water cell, respectively. Using identical sets of variables, an empirical relationship was developed by Yagow et al (1998):

$$SESDR = \exp(-0.4233 * L * Sf) \tag{7}$$

$$Sf = \exp(-16.1 * (R / L + 0.057)) - 0.6 \tag{8}$$

where both variables are expressed in m. Tim *et al.,* (1992) suggested a more general form of the SESDR that was presented as:

$$SESDR = \exp(-k * S * L) \tag{9}$$

where k is a coefficient that varies with land cover, S is the slope gradient, and L is the flow length.

Based on theoretical consideration of the transporting capacity of overland flow, Bradbury (1997) suggested that the SESDR be seen as a function of the minimum transporting capacity along the flow path. With prior knowledge of the relationship between total overland flow discharge and total annual rainfall amount (P), the estimation of sediment transport capacity (ST) can be simplified as follow:

$$ST = F^{0.5} P^{0.7} S^{1.67} \tag{10}$$

where S is the slope and F is a flow parameter determined by calculating the number of flow paths from each pixel within a DEM which pass through the pixel under study. The specification of the exponents within the equation was based on the work of Govers (1990). In order to convert the minimum transport capacity to a value of SESDR, a calibrated look up table was provided.

References:

Bradbury, P.A., 1997. CALSITE: A catchment planing tool for simulating soil erosion and sediment yield. International Conference on Integrated River Basin Development, 13 - 16 September 1997. H R Wallingford

Clark, C. D. and P.G. Waldo, 1986. Sediment yield from small and medium watersheds. In *Proceedings of the Fourth Interagency Sedimentation Conference*, 3-19 to 3-28

Ferro, V. and M. Minacaplli, 1995. Sediment delivery processes at basin scale. *Hydrological*

Govers, G., 1990. Empirical relationships for the transport capacity of overland flow. In *Erosion, Transport, and Deposition Processes* (Proceedings of the Jerusalem Workshop, March-April 1987), IAHS Publ. No. 189, 45-62

Hession, W. C. and V. O. Shanholtz, 1988. A Geographic Information for targeting nonpoint-source agricultural pollution. *Journal of Soil and Water Conservation*, Vol. 43(3), 264-266

Kothyari, U. C. and S. K. Jain, 1997. Sediment yield estimation using GIS. *Hydrological Sciences Journal,* Vol. 42(6), 833-843

Tim, U.S., S. Mostaghimi, and V.O.Shanholtz, 1992. Identification of critical nonpoint pollution source areas using geographic information systems and water quality modelling. *Water Resources Bulletin*, Vol. 28(5), 877-887

USEPA, 1980. An approach to water resources evaluation of non-point silvicultural sources (A Procedural handbook). *WITS report*, IV.52 – IV.58.

Yagow, E. R., V. O. Shanholtz, B. A. Julian, and J. M. Flagg, 1988. A water quality module for CAMPS. *American Society of Agricultural Engineers meeting presentation*, Paper No 88-2653.

2.3 AML (ARC/INFO Macro Language) source files

D50.aml

```
&args in_gd1 in_gd2 out_gd
/* program purpose: derive d50 value in Phi unit from the sand and silt
/*         percentage using the British classification system
/* program inputs:
/*     in_gd1: sand fraction in percent
/*     in_gd2: silt fraction in percent
/*     out_gd: estimated D50 in Phi unit
/* the adopted classification scheme (in Phi unit):
/*     < 4 sand; 4-9: silt; 9-13 clay
/* programmer: Yusheng Zhang(Y.S.Zhang@ex.ac.uk)

&message &on
&fullscreen &on
/* check current program module
&if [locase [show program]] ne grid &then
&return &warning Run this routine in GRID module

/* check input and output specification
&if [null %in_gd1%] || [null %in_gd2%] | [null %out_gd%] &then
&return &warning Usage: d50.aml in_sand in_silt out_d50

&if ^ [exist %in_gd1% -grid] | ^ [exist %in_gd2% -grid] &then
&return &warning input grid %in_gd1% or %in_gd2% does not exist

&if [exist %out_gd% -directory] &then
&return &warning output grid exists in the workspace
&do i = 1 &to 11
&if [exist tmp_%i% -grid] &then
kill tmp_%i% all
&end

/* setup spatial analysis environment
mapex %in_gd1%
&describe %in_gd1%
setwindow %in_gd1%
setcell %GRD$DX%

tmp_1 = %in_gd1% + %in_gd2%
tmp_2 = setnull(tmp_1 <= %in_gd1%, tmp_1)
kill tmp_1 all
/* estimated parameters with sand and silt percentages
tmp_3 = -1.0 * %in_gd1% / 25.0 + tmp_2 / 50.0
tmp_4 = %in_gd1% * 8.0 / 25.0 - 3.0 * tmp_2 / 50.0
tmp_5 = %in_gd1% * 9.0 / 25.0 - 2.0 * tmp_2 / 25.0
/* estimated parameters with silt and clay percentages
tmp_6 = 25.0 / 9.0 - tmp_2 / 20.0 + %in_gd1% / 45.0
tmp_7 = 17.0 * tmp_2 / 20.0 - 22.0 * %in_gd1% / 45.0 - 325.0 / 9.0
tmp_8 = 100.0 - 13.0 * tmp_2 / 5.0 + 13.0 * %in_gd1% / 5.0
/* estimated coefficients for the relation: y = a*x^2+b*x+c where x is
/* the particle size in Phi unit and y is the cumulative mass coarser
docell
if (tmp_2 >= 50) {
tmp_9 = sqrt(tmp_4 * tmp_4 - 4.0 * tmp_3 * tmp_5 + 200.0 * tmp_3)
```

```
tmp_10 = ( tmp_9 - tmp_4 ) / tmp_3
tmp_11 = (-1.0 * tmp_9 - tmp_4 ) / tmp_3
tmp_1 = ( 50 - tmp_5 ) / tmp_4
}else {
tmp_9 = sqrt(tmp_7 * tmp_7 - 4.0 * tmp_6 * tmp_8 + 200.0 * tmp_6)
tmp_10 = ( tmp_9 - tmp_7 ) / tmp_6
tmp_11 = (-1.0 * tmp_9 - tmp_7 ) / tmp_6
tmp_1 = ( 50 - tmp_7 ) / tmp_6
}end

docell
/* dealing with linear relations
if (tmp_2 >= 50 && tmp_3 == 0)
%out_gd% = tmp_1
else if (tmp_2 < 50 && tmp_6 == 0)
%out_gd% = tmp_1
else if (tmp_10 > 0 && tmp_10 < 26)
%out_gd% = 0.5 * tmp_10
else
%out_gd% = 0.5 * tmp_11
end
/* clear up the temporary grids
&do i = 1 &to 11
&if [exist tmp_%i% -grid] &then
kill tmp_%i% all
&end
&return
```

slopeshp.aml

```
&args in_gd out_gd base_gd
/* purpose: estimate slope shape factor from a DEM
/* in_gd: DEM with a cell size of 50 m
/* out_gd: slope shape factor at 1000 m resolution
/* base_gd: 1000m grid for specifying output grid orientation and
/*   spatial extent. If no grid is given, the in_gd will be
/*   used to derive those data
/* programmer: Zhang Yusheng (Y.S.Zhang@ex.ac.uk)
/* date: debugged on the 23rd of July 2001
&message &on
&fullscreen &on
/* check current program module
&if [locase [show program]] ne grid &then
&return &warning Run this routine in GRID module
/* check input and output specification
&if [null %in_gd%] | [null %out_gd%] &then
&return &warning Usage: sshape.aml in_gd out_gd base_gd

&if [null %base_gd%] &then
&s base_gd %in_gd%

&if ^ [exist %in_gd% -grid] | ^ [exist %base_gd% -grid] &then
&return &warning input grid %in_gd% or %base_gd% does not exist

&if [exist %out_gd% -grid] | [exist %out_gd% -directory] &then
&return &warning output grid %out_dem% exists
```

```
&describe %in_gd%
&if %GRD$DX% <> 50 &then
&return &warning input grid %in_gd% has invalid cell size

&do i = 1 &to 4
&if [exist tmp_%i% -grid] &then
kill tmp_%i% all
&end
/* setup spatial analysis environment
mapex %in_gd%
&describe %in_gd%
setwindow %in_gd%
setcell 50

/* calculate slope weighted surface curvature
tmp_3 = curvature (%in_gd%,tmp_1,#,tmp_2)
kill tmp_3 all
tmp_3 = cos(tmp_2 / DEG)
kill tmp_2 all
tmp_2 = con(tmp_1 >= 0, tmp_1 / tmp_3, 0)
tmp_4 = con(tmp_1 < 0, abs(tmp_1) / tmp_3, 0)
kill tmp_1 all

/* sum up convexity and concavity within 1000 m spatial extent
&type start focalsum operation
tmp_1 = focalsum(tmp_2,rectangle,20,20,data)
kill tmp_2 all
tmp_2 = focalsum(tmp_4,rectangle,20,20,data)
&type finish focalsum operation
kill tmp_4 all
/* calculate the ratio of convexity
kill tmp_3 all
tmp_3 = tmp_1 / (tmp_1 + tmp_2)
kill tmp_1 all
kill tmp_2 all

/* resampling
mapex %base_gd%
setwindow %base_gd%
setcell 1000
%out_gd% = resample(tmp_3)
kill tmp_3 all
&return
```

drainden.aml

```
&args in_gd out_gd river_cv base_gd
/* purpose: estimate median distance from cell centre to a river cover
/* in_gd: DEM with a cell size of 50 m
/* out_gd: distance at 1000 m resolution
/* river_cv: watercourse coverage (1: 50000)
/* base_gd: 1000m grid for specifying output grid orientation
/*   and spatial extent. If no grid is given, the in_gd will
/*   be used to derive those data
/* programmer: Zhang Yusheng (Y.S.Zhang@ex.ac.uk)
/* date: debugged on the 14th of September, 2001

&message &on
```

```
&fullscreen &on
/* check current program module
&if [locase [show program]] ne grid &then
&return &warning Run this routine in GRID module
/* check input and output specification
&if [null %in_gd%] | [null %out_gd%] | [null %river_cv%] &then
&return &warning Usage: drainden.aml in_gd out_gd river_cv base_gd

&if [null %base_gd%] &then
&s base_gd %in_gd%

&if ^ [exists %in_gd% -grid] | ^ [exist %base_gd% -grid] &then
&return &warning input grid %in_gd% or %base_gd% does not exist
&if ^ [exists %river_cv% -arc] &then
&return &warning linear coverage %river_cv% does not exist

&if ^ [exists %river_cv%.aat -info] &then
build %river_cv% line

&if [exist %out_gd% -grid] | [exist %out_gd% -directory] &then
&return &warning output grid %out_dem% exists

&do i = 1 &to 3
&if [exist tmp_%i% -grid] | [exist tmp_%i% -cover] &then
kill tmp_%i% all
&end

/* setup spatial analysis environment
mapex %in_gd%
&describe %in_gd%
setwindow %in_gd%
setcell %GRD$DX%
&s var0 [truncate [calc 1000 / %GRD$DX% ]]
&s var1 %GRD$XMAX% * %GRD$YMAX%
tmp_1 = gridpoint(%in_gd%)
&type start near operation
arc near tmp_1 %river_cv% line %var1%
&type finish near operation
tmp_2 = pointgrid(tmp_1,distance)
kill tmp_1 all
/* sum up within 1000 m spatial extent
&type start focalmedian operation
tmp_1 = focalmedian(tmp_2,rectangle,%var0%,%var0%,data)
&type finish focalmedian operation
/*kill tmp_2 all

/*resampling
mapex %base_gd%
setwindow %base_gd%
setcell 1000
%out_gd% = resample(tmp_1)
kill tmp_1 all
&return
```

2.4 Look up table for the specification of the Manning's roughness n*

Land cover group	Recommended ' n
Sea / estuary	Watercourse
Inland water	Water course
Beach and coastal bare	Water course
Saltmarsh	Water course
Upland bog	Water course
Lowland bog	Water course
Continuous urban	0.9
Suburban / rural development	0.7
Deciduous woodland	0.9
Coniferous woodland	0.9
Felled forest	0.9
Tilled land	0.04 (smooth) 0.3 (rough)
Grass heath	0.24
Mown / grazed turf	0.24
Meadow / verge / semi-natural	0.24
Rough / marsh grass	0.24
Moorland grass	0.24
Open shrub moor	0.15
Dense shrub moor	0.3
Bracken	0.15
Open shrub heath	0.25
Open shrub heath	0.35
Scrub / orchard	0.2
Ruderal weed	0.5

*The table was created to highlight the contrast between major land use groups, such as arable land, grassland, and forest. While the actual values are open to question, the relative rankings are thought to be sufficiently accurate for the project. Its use for other purposes should be treated with caution.

Appendix 3

Data relating to spatial data processing, analysis and mapping

3.1 LANDCOVER MAP 1990

3.1.1 INTRODUCTION

The Land cover map of Great Britain (LCMGB) was produced by The Centre for Ecology and Hydrology (CEH) using supervised maximum likelihood classifications of Landsat Thematic Mapper (TM) data. The map, resampled to a 25 m grid, records 25 cover types, consisting of sea and inland water, beaches and bare ground, developed and arable land, and 18 types of semi-natural vegetation - these are described below, and more details can be obtained from the CEH website:
http://www.ceh.ac.uk/data/lcm/index.htm.

3.1.2 Description of Land Cover classes

The following descriptions outline the Landsat-derived cover types used in the Land Cover Map of Great Britain. The classes chosen represent an aggregation of many subclasses: for example, wheat, barley and oilseed rape are subclasses of the 'arable' class. These subclasses have been reduced to a short- list of target 'classes' which are considered ecologically meaningful, consistently recognisable from the selected imagery, and realistic in terms of their likely accuracy.

A – SEA / ESTUARY

This category includes all open sea and coastal waters, including estuaries, normally inland to the point where the waterway is less than 30 m wide or its continuity is broken by a bridging point. It is not intended to accurately show the limit of saline or tidal waters, which may extend much further inland. **Fuller key-name: Sea.**

B - INLAND WATER

Fuller key-name: inland fresh waters and estuarine waters above the first bridging point or barrier. **This category carries the label '2' in the 25 'target' class dataset.**

C - COASTAL BARE GROUND (BEACH / MUDFLATS / CLIFFS)

Fuller key-name: bare coastal mud, silt, sand, shingle and rock, including coastal accretion and erosion features above high water. This category carries the label '3' in the 25 'target' cover-type digital data set.

D - SALTMARSH

Fuller key name: intertidal seaweed beds and saltmarshes up to normal levels of high water spring tides. **This category carries the label '4' in the 25 'target' class dataset.**

E - ROUGH PASTURE / DUNE GRASS / GRASS MOOR

Grass Heath – Fuller key-name: semi-natural, mostly acid, grasslands of dunes, heaths and lowland-upland margins. This category carries the label '5' in the 25 'target' class dataset.

Moorland Grass – Fuller key-name: montane/hill grasslands, mostly unenclosed Nardus/Molinia moorland. This category carries the label '9' in the 25 'target' class dataset.

F - PASTURE / MEADOW / AMENITY GRASS

Mown / Grazed Turf – Fuller key-name: pastures and amenity swards, mown or grazed, to form a turf throughout the growing season. **This category carries the label '6' in the 25 'target' class dataset.**

Meadow / Verge / Semi-natural swards – Fuller key-name: Meadows, verges, low intensity amenity grasslands and semi-natural cropped swards, not maintained as a short turf. **This category carries the label '7' in the 25 'target' class dataset.**

G - MARSH / ROUGH GRASS

Ruderal weed – Fuller key-name: ruderal weeds colonising natural and man-made bare ground. This category carries the label '19' in the 25 'target' class dataset.

Felled Forest – Fuller key-name: felled forest, with ruderal weeds and rough grass. This category carries the label '23' in the 25 'target' class dataset.

Rough / Marsh Grass – Fuller key-name: lowland marsh/rough grasslands, mostly uncropped and unmanaged, forming grass and herbaceous communities, of mostly perennial species, with high winter-litter content. This category carries the label '8' in the 25 'target' class dataset.

H - GRASS / SHRUB HEATH

Open Shrub Heath – Fuller key-name: lowland, dwarf shrub/grass heathland. This category carries the label '25' in the 25 'target' class dataset.

Open Shrub Moor – Fuller key-name: upland, dwarf shrub/grass moorland. This category carries the label '10' in the 25 'target' class dataset.

I - SHRUB HEATH

Dense Shrub Heath – Fuller key-name: lowland evergreen shrub-dominated heathland. This category carries the label '13' in the 25 'target' class dataset.

Dense Shrub Moor – Fuller key-name: upland evergreen dwarf shrub-dominated moorland. This category carries the label '11' in the 25 'target' class dataset.

J - BRACKEN

Bracken – Fuller key-name: bracken-dominated herbaceous communities. This category carries the label '12' in the 25 'target' class dataset.

K - DECIDUOUS / MIXED WOOD

Scrub / Orchard – Fuller key-name: deciduous scrub and orchards. This category carries the label '14' in the 25 'target' class dataset.

Deciduous Woodland – Fuller key-name: Deciduous broadleaved and mixed woodlands. This category carries the label '15' in the 25 'target' class dataset.

L - CONIFEROUS / EVERGREEN WOODLAND

Fuller key-name: Conifer and broadleaved evergreen trees. This category carries the label '16' in the 25 'target' class dataset.

M - BOG (HERBACEOUS)

Lowland bog – Fuller key-name: lowland herbaceous wetlands with permanent or temporary standing water. This category carries the label '24' in the 25 'target' class dataset.

Upland bog – Fuller key-name: lowland herbaceous wetlands with permanent or temporary standing water. This category carries the label '17' in the 25 'target' class dataset.

N - TILLED LAND (ARABLE CROPS)
Fuller key-name: arable and other seasonally or temporarily bare ground. This category carries the label '18' in the 25 'target' class dataset.

O - SUBURBAN / RURAL DEVELOPMENT
Fuller key-name: suburban and rural developed land comprising buildings and/or roads but with some cover of permanent vegetation. This category carries the label '20' in the 25 'target' class dataset.

P - URBAN DEVELOPMENT
Fuller key-name: industrial, urban and any other developments, lacking permanent vegetation. This category carries the label '21' in the 25 'target' class dataset.

Q - INLAND BARE GROUND
Fuller key-name: ground bare of vegetation, surfaced with 'natural' materials. This category carries the label '22' in the 25 'target' class dataset.